Annals of PDE (2022) 8:24
https://doi.org/10.1007/s40818-022-00140-7

MANUSCRIPT

Asymptotically self-similar blowup of the Hou-Luo model for the 3D Euler equations

Jiajie Chen[1,2] · **Thomas Y. Hou**[1] · **De Huang**[1,3]

Received: 12 June 2021 / Accepted: 27 October 2022

Abstract
Inspired by the numerical evidence of a potential 3D Euler singularity [54, 55], we prove finite time singularity from smooth initial data for the HL model introduced by Hou-Luo in [54, 55] for the 3D Euler equations with boundary. Our finite time blowup solution for the HL model and the singular solution considered in [54, 55] share some essential features, including similar blowup exponents, symmetry properties of the solution, and the sign of the solution. We use a dynamical rescaling formulation and the strategy proposed in our recent work in [11] to establish the nonlinear stability of an approximate self-similar profile. The nonlinear stability enables us to prove that the solution of the HL model with smooth initial data and finite energy will develop a focusing asymptotically self-similar singularity in finite time. Moreover the self-similar profile is unique within a small energy ball and the C^γ norm of the density θ with $\gamma \approx 1/3$ is uniformly bounded up to the singularity time.

1 Introduction

The three-dimensional (3D) incompressible Euler equations are one of the most fundamental equations in fluid dynamics. Despite their wide range of applications, the global well-posedness of the 3D incompressible Euler equations is one of the most outstanding open questions in the theory of nonlinear partial differential equations. The interested readers may consult the excellent surveys [14, 32, 40, 46, 57] and the

✉ Jiajie Chen
jiajie.chen@cims.nyu.edu; jchen@caltech.edu

Thomas Y. Hou
hou@cms.caltech.edu

De Huang
dhuang@math.pku.edu.cn; dhuang@caltech.edu

1 Applied and Computational Mathematics, Caltech, Pasadena, CA 91125, USA

2 Courant Institute, NYU, New York, NY 10012, USA

3 School of mathematical sciences, Peking University, Beijing 100871, China

Published online: 13 November 2022

references therein. The difficulty associated with the global regularity of the 3D Euler equations can be described by the vorticity equation:

$$\omega_t + u \cdot \nabla \omega = \omega \cdot \nabla u, \tag{1.1}$$

where $\omega = \nabla \times u$ is the *vorticity vector* of the fluid, and u is related to ω via the *Biot-Savart law*. Formally, ∇u has the same scaling as ω, which implies that the vortex stretching term $\omega \cdot \nabla u$ formally scales like ω^2. However, ∇u is related to ω through the Riesz transform. Various previous studies indicate that the nonlocal nature of the vortex stretching term and the local geometric regularity of the vorticity vector may lead to dynamic depletion of the nonlinear vortex stretching (see e.g. [15, 22, 41]), which may prevent singularity formation in finite time.

In [54, 55], Luo and Hou investigated the 3D axisymmetric Euler equations with a solid boundary and presented some convincing numerical evidence that the 3D Euler equations develop a potential finite time singularity. They considered a class of smooth initial data with finite energy that satisfy certain symmetry properties. The potential singularity occurs at a stagnation point of the flow along the boundary. The presence of the boundary and the hyperbolic flow structure near the singularity play an important role in the singularity formation. To understand the mechanism for this potential 3D Euler singularity, Hou and Luo [54] proposed the following one-dimensional model along the boundary at $r = 1$:

$$\begin{aligned} &\omega_t + u\omega_x = \theta_x, \\ &\theta_t + u\theta_x = 0, \quad u_x = H\omega. \end{aligned} \tag{1.2}$$

Here $u = u^z$, $\omega = \omega^\phi$, and $\theta = (u^\phi)^2$, with u^ϕ and ω^ϕ being the angular velocity and angular vorticity, respectively. Numerical study presented in [54] shows that the HL model develops a finite time singularity from smooth initial data with blowup scaling properties surprisingly similar to those observed for the 3D Euler equations. By exploiting the symmetry properties of the solution and some monotonicity property of the velocity kernel, Choi et al have been able to prove that the HL model develops a finite time singularity in [12] using a Lyapunov functional argument. Part of our analysis to be presented is inspired by the sign property of a quadratic interaction term between u and ω obtained in [12]. However, there seems to be some essential difficulties in extending the method in [12] to the 3D Euler equations.

There has been a number of subsequent developments inspired by the singularity scenario reported in[54, 55], see e.g. [12, 13, 47, 48] and the excellent survey article [46]. Although various simplified models have been proposed to study the singularity scenario reported in[54, 55], currently there is no rigorous proof of the Luo-Hou blowup scenario with smooth data. Recently, Elgindi [24] (see also [25]) proved an important result that the 3D axisymmetric Euler equations without swirl can develop a finite time singularity for $C^{1,\alpha}$ initial velocity. In a setting similar to the Luo-Hou scenario, singularity formation of the 2D Boussinesq and the 3D axisymmetric Euler equations with $C^{1,\alpha}$ velocity and boundary has been established by the first two authors [7].

One of our goals is to establish the finite time self-similar blowup of (1.2) of the form

$$\omega_*(x,t) = \frac{1}{(1-t)|c_{\omega,\infty}|}\omega_\infty\left(\frac{x}{(1-t)^\lambda}\right),$$
$$\theta_*(x,t) = \frac{1}{(1-t)^{2-\lambda}|c_{\omega,\infty}|}\theta_\infty\left(\frac{x}{(1-t)^\lambda}\right), \tag{1.3}$$

where $\lambda = c_{l,\infty}|c_{\omega,\infty}|^{-1}$ is the blowup exponent and $c_{l,\infty}, c_{\omega,\infty}$ are the scaling exponents. The main result of this paper is stated by the informal theorem below, which shows the existence of the self-similar profile with sharp estimate of the blowup exponent λ. A more precise and stronger statement will be given by Theorem 2 in Section 2.

Theorem 1 *There is a family of initial data (θ_0, ω_0) with $\theta_{0,x}, \omega_0 \in C_c^\infty$, such that the solution of the HL model (1.2) will develop a focusing asymptotically self-similar singularity in finite time. The self-similar blowup profile $(\theta_\infty, \omega_\infty)$ is unique within a small energy ball and its associated scaling exponents $c_{l,\infty}, c_{\omega,\infty}$ satisfy $|\lambda - 2.99870| \le 6\cdot 10^{-5}$ with $\lambda = c_{l,\infty}|c_{\omega,\infty}|^{-1}$. Moreover, the C^γ norm of θ is uniformly bounded up to the blowup time T, and the C^β norm of θ blows up at T for any $\beta \in (\gamma, 1]$ with $\gamma = \frac{\lambda-2}{\lambda}$.*

The blowup exponent $\lambda \approx 2.99870$ in the HL model is surprisingly close to the blowup exponent $\lambda \approx 2.9215$ of the 3D Euler equations considered by Luo-Hou [54, 55]. In order to construct the self-similar profile $(\omega_\infty, \theta_\infty, c_{l,\infty}, c_{\omega,\infty})$ in (1.3), we first construct an approximate self-similar profile $(\bar\omega, \bar\theta, \bar c_l, \bar c_\omega)$ and will prove that $(\bar\omega, \bar\theta, \bar c_l, \bar c_\omega)$ is close to the exact self-similar profile in some suitable energy norm. See more details in Theorem 2 in Section 2. An important property that characterizes the stable nature of the blowup in the HL model is that $\bar c_l x + \bar u \ge 0.49x$, $\bar c_l = 3$, $\bar u < 0$ for any $x \ge 0$, here $\bar u, \bar c_l$ are the velocity and the scaling exponent of the approximate self-similar profile. We use this property to extract the main damping effect from the linearized operator in the near field using some carefully designed singular weights.

As we will show later, $\bar c_l x + \bar u$ is the velocity field for the linearized equation in the dynamic rescaling formulation. The inequality $\bar c_l x + \bar u \ge 0.49x$, $x \ge 0$ implies that the perturbation is transported from the near field to the far field and then damped by the damping term $\bar c_\omega \omega$ in the ω equation and by $2\bar c_\omega \theta_x$ in the θ_x equation. This is the main physical mechanism that generates the dynamic stability of the self-similar blowup in the HL model. We believe that this also captures the dynamic stability of the blowup scenario considered by Luo-Hou along the boundary [54, 55], whose numerical evidence has been reported in [53].

There are four important components of our analysis for the HL model. The first one is to construct the approximate steady state with sufficiently small residual error by decomposing it into a semi-analytic part that captures the far field behavior of the solution and a numerically computed part that has compact support. The approximate steady state gives an approximate self-similar profile discussed above. See more discussion in Section 4. The second one is that we extract the damping effect from the local terms in the linearized equations by using carefully designed singular weights. The third one is that the contributions from the advection terms are relatively weak compared with those coming from the vortex stretching terms. As a result, we can treat

those terms coming from advection as perturbation to those from vortex stretching. The last one is to apply some sharp functional inequalities to control the nonlocal terms and take into account cancellation among various nonlocal terms. This enables us to show that the contributions from the nonlocal terms are relatively small compared with those from the local terms and can be controlled by the damping terms. We refer to Section 2 for more detailed discussion of the main ingredients in our stability analysis.

We believe that the analysis of the 2D Boussinesq equations and 3D Euler equations with smooth initial data and boundary would benefit from the four important components mentioned above. The stability analysis of the HL model is established based on some weighted L^2 space. For the 2D Boussinesq equations and 3D Euler equations, a wider class of functional spaces, e.g. weighted L^p or weighted C^α spaces, can be explored to derive larger damping effect from the linearized equations and to further establish stability analysis.

There is an interesting implication of our blowup results for the self-similar solution (ω_*, θ_*) defined in (1.3). In Section 6.1, we show that the profile satisfies $\lim_{x\to\infty} \theta_\infty(x)|x|^{-\gamma} = C$ for some $C > 0$ (see (1.3)). Thus, we have $\lim_{t\to 1} \theta_*(x,t) \to C|x|^\gamma$ for any $x \neq 0$. Since $0 < \gamma < 1$, the self-similar solution forms a cusp singularity at $x = 0$ as $t \to 1$. Moreover, from Theorem 1, for a class of initial data θ_0, the C^γ norm of the singular solution θ is uniformly bounded up to the blowup time. Note that from Theorem 1, we have $|\gamma - 0.33304| < 2 \cdot 10^{-5}$, thus $\gamma \approx \frac{1}{3}$ and $\lim_{t\to 1} \theta_*(x,t) = C|x|^\gamma \approx C|x|^{1/3}$. Similarly, we can generalize the method of analysis to prove $\lim_{t\to 1} \omega_*(x,t) = C_2|x|^{(\gamma-1)/2} \approx C_2|x|^{-1/3}$. Interestingly, the limiting behavior is closely related to a family of explicit solutions of (1.2) discovered by Hoang and Radosz in [39]

$$\omega(x,t) = k|x|^{-1/3}\mathrm{sgn}(x), \quad \theta(x,t) = c_1k^2|x|^{1/3} + c_2k^3t, \tag{1.4}$$

where $c_1, c_2 > 0$ are suitable constants and $k > 0$ is arbitrary. We remark that from Theorem 1, the $C^{1/3}$ norm of θ from a class of smooth initial data that we consider blows up at the singularity time since $\frac{1}{3} > \gamma$, while the non-smooth θ in (1.4) remains in $C^{1/3}$ for all time.

The cusp formation and the Hölder regularity on θ are related to the $C^{1/2}$ conjecture by Silvestre and Vicol in [68] and the cusp formation on the Cordoba-Cordoba-Fontelos (CCF) model [11, 17, 45, 52], which is the $\theta-$equation in (1.2) coupled with $u = H\theta$. The cusp formation of a closely related model was established in [38], and the $C^{1/2}$ conjecture was studied in [26, 28] for a class of $C^{1,\alpha}$ initial data with small α. Using the same method for the HL model, we have obtained an approximate self-similar profile for the CCF model with residual $O(10^{-8})$ and $\gamma = 0.5414465$, which is accurate up to six digits. This blowup exponent γ is qualitatively similar to that obtained in [56] for the generalized Constantin-Lax-Majda model (gCLM) (see[64]) with $a = -1$. In a follow-up work, we will generalize our method of analysis to study the cusp formation of the CCF model, and rigorously prove that $\theta \in C^\gamma$ up to the singularity time with $\gamma > 1/2$. Moreover, the C^β norm of θ will blow up at the singularity time for any $\beta > \gamma$.

There has been a lot of effort in studying potential singularity of the 3D Euler equations using various simplified models. In [13, 37, 39, 49], the authors proposed several simplified models to study the Hou-Luo blowup scenario [54, 55] and established finite time blowup of these models. In these works, the velocity is determined by a simplified Biot-Savart law in a form similar to the key lemma in the seminal work of Kiselev-Sverak [48]. In [42], Hou and Liu established the self-similar singularity of the CKY model [13] using the property that the CKY model can be reformulated as a local ODE system. The HL model does not enjoy a similar local property, and our method to prove self-similar singularity is completely different from that in [42]. In [27, 29] , Elgindi and Jeong proved finite time singularity formation for the 2D Boussinesq and 3D axisymmetric Euler equations in a domain with a corner using $\mathring{C}^{0,\alpha}$ data.

Several other 1D models, including the Constantin-Lax-Majda (CLM) model [16], the De Gregorio (DG) model [20, 21], and the gCLM model [64], have been introduced to study the effect of advection and vortex stretching in the 3D Euler. Singularity formation from smooth initial data has been established for the CLM model in [16], for the DG model in [11], and for the gCLM model with various parameters in [2, 5, 6, 11, 26, 28]. In the viscous case, singularity formation of the gCLM model with some parameters has been established in [6, 66].

The rest of the paper is organized as follows. In Section 2, we outline some main ingredients in our stability analysis by using the dynamic rescaling formulation. Section 3 is devoted to linear stability analysis. In Section 4, we discuss some technical difficulty in obtaining an approximate steady state with a residual error of order 10^{-10}. In Section 5, we perform nonlinear stability analysis and establish the finite time blowup result. In Section 6, we estimate the Hölder regularity of the singular solution. In Section 7, we give a formal derivation to demonstrate that both the HL model and the 2D Boussinesq equations with $C^{1,\alpha}$ initial data for velocity and θ and with boundary have the same leading system for small α. We make some concluding remarks in Section 8. Some technical estimates and derivations are deferred to the Appendix.

2 Outline of the main ingredients in the stability analysis

In this section, we will outline the main ingredients in our stability analysis by using the dynamic rescaling formulation for the HL model. The most essential part of our analysis lies in the linear stability. We need to use a number of techniques to extract the damping effect from the linearized operator around the approximate steady state of the dynamic rescaling equations and obtain sharp estimates of various nonlocal terms. Since the damping coefficient we obtain is relatively small (about 0.03), we need to construct an approximate steady state with a very small residual error of order 10^{-10}. This is extremely challenging since the solution is supported on the whole real line with a slowly decaying tail in the far field. We use analytic estimates and numerical analysis with rigorous error control to verify that the residual error is small in the energy norm. See detailed discussions in Section 4 and Section 10 of the Supplementary Material [10].

Passing from linear stability to nonlinear stability is relatively easier since the perturbation is quite small due to the small residual error. Yet we need to verify various inequalities involving the approximate steady state using the interval arithmetic [33, 63, 65] and numerical analysis with computer assistance. The most essential part of the linear stability analysis can be established based on the grid point values of the approximate steady state constructed on a relatively coarse grid, which does not involve the lengthy rigorous verification. See more discussion in Section 3.13. The reader who is not interested in the rigorous verification can skip the lengthy verification process presented in the Supplementary Material [10].

2.1 Dynamic rescaling formulation

An essential tool in our analysis is the dynamic rescaling formulation. Let $\omega_{phy}(x,t)$, $\theta_{phy}(x,t)$ be the solutions of the physical equations (1.2), then it is easy to show that

$$\omega(x,\tau) = C_\omega(\tau)\omega_{phy}(C_l(\tau)x, t(\tau)), \quad \theta(x,\tau) = C_\theta(\tau)\theta_{phy}(C_l(\tau)x, t(\tau))$$

are the solutions to the dynamic rescaling equations

$$\omega_\tau + (c_l x + u)\omega_x = c_\omega \omega + \theta_x, \quad \theta_\tau + (c_l x + u)\theta_x = c_\theta \theta, \quad u_x = H\omega, \tag{2.1}$$

where $t(\tau) = \int_0^\tau C_\omega(s)ds$ and

$$C_\omega(\tau) = \exp\left(\int_0^\tau c_\omega(s)ds\right), \; C_l(\tau) = \exp\left(\int_0^\tau -c_l(s)ds\right),$$
$$C_\theta(\tau) = \exp\Big(\int_0^\tau c_\theta(s)ds\Big).$$

In order for the dynamic rescaling formulation to be equivalent to the original HL model, we must enforce a relationship among the three scaling parameters, c_l, c_ω and c_θ, i.e. $c_\theta = c_l + 2c_\omega$.

The dynamic rescaling formulation was introduced in [50, 59] to study the self-similar blowup of the nonlinear Schrödinger equations. This formulation is closely related the modulation technique, which has been developed by Merle, Raphael, Martel, Zaag and others, see e.g. [44, 58, 60–62]. The dynamic rescaling formulation and modulation technique have been very effective in analyzing singularity formation for many nonlinear PDEs including the nonlinear Schrödinger equation [44, 60], the nonlinear wave equation [62], the nonlinear heat equation [61], the generalized KdV equation [58], the De Gregorio model and the generalized Constantin-Lax-Majda model [5, 6, 11], and singularity formation in 3D Euler equations [7, 24].

To simplify our presentation, we still use t to denote the rescaled time in (2.1). Taking the x derivative on the θ equation in (2.1) yields

$$\begin{aligned} &\omega_t + (c_l x + u)\omega_x = c_\omega \omega + \theta_x, \\ &(\theta_x)_t + (c_l x + u)\theta_{xx} = (c_\theta - c_l - u_x)\theta_x = (2c_\omega - u_x)\theta_x, \quad u_x = H\omega, \end{aligned} \tag{2.2}$$

where $c_\theta = c_l + 2c_\omega$. We still have two degrees of freedom in choosing c_l, c_ω to uniquely determine the dynamic rescaled solution. We impose the following normalization conditions on c_ω, c_l

$$c_l = 2\frac{\theta_{xx}(0)}{\omega_x(0)}, \quad c_\omega = \frac{1}{2}c_l + u_x(0). \tag{2.3}$$

These two normalization conditions play the role of forcing

$$\theta_{xx}(t,0) = \theta_{xx}(0,0), \quad \omega_x(t,0) = \omega_x(0,0) \tag{2.4}$$

for all time. Our study shows that enforcing $\theta_{xx}(t,0)$ to be independent of time is essential for stability by eliminating a dynamically unstable mode in the dynamic rescaling formulation.

2.2 Main result

Throughout this paper, we will consider solution of (2.1) with odd ω, θ_x and $\theta(t,0) = 0$. Under this setting, it is not difficult to show that the odd symmetries of θ_x, ω, u and the condition $\theta(t,0) = 0$ are preserved by the equations.

Due to the symmetry, we restrict the inner product and L^2 norm to $\mathbb{R}_+$

$$\langle f, g\rangle \triangleq \int_0^\infty fg dx, \quad ||f||_2^2 = \int_0^\infty f^2 dx. \tag{2.5}$$

Let ψ, φ be the singular weights defined in (3.8), and λ_i be the parameter given in (C.3). We use the following energy in our energy estimates

$$\begin{aligned} E^2(f,g) \triangleq\ & ||f\psi^{1/2}||_2^2 + \lambda_1||g\psi^{1/2}||_2^2 + \lambda_2\frac{\pi}{2}(Hg(0))^2 + \lambda_3\langle f, x^{-1}\rangle^2 \\ & + \lambda_4(||D_x f\psi^{1/2}||_2^2 + \lambda_1||D_x g\varphi^{1/2}||_2^2), \end{aligned} \tag{2.6}$$

where $Hg(0) = -\frac{1}{\pi}\int_{\mathbb{R}} gx^{-1}dx$ is related to c_ω in (2.3). Our main result is the following.

Theorem 2 *Let $(\bar\theta, \bar\omega, \bar c_l, \bar c_\omega)$ be the approximate self-similar profile constructed in Section 4, and $E_* = 2.5\cdot 10^{-5}$. For odd initial data $\theta_{0,x}, \omega_0$ of (2.1) with $\theta_0(0) = 0$ and a small perturbation to $(\bar\theta_x, \bar\omega)$, $E(\theta_{0,x} - \bar\theta_x, \omega_0 - \bar\omega) \le E_*$, we have (a) $E(\theta_x - \bar\theta_x, \omega - \bar\omega) \le E_*$ for all time.*

(b) The solution $(\theta, \omega, c_l, c_\omega)$ converges to a steady state of (2.1) $(\theta_\infty, \omega_\infty, c_{l,\infty}, c_{\omega,\infty})$

$$\begin{aligned} &||(\theta_x(t) - \theta_{\infty,x})\psi^{1/2}||_2 + ||(\omega(t) - \omega_\infty)\varphi^{1/2}||_2 + ||c_l(t) - c_{l,\infty}||_2 \\ &+||c_\omega(t) - c_{\omega,\infty}||_2 \le Ce^{-\kappa_2 t} \end{aligned}$$

exponentially fast, for some $\kappa_2 > 0, C > 0$. Moreover, $(\theta_\infty, \omega_\infty, c_{l,\infty}, c_{\omega,\infty})$ enjoys the regularity $E(\theta_{x,\infty} - \bar\theta_x, \omega_\infty - \bar\omega) \le E_*$, and is the unique steady state in the class

$E(\theta_x - \bar{\theta}_x, \omega - \bar{\omega}) \le E_*$ *with normalization conditions* (2.3)*and* $\theta(0) = 0$*, and odd assumption on* θ_x, ω.

(c) Let $\gamma = \frac{c_{\theta,\infty}}{c_{l,\infty}} = \frac{c_{l,\infty}+2c_{\omega,\infty}}{c_{l,\infty}}$. *We have* $|\frac{c_{\omega,\infty}}{c_{l,\infty}} - 2.99870| \le 6 \cdot 10^{-5}$. *Moreover, the solution enjoys the Hölder estimates* $\theta_\infty \in C^\gamma$ *and* $\sup_{t\ge 0} ||\theta||_{C^\gamma} \lesssim 1$.

(d) For the physical equations (1.2) *with the above initial data, the solution blows up in finite time* T *with the following blowup estimates for any* $\gamma < \beta \le 1$

$$||\theta_{phy}(t)||_{C^\beta} \gtrsim (T-t)^{-\delta}, \quad \delta = \frac{2(\beta-\gamma)}{1-\gamma} > 0.$$

If in addition $\theta_{0,x}|x|^{1-\gamma} \in L^\infty$, *the* C^γ *norm is uniformly bounded up to the blowup time:* $\sup_{t\in[0,T)} ||\theta_{phy}(t)||_{C^\gamma} \lesssim 1$.

The assumption $\theta_{0,x}|x|^{1-\gamma} \in L^\infty$ in (d) is to ensure the decay $|\theta_{0,x}| \le C|x|^{\gamma-1}$, which is consistent with $\theta_0 \in C^\gamma$. In fact, if $\theta_0 \in C^\gamma$, we get $|\theta_0(x)| \lesssim 1 + |x|^\gamma$. Then, formally, $\theta_{0,x}$ has a decay rate $|x|^{\gamma-1}$.

2.3 Main ingredients in our stability analysis

The key step to prove Theorem 2 is the stability analysis. We will outline several important ingredients to establish it in this subsection

2.3.1 The stability of the linearized operator

The most essential part of our analysis is the linear stability of the linearized operator around the approximate steady state $(\bar{\theta}, \bar{\omega}, \bar{c}_l, \bar{c}_\omega)$. To simplify our notation, we still use ω, u, θ, c_l, and c_ω to denote the perturbation. The linearized system for the perturbation is given below by neglecting the nonlinear and error terms:

$$\begin{aligned} \partial_t\theta_x + (\bar{c}_l x + \bar{u})\theta_{xx} &= (2\bar{c}_\omega - \bar{u}_x)\theta_x + (2c_\omega - u_x)\bar{\theta}_x - u\bar{\theta}_{xx}, \\ \omega_t + (\bar{c}_l x + \bar{u})\omega_x &= \bar{c}_\omega\omega + \theta_x + c_\omega\bar{\omega} - u\bar{\omega}_x, \quad c_\omega = u_x(t,0), \quad c_l = 0. \end{aligned} \tag{2.7}$$

The condition $c_\omega = u_x(t,0)$, $c_l = 0$ is a consequence of the normalization conditions (2.4). There are two groups of terms in the above system, one representing the local terms and the other representing the nonlocal terms. Among the nonlocal terms, we can further group them into three subgroups, one from the vortex stretching term, one from the advection term, and the remaining from the rescaling factor c_ω.

As in our previous works [7, 11], we design some singular weights to extract the damping effect from the local terms. As we mentioned before, we will use $\bar{c}_l x + \bar{u} \ge 0.49x$ to extract an $O(1)$ damping effect. Since the damping coefficient that we can extract from the local terms is relatively small and the linearized operator is not a normal operator, we typically expect to have a transient growth for a standard energy norm of the solution to (2.7). This will present considerable difficulty for us to obtain nonlinear stability since the approximate steady state also introduces a residual error. To overcome this difficulty, we need to design a weighted energy norm carefully so

that the energy of the solution to the linearized equations decreases monotonically in time. We remark that weighted energy estimates with singular weights have also been used in [5, 6, 24, 43] for nonlinear stability analysis.

2.3.2 Control of nonlocal terms

The most challenging part of the linear stability analysis is how to control several nonlocal terms that are of $O(1)$. It is essential to obtain sharp estimates of these nonlocal terms by applying sharp weighted functional inequalities, e.g. Lemma A.8, and taking into account the cancellation among different nonlocal terms and the structure of the coupled system. We have also used the L^2 isometry property and several other properties of the Hilbert transform in an essential way. We remark that some of these properties of the Hilbert transform have been used in the previous works, see, e.g. [2, 6, 11, 18, 28]. Based on our observation that the blowup is driven by vortex stretching and the advection is relatively weak compared with vortex stretching, we will treat the nonlocal terms that are generated by the advection terms, e.g. $u\bar{\theta}_{xx}$ in (2.7), as perturbation to the linearized vortex stretching terms, e.g. $u_x\bar{\theta}_x$ in (2.7). We will use the following five strategies in our analysis.

(1) The decomposition of the velocity field. We first denote $\tilde{u} \triangleq u - u_x(0)x$ and choose a constant $c = 1/(2p-1)$ where p is related to the order of the singular weight $|x|^{-p}$ being used. We further decompose $\tilde{u}$ into a main term and a remainder term as follows:

$$\tilde{u} = cx\tilde{u}_x + (\tilde{u} - cx\tilde{u}_x) \triangleq \tilde{u}_M + \tilde{u}_R, \tag{2.8}$$

where $\tilde{u}_M = cx\tilde{u}_x$ and $\tilde{u}_R = (\tilde{u} - cx\tilde{u}_x)$. The contribution from the remainder term $\tilde{u}_R$ is smaller than $x\tilde{u}_x$ due to an identity (see Appendix B.1)

$$||(\tilde{u} - \frac{1}{2p-1}\tilde{u}_x x)x^{-p}||_2^2 = \frac{1}{(2p-1)^2}\int_{\mathbb{R}_+} \frac{\tilde{u}_x^2}{x^{2p-2}}dx. \tag{2.9}$$

We can choose $p = 3$ in the near field, which enables us to gain a small factor of $1/5$ in estimating the $\tilde{u}_R$ term in terms of the weighted norm of $\tilde{u}_x$.

(2) Exploiting the nonlocal cancellation between $\tilde{u}_x$ and ω. For the main term $\tilde{u}_M = cx\tilde{u}_x$ and the vortex stretching term $-u_x\bar{\theta}_x$, we use an orthogonality between $\tilde{u}_x$ and ω

$$\langle \tilde{u}_x, \omega x^{-3}\rangle = \langle H\omega - H\omega(0), \omega x^{-3}\rangle \ = \ 0 \tag{2.10}$$

(see Lemma A.4). We will use similar orthogonal properties to exploit the cancellation between $-\tilde{u}_x\bar{\theta}_x$ in the θ_x equation and θ_x in the ω equation in (2.7) by performing the weighted L^2 estimates for θ_x and ω together. To illustrate this idea, we consider the following model:

Model 1 for nonlocal interaction

$$\partial_t\theta_x = -(u_x - u_x(0))\bar{\theta}_x, \quad \omega_t = \theta_x. \tag{2.11}$$

The above system is derived by dropping other terms in (2.7). The profile $\bar{\theta}_x$ satisfies $\bar{\theta}_x(0) = 0$ and $\bar{\theta}_x > 0$ for $x > 0$.

By performing $L^2(\rho_1)$ estimate on θ_x and $L^2(\rho_2)$ estimate on ω, we get

$$\frac{1}{2}\frac{d}{dt}(\langle\theta_x, \theta_x\rho_1\rangle + \langle\omega, \omega\rho_2\rangle) = -\langle(u_x - u_x(0))\bar{\theta}_x\rho_1, \theta_x\rangle + \langle\omega\rho_2, \theta_x\rangle \triangleq I \tag{2.12}$$

From (2.10), we know that $(u_x - u_x(0))x^{-2}$ and ωx^{-1} are orthogonal. Formally, I is the sum of the projections of θ_x onto two directions that are orthogonal. To exploit this orthogonality, we choose $\rho_1 = (\mu x\bar{\theta}_x)^{-1}\rho_2$ with any $\mu > 0$. We can rewrite I as follows

$$I = \langle -(u_x - u_x(0))x^{-2}, \theta_x\bar{\theta}_x\rho_1 x^2\rangle + \langle\mu\omega x^{-1}, \theta_x\bar{\theta}_x\rho_1 x^2\rangle \triangleq \langle A + B, \theta_x\bar{\theta}_x\rho_1 x^2\rangle,$$

where $A = -(u_x - u_x(0))x^{-2}$ and $B = \mu\omega x^{-1}$. Applying the Cauchy-Schwarz inequality yields

$$I \le ||A + B||_2||\theta_x\bar{\theta}_x\rho_1 x^2||_2.$$

The equality can be achieved if $\theta_x\bar{\theta}_x\rho_1 x^2 = c(A + B)$ for some c. Expanding $||A + B||_2$ and using Lemma A.4 with $f = \omega$ and $g = u$, we get

$$||A + B||_2^2 = ||A||_2^2 + ||B||_2^2 + 2\langle A, B\rangle = ||A||_2^2 + ||B||_2^2, \tag{2.13}$$

which is sharper than the trivial estimate $||A + B||_2 \le ||A||_2 + ||B||_2$. The $||A||_2^2$ term can be further bounded by $||\omega x^{-1}||_2^2$ using the L^2 isometry of the Hilbert transform in Lemma A.2. The $||B||_2^2$ term can be bounded by the weighted L^2 norm of ω directly.

(3) Additional damping effect from c_ω. Another nonlocal term in (2.7) is $c_\omega = u_x(t, 0) = H(\omega)(t, 0)$. Physically, the role of c_ω is to rescale the amplitude of the blowup profile ω in the original physical variable so that the magnitude of the dynamic rescaled profile remains $O(1)$ for all time. Thus, we expect that the dynamic rescaling parameter c_ω should also offer some stabilizing effect to the blowup profile and the linearized system (2.7). Indeed, by deriving an ODE for c_ω, we can extract an additional damping term, which will be used to control other nonlocal terms associated with c_ω. To illustrate this idea, we consider the following model:

Model 2 for the c_ω term

$$\partial_t\theta_x = c_\omega\bar{f}, \quad \partial_t\omega = \theta_x + c_\omega\bar{g}, \tag{2.14}$$

where $\bar{f}, \bar{g}$ are odd and $\bar{f}, \bar{g} > 0$ for $x > 0$ with $\bar{f}x^{-1}, \bar{g}x^{-1} \in L^1$. Note that the profile satisfies that $\bar{\theta}_x - x\bar{\theta}_{xx}, \bar{\omega} - x\bar{\omega}_x$ are odd and positive for $x > 0$. This system models the c_ω terms in (2.7) with coupling θ_x in ω equation by dropping other terms. Recall

$$c_\omega = -\frac{1}{\pi}\int_{\mathbb{R}}\frac{\omega}{x}dx = -\frac{2}{\pi}\langle\omega, x^{-1}\rangle.$$

Obviously, it can be bounded by some weighted L^2 norm of ω using the Cauchy-Schwarz inequality. Yet, the constant in this estimate is large. Denote $A = \langle \bar{f}, x^{-1}\rangle$, $B = \langle \bar{g}, x^{-1}\rangle$. By definition, $A, B > 0$. We derive an ODE for c_ω using the ω equation

$$\partial_t \langle \omega, x^{-1}\rangle = c_\omega \langle \bar{g}, x^{-1}\rangle + \langle \theta_x, x^{-1}\rangle = -\frac{2}{\pi} B\langle \omega, x^{-1}\rangle + \langle \theta_x, x^{-1}\rangle.$$

We see that the c_ω term in the ω equation in (2.14) has a damping effect, which is not captured by the weighted L^2 estimates. To handle the coupled term, we also derive an ODE for $\langle \theta_x, x^{-1}\rangle$ using the θ_x equation

$$\partial_t \langle \theta_x, x^{-1}\rangle = c_\omega \langle \bar{f}, x^{-1}\rangle = -\frac{2}{\pi} A\langle \omega, x^{-1}\rangle.$$

Multiplying both sides of these ODEs by $\langle \omega, x^{-1}\rangle$ or $\langle \theta_x, x^{-1}\rangle$, we yield

$$\begin{aligned} &\frac{1}{2}\frac{d}{dt}\langle \omega, x^{-1}\rangle^2 = -\frac{2}{\pi} B\langle \omega, x^{-1}\rangle^2 + \langle \theta_x, x^{-1}\rangle\langle \omega, x^{-1}\rangle, \\ &\frac{1}{2}\partial_t \langle \theta_x, x^{-1}\rangle^2 = -\frac{2}{\pi} A\langle \theta_x, x^{-1}\rangle\langle \omega, x^{-1}\rangle. \end{aligned} \tag{2.15}$$

The $\langle \theta_x, x^{-1}\rangle\langle \omega, x^{-1}\rangle$ terms in the above ODEs have cancellation. This implies that the c_ω term in the θ_x equation and θ_x term in the ω equation have cancellation, which is not captured by the weighted L^2 estimate. We will derive similar ODEs in the analysis of (2.7) and obtain damping term similar to $-\frac{2}{\pi} B\langle \omega, x^{-1}\rangle^2$ in the above ODEs, which enables us to control the c_ω terms in (2.7) effectively.

(4) Estimating the u term in (2.7). To estimate the u terms in (2.7) effectively, we have two approaches. The first approach is to exploit the cancellation between u and ω similar to that in Model 1. See Lemma A.4. The second approach is to decompose $\tilde{u}$ into the main term $\tilde{u}_M = cx\tilde{u}_x$ and an error term $\tilde{u}_R$ as (3.17). For $\tilde{u}_M$, we employ the estimates on u_x discussed previously. The error term $\tilde{u}_R$ enjoys better estimate (2.9) and is treated as a perturbation.

(5) Obtaining sharp estimates for other interaction terms. To obtain sharper estimates for a number of quadratic interaction terms, we introduce a number of parameters in various intermediate steps and optimize these parameters later by solving a constrained optimization problem. In the ODE for c_ω and the weighted L^2 estimates, we need to control a number of quadratic interaction terms, e.g. $\langle \omega, x^{-1}\rangle \cdot \langle \theta_x, x^{-1}\rangle$. We treat these interaction terms as the products of projection of θ_x and ω onto some low dimensional subspaces and reduce them to some quadratic forms in a finite dimensional space. This connection enables us to reduce the problem of obtaining sharp estimates of these terms to computing the largest eigenvalue $\lambda_{\max}$ of a matrix. We then compute $\lambda_{\max}$ as part of the constrained optimization problem to determine these parameters and obtain a sharper upper bound in the energy estimate.

3 Linear stability

In this section, we establish the linear stability of (3.6) in some weighted L^2 spaces.

3.1 Linearized operators around approximate steady state

The approximate steady state of (2.2) $(\bar{\theta}_x, \bar{\omega})$ we construct are odd with scaling factors

$$\bar{c}_l = 3, \quad |\bar{c}_\omega + 1.00043212| < 10^{-8}, \quad \bar{c}_\omega \approx -1.$$

It has regularity $\bar{\omega}, \bar{\theta}_x \in C^3$ and decay rates $\partial_x^i \bar{\omega} \sim x^{\alpha - i}$, $\partial_x^i \bar{\theta}_x \sim x^{2\alpha - i}$, $i = 0, 1, 2$ with α slightly smaller than $-1/3$. One can find plots of $(\bar{\omega}, \bar{\theta}_x)$ (with particular rescaling) in Figure 2 in Section 5.5. See detailed discussion in Section 4. Note that we do not require a C^∞ approximate steady state in our analysis, since the C^3 approximate steady state is regular enough for us to perform weighted H^1 estimates and establish its nonlinear stability.

Linearizing around the approximate steady state $(\bar{\theta}_x, \bar{\omega})$, we obtain the equations for the perturbation

$$\begin{aligned} \partial_t \theta_x + (\bar{c}_l x + \bar{u})\theta_{xx} &= (2\bar{c}_\omega - \bar{u}_x)\theta_x + (2c_\omega - u_x)\bar{\theta}_x - u\bar{\theta}_{xx} + F_\theta + N(\theta), \\ \omega_t + (\bar{c}_l x + \bar{u})\omega_x &= \bar{c}_\omega \omega + \theta_x + c_\omega \bar{\omega} - u\bar{\omega}_x + F_\omega + N(\omega), \end{aligned} \tag{3.1}$$

where the error terms F_θ, F_ω and the nonlinear terms $N(\theta)$, $N(\omega)$ read

$$\begin{aligned} F_\theta &= (2\bar{c}_\omega - \bar{u}_x)\bar{\theta}_x - (\bar{c}_l x + \bar{u}) \cdot \bar{\theta}_{xx}, \quad F_\omega = \bar{\theta}_x + \bar{c_\omega}\bar{\omega} - (\bar{c}_l x + \bar{u}) \cdot \bar{\omega}_x, \\ N(\theta) &= (2c_\omega - u_x)\theta_x - u\theta_{xx}, \quad N(\omega) = c_\omega \omega - u\omega_x. \end{aligned} \tag{3.2}$$

We consider odd initial perturbation $\omega_0, \theta_{0,x}$ with $\omega_{0,x}(0) = 0, \theta_{0,xx}(0) = 0$. Note that the normalization conditions (2.3),(2.4) implies

$$c_\omega = u_x(0), \quad c_l = 0, \quad \theta_{xx}(t, 0) = \theta_{0,xx}(0) = 0, \quad \omega_x(t, 0) = \omega_{0x}(0) = 0, \tag{3.3}$$

for the perturbation. Since ω, θ_x are odd, these normalization conditions imply that near $x = 0$, $\omega = O(x^3)$, $\theta_x = O(x^3)$ for sufficient smooth solution. This important property enables us to use a more singular weight in our stability analysis to extract a larger damping coefficient.

We rewrite the c_ω and u terms as follows

$$\begin{aligned} (2c_\omega - u_x)\bar{\theta}_x - u\bar{\theta}_{xx} &= -(u_x - u_x(0))\bar{\theta}_x - (u - u_x(0)x)\bar{\theta}_{xx} + c_\omega(\bar{\theta}_x - x\bar{\theta}_{xx}), \\ c_\omega \bar{\omega} - u\bar{\omega}_x &= -(u - u_x(0)x)\bar{\omega}_x + c_\omega(\bar{\omega} - x\bar{\omega}_x) \end{aligned} \tag{3.4}$$

Denote $\Lambda = (-\Delta)^{1/2}$. From $\partial_x u = H\omega$ and $\Lambda = \partial_x H$, we have $u(x) = -\Lambda^{-1}\omega(x) = \frac{1}{\pi}\int \log|x - y|\omega(y)dy$. Using this notation, we get $u - u_x(0)x =$

$-\Lambda^{-1}\omega - H\omega(0)x$. We introduce the following linearized operators

$$\begin{aligned}
\mathcal{L}_{\theta 1}(f,g) &= -(\bar{c}_l x+\bar{u})f_x + (2\bar{c}_\omega - \bar{u}_x)f - (Hg - Hg(0))\bar{\theta}_x \\
&\quad - (-\Lambda^{-1}g - Hg(0)x)\bar{\theta}_{xx}, \\
\mathcal{L}_{\omega 1}(f,g) &= -(\bar{c}_l x+\bar{u})g_x + \bar{c}_\omega g + f - (-\Lambda^{-1}g - Hg(0)x)\bar{\omega}_x, \\
\mathcal{L}_{\theta}(f,g) &= \mathcal{L}_{\theta 1}(f,g) + Hg(0)(\bar{\theta}_x - x\bar{\theta}_{xx}), \\
\mathcal{L}_{\omega}(f,g) &= \mathcal{L}_{\omega 1}(f,g) + Hg(0)(\bar{\omega} - x\bar{\omega}_x).
\end{aligned} \tag{3.5}$$

Using these operators, we can rewrite (3.1) as follows

$$\begin{aligned}
\partial_t\theta_x &= \mathcal{L}_{\theta 1}(\theta_x,\omega) + c_\omega(\bar{\theta}_x - x\bar{\theta}_{xx}) + F_\theta + N(\theta), \\
\partial_t\omega &= \mathcal{L}_{\omega 1}(\theta_x,\omega) + c_\omega(\bar{\omega} - x\bar{\omega}_x) + F_\omega + N(\omega).
\end{aligned} \tag{3.6}$$

Clearly, $\mathcal{L}_\theta, \mathcal{L}_\omega$ are the linearized operators associated to (3.1). The motivation of introducing $\mathcal{L}_{\theta 1}, \mathcal{L}_{\omega 1}$ is that the estimates of these operators will be used importantly in both the weighted L^2 and weighted H^1 estimates.

3.2 Singular weights

For some $e_1, e_2, e_3 > 0$ determined by the profile $(\bar{\omega}, \bar{\theta})$, we introduce

$$\begin{aligned}
&\xi_1 = e_1 x^{-2/3} - (\bar{\theta}_x + \frac{1}{5}x\bar{\theta}_{xx}), \quad \xi_2 = e_2 x^{-2/3} - (\bar{\theta}_x + \frac{3}{7}x\bar{\theta}_{xx}), \\
&\xi_3 = -\frac{e_3}{3}x^{-4/3} - \bar{\omega}_x.
\end{aligned} \tag{3.7}$$

Following the guideline of the construction of the singular weight in [11], we design different parts of the singular weight that have different decays as follows

$$\begin{aligned}
&\psi_n = \frac{1}{\bar{\theta}_x + \frac{1}{5}x\bar{\theta}_{xx} + \chi\xi_1}(\alpha_1 x^{-4} + \alpha_2 x^{-3}), \quad \psi_f = \frac{1}{\bar{\theta}_x + \frac{3}{7}x\bar{\theta}_{xx} + \chi\xi_2}\alpha_3 x^{-4/3}, \\
&\varphi_s = \alpha_4 x^{-4}, \quad \varphi_n = \alpha_5(\alpha_1 x^{-3} + \alpha_2 x^{-2}), \quad \varphi_f = \alpha_6 x^{-2/3},
\end{aligned} \tag{3.8}$$

where the parameters are positive and chosen in (C.2), and the cutoff function χ defined in Appendix B.2 is supported in $|x| \geq \rho_2$ for $\rho_2 > 10^8$. The subscripts f, n, s are short for *far, near, singular*. We use the following weights in the weighted Sobolev estimate

$$\psi = \psi_n + \psi_f, \quad \varphi = \varphi_s + \varphi_n + \varphi_f. \tag{3.9}$$

We introduce χ, ξ_1, ξ_2 and add them in the definition of ψ_n, ψ_f for the following purposes. Firstly, recall from the beginning of Section 3.1 that $\bar{\theta}_x + cx\bar{\theta}_{xx}$ with $c = \frac{1}{5}$ or $c = \frac{3}{7}$ has decay $x^{2\alpha}$ which is close to $x^{-2/3}$. In particular, for sufficient large x, it can be well approximated by $ex^{-2/3}$ for some constant e. The parameters e_1, e_2 in (3.7)

are determined in this way. Secondly, in the far field, where $\chi(x) = 1$, the weights ψ_n, ψ_f reduce to $c_1 x^{-7/3}$, $c_2 x^{-2/3}$ for some c_1, c_2, respectively. These explicit powers are much simpler than the weights in the near field and have forms similar to those in φ. They will be useful for the analytic estimates (see Section 3.6) and simplify the computer-assisted verification of the estimates in the far field. We introduce ξ_3 similar to ξ_1, ξ_2 and it will be used later.

Remark 3.1 Since χ is supported in $|x| > 10^8$ and the profile $(\bar{\omega}, \bar{\theta}_x)$ decays for large $|x|$, we gain a small factor in the estimates of the terms involving χ. Thus, the upper bound in these estimates are very small. The reader can safely skip the technicalities due to the χ terms.

3.2.1 The form of the singular weights

We add $\bar{\theta}_x, \bar{\theta}_{xx}$ terms in the denominators in ψ_n, ψ_f to cancel the variable coefficients in our energy estimates. In Model 1 in Section 2.3.2, we have chosen $\rho_1 = (\mu x \bar{\theta}_x)^{-1} \rho_2$ so that we can combine the estimates of two interactions in (2.12). Here, we design ψ_n, φ_n with a similar relation $\psi_n = \frac{1}{f} x^{-1} \varphi_n$, $f = \bar{\theta}_x + \frac{1}{5} x \bar{\theta}_{xx} + \chi \xi_1$ for the same purpose. Similar consideration applies to ψ_f, φ_f. See also estimates (3.18), (3.23). This idea has been used in [7, 11] for stability analysis.

The profile satisfies $\bar{\theta}_x + \frac{1}{5} x \bar{\theta}_{xx}, \bar{\theta}_x + \frac{3}{7} x \bar{\theta}_{xx} > 0$ for $x > 0$. The weight ψ is of order x^{-5} for x close to 0, while it is of order $x^{-2/3}$ for large x. We choose φ of order x^{-4} near 0 so that we can apply the sharp weighted estimates in Lemma A.8 to control u_x and u.

We will use the following notations repeatedly

$$\tilde{u} \triangleq u - u_x(0)x, \quad \tilde{u}_x = u_x - u_x(0). \tag{3.10}$$

3.3 Weighted L^2 estimates

Performing weighted L^2 estimates on (3.6) with weights ψ, φ, we obtain

$$\begin{aligned}
\frac{1}{2}\frac{d}{dt}\langle \theta_x, \theta_x \psi \rangle &= \langle \mathcal{L}_{\theta 1} \theta_x, \theta_x \psi \rangle + c_\omega \langle \bar{\theta}_x - x \bar{\theta}_{xx}, \theta_x \psi \rangle + \langle N(\theta), \theta_x \psi \rangle + \langle F_\theta, \theta_x \psi \rangle \\
&= \Big(- \langle (\bar{c}_l x + \bar{u}) \theta_{xx}, \theta_x \psi \rangle + \langle (2\bar{c}_\omega - \bar{u}_x) \theta_x, \theta_x \psi \rangle \Big) \\
&\quad + \Big(- \langle (u_x - u_x(0)) \bar{\theta}_x + (u - u_x(0)x) \bar{\theta}_{xx}, \theta_x \psi \rangle + c_\omega \langle \bar{\theta}_x - x \bar{\theta}_{xx}, \theta_x \psi \rangle \Big) \\
&\quad + \langle N(\theta), \theta_x \psi \rangle + \langle F_\theta, \theta_x \psi \rangle \triangleq D_1 + Q_1 + N_1 + F_1, \\
\frac{1}{2}\frac{d}{dt}\langle \omega, \omega \varphi \rangle &= \langle \mathcal{L}_{\omega 1} \omega, \omega \varphi \rangle + c_\omega \langle \bar{\omega}_x - x \bar{\omega}_{xx}, \omega_x \varphi \rangle + \langle N(\omega), \omega \varphi \rangle + \langle F_\omega, \omega \varphi \rangle \\
&= \Big(- \langle (\bar{c}_l x + \bar{u}) \omega_x, \omega \varphi \rangle + \langle \bar{c}_\omega \omega, \omega \varphi \rangle \Big) + \Big(\langle \theta_x, \omega \varphi \rangle - \langle (u - u_x(0)x) \bar{\omega}_x, \omega \varphi \rangle \\
&\quad + c_\omega \langle \bar{\omega} - x \bar{\omega}_x, \omega \varphi \rangle \Big) + \langle N(\omega), \omega \varphi \rangle + \langle F_\omega, \omega \varphi \rangle \triangleq D_2 + Q_2 + N_2 + F_2.
\end{aligned} \tag{3.11}$$

Our goal in the remaining part of this Section is to establish an estimate similar to

$$D_1 + \lambda_1 D_2 + Q_1 + \lambda_1 Q_2 \le -c(||\theta_x \psi^{1/2}||_2^2 + \lambda_1 ||\omega\varphi^{1/2}||_2^2), \tag{3.12}$$

for some $\lambda_1 > 0$ with $c > 0$ as large as possible. This implies the linear stability of (3.6) with $N_i, F_i = 0$ in the energy norm $||\theta_x \psi^{1/2}||_2^2 + \lambda_1 ||\omega\varphi^{1/2}||_2^2$. The actual estimate is slightly more complicated and we will add $c_\omega^2, \langle \theta_x, x^{-1}\rangle^2$ to the energy. We ignore the term c_ω and $\langle \theta_x, x^{-1}\rangle^2$ for now to illustrate the main ideas. See (3.57).

The D_1, D_2 terms only involve the local terms about θ_x, ω and we treat them as damping terms. The Q_i term denotes the quadratic terms other than D_i in the weighted L^2 estimates; The N_i and F_i terms represent the nonlinear terms and error terms in (3.6).

For D_1, D_2, performing integration by parts on the transport term, we obtain

$$D_1 = \langle D_\theta, \theta_x^2 \psi\rangle, \quad D_2 = \langle D_\omega, \omega^2 \varphi\rangle, \tag{3.13}$$

where D_θ, D_ω are given by

$$D_\theta = \frac{1}{2\psi}((\bar{c}_l x + \bar{u})\psi)_x + 2\bar{c}_\omega - \bar{u}_x, \quad D_\omega = \frac{1}{2\varphi}((\bar{c}_l x + \bar{u})\varphi)_x + \bar{c}_\omega.$$

We will verify that $D_\theta, D_\omega \le -c < 0$ for some constant $c > 0$ in (D.4), Appendix D. The weight ψ in (3.9) involves three parameters $\alpha_1, \alpha_2, \alpha_3$. We choose the approximate values of α_i with $\alpha_i > 0$ so that $D_\theta \le -c$ with c as large as possible and varies slowly. This enables us to obtain a large damping coefficient. After we choose $\alpha_1, \alpha_2, \alpha_3$, we choose positive α_4, α_5 and α_6 in the weight φ in (3.9) so that $D_\omega \le -c_1$ with c_1 as large as possible and varies slowly. The final values are given in (C.2). See also Figure 1 for plots of the grid point values of D_θ, D_ω.

Using the notations in (3.10), we can rewrite $Q_1 + \lambda_1 Q_2$ as follows

$$\begin{aligned} Q_1 + \lambda_1 Q_2 = &-\langle \tilde{u}_x \bar{\theta}_x + \tilde{u}\bar{\theta}_{xx}, \theta_x \psi\rangle + \lambda_1 \langle \omega, \theta_x \varphi\rangle - \lambda_1 \langle \tilde{u}\bar{\omega}_x, \omega\varphi\rangle \\ &+ c_\omega \langle (\bar{\theta}_x - x\bar{\theta}_{xx}), \theta_x \psi\rangle + \lambda_1 c_\omega \langle (\bar{\omega} - x\bar{\omega}_x), \omega\varphi\rangle. \end{aligned} \tag{3.14}$$

The terms in $Q_1 + \lambda_1 Q_2$ are the interactions among u, ω, θ_x and do not have a favorable sign. Our goal is to prove that they are perturbation to the damping terms D_1, D_2 and establish (3.12). This is challenging since the coefficients of the quadratic terms in $Q_1 + \lambda_1 Q_2$ and in D_i are comparable.

3.3.1 Decompositions on Q_i

Recall different parts of the weights in (3.8). They provide a natural decomposition of the global interaction among u, ω, θ_x into the near field and the far field interaction. We have a straightforward partition of unity

$$\psi_n \psi^{-1} + \psi_f \psi^{-1} = 1, \quad \varphi_n \varphi^{-1} + \varphi_f \varphi^{-1} + \varphi_s \varphi^{-1} = 1. \tag{3.15}$$

According to different singular orders and decay rates of the weights in (3.8), $\psi_f\psi^{-1}$, $\varphi_f\varphi^{-1}$ are mainly supported in the far field, $\psi_n\varphi^{-1}$ in the near field, $\varphi_n\varphi^{-1}$ near $|x| \approx 1$, and $\varphi_s\varphi^{-1}$ near 0. Next, we decompose the interaction using these weights. Using $\psi = \psi_f + \psi_n$, we get

$$\begin{aligned}
&-\langle \tilde{u}_x\bar{\theta}_x, \theta_x\psi\rangle = -\langle \tilde{u}_x(\bar{\theta}_x + \chi\xi_1), \theta_x\psi_n\rangle\\
&-\langle \tilde{u}_x(\bar{\theta}_x + \chi\xi_2), \theta_x\psi_f\rangle + \langle \tilde{u}_x\chi(\xi_1\psi_n + \xi_2\psi_f), \theta_x\rangle.
\end{aligned}$$

We decompose the first two terms on the right hand side of (3.14) as follows

$$\begin{aligned}
&-\langle \tilde{u}_x\bar{\theta}_x + \tilde{u}\bar{\theta}_{xx}, \theta_x\psi\rangle + \lambda_1\langle\omega, \theta_x\varphi\rangle\\
&= \Big(-\langle \tilde{u}_x(\bar{\theta}_x + \chi\xi_2) + \tilde{u}\bar{\theta}_{xx}, \theta_x\psi_f\rangle + \lambda_1\langle\theta_x, \omega\varphi_f\rangle\Big)\\
&\quad + \Big(-\langle \tilde{u}_x(\bar{\theta}_x + \chi\xi_2) + \tilde{u}\bar{\theta}_{xx}, \theta_x\psi_n\rangle + \lambda_1\langle\theta_x, \omega\varphi_n\rangle\Big) + \lambda_1\langle\theta_x, \omega\varphi_s\rangle\\
&\quad + \langle \tilde{u}_x\chi(\xi_1\psi_n + \xi_2\psi_f), \theta_x\rangle \triangleq I_f + I_n + I_s + I_{r1}.
\end{aligned} \tag{3.16}$$

The subscripts f, n, s, r are short for *far, near, singular, remainder*. Denote $I_{u\omega} = -\lambda_1\langle\tilde{u}\bar{\omega}_x, \omega\varphi\rangle$ in (3.14). The main terms in (3.14) are I_f, I_n and I_s. From the above discussion on (3.15), the interactions in I_n, I_f, I_s are mainly supported in different regions. Since u depends on ω linearly, $I_{u\omega}$ can be seen as the interaction between ω and itself. This type of interaction is different from I_n, I_f, I_s. Since $c_\omega = u_x(0) = -\frac{1}{\pi}\int_{\mathbb{R}}\omega dx$, the terms $c_\omega\langle(\bar{\theta}_x - x\bar{\theta}_{xx}), \theta_x\psi\rangle$, $\lambda_1 c_\omega\langle(\bar{\omega} - x\bar{\omega}_x), \omega\varphi\rangle$ in (3.14) are the projections of ω, θ_x onto some rank-1 space. The estimate of the c_ω terms is smaller than that of I_n, I_f, I_s, $I_{u\omega}$. The term I_{r1} is very small compared to other terms and will be estimated directly.

We will exploit the structure of the interactions in (3.14) using the above important decompositions.

3.4 Outline of the estimates

In order to establish the weighted L^2 estimates similar to (3.12), we first develop sharp estimates on each term in the above decomposition. In these estimates, we introduce several parameters, when we apply the Cauchy-Schwarz or Young's inequality. These parameters are important in our estimates. Since the coefficients in the damping term D_1, D_2 (3.13) are relative small, we can treat the interaction term as perturbation to the damping term using the energy estimates, only for certain range of parameters. See more discussion in Remark 3.3. Thus, the upper bound in these estimates depend on several parameters. Then, using these estimates, we reduce the estimate similar to (3.12) to some inequality constraints on the parameters with explicit coefficients. See (3.40) for an example. Finally, to obtain an overall sharp energy estimate, e.g. (3.12) with $c > 0$ as large as possible, we determine these parameters guided by solving a constrained optimization problem.

In our energy estimates, to obtain the sharp weighted estimates of xu_x, u with singular weight x^{-2p} by applying Lemma A.8, we can only use a few exponents

$p = 3, 2, \frac{5}{3}$. Thus, we need to perform the energy estimates very carefully. The linear combinations of different powers in Lemma A.8, e.g. $\alpha x^{-4}+\beta x^{-2}$, plays a role similar to that of interpolating different singular weights, e.g. x^{-4}, x^{-2}. It enables us to obtain sharp weighted estimates with singular weight x^{-2q} and intermediate exponent q. In our weighted estimates of u_x, u, we choose some weights with a few parameters, see e.g. (3.33). Moreover, to generalize the cancellations and estimates in the Model 1 in Section 2.3.2 to the more complicated linearized system (2.7), we also need to perform the energy estimates carefully so that we can apply the cancellation in Lemma A.4.

3.5 Estimates of the interaction in the near field I_n

We use ideas in Model 1 in Section 2.3.2 to estimate the main term introduced below and ideas in Section 2.3.2 to estimate u.

Firstly, we choose $c = \frac{1}{5}$ in the decomposition 2.8 $\tilde{u} = \frac{1}{5}x\tilde{u}_x + \tilde{u} - \frac{1}{5}x\tilde{u}_x$, and decompose $\tilde{u}_x(\bar{\theta}_x+\chi\xi_1)+\tilde{u}\bar{\theta}_{xx}$ into the main term $\mathcal{M}$ and the remainder $\mathcal{R}$ as follows

$$\tilde{u}_x(\bar{\theta}_x + \chi\xi_1) + \tilde{u}\bar{\theta}_{xx} = \tilde{u}_x(\bar{\theta}_x + \frac{1}{5}\bar{\theta}_{xx}x + \chi\xi_1) + (\tilde{u} - \frac{1}{5}\tilde{u}_x x)\bar{\theta}_{xx} \triangleq \mathcal{M} + \mathcal{R}. \tag{3.17}$$

This term also appears in I_f and we will use another decomposition in Section 3.6. Recall I_n in (3.16). Using the above decomposition, we yield

$$\begin{aligned} I_n &= -\langle \tilde{u}_x(\bar{\theta}_x + \chi\xi_1) + \tilde{u}\bar{\theta}_{xx}, \theta_x\psi_n\rangle + \lambda_1\langle\omega, \theta_x\varphi_n\rangle \\ &= \Big(- \langle \mathcal{M}, \theta_x\psi_n\rangle + \lambda_1\langle\omega, \theta_x\varphi_n\rangle\Big) + \langle -\mathcal{R}, \theta_x\psi_n\rangle \triangleq I_{\mathcal{M}} + I_{\mathcal{R}}. \end{aligned}$$

The estimates of $I_{\mathcal{M}}$ are similar to that in Model 1 in Section 2.3.2. Recall the formulas of ψ_n, φ_n in (3.8). Using Young's inequality $ab \le t_2a^2 + \frac{1}{4t_2}b^2$ for $t_2 > 0$, we obtain

$$\begin{aligned} I_{\mathcal{M}} &= -\langle \tilde{u}_x, \theta_x(\alpha_2 x^{-3} + \alpha_1 x^{-4})\rangle + \langle \omega, \theta_x\lambda_1\alpha_5(\alpha_2 x^{-2} + \alpha_1 x^{-3})\\ &= \langle -\tilde{u}_x x^{-2} + \lambda_1\alpha_5\omega x^{-1}, \theta_x(\alpha_2 x^{-1} + \alpha_1 x^{-2})\rangle \\ &\le t_2|| - \tilde{u}_x x^{-2} + \lambda_1\alpha_5\omega x^{-1}||_2^2 + \frac{1}{4t_2}||\theta_x(\alpha_2 x^{-1} + \alpha_1 x^{-2})||_2^2. \end{aligned} \tag{3.18}$$

Remark 3.2 We design the special form ψ_n in (3.8) so that the denominator in ψ_n and the coefficient $\bar{\theta}_x + \frac{1}{5}\bar{\theta}_{xx}x + \chi\xi_1$ in $\mathcal{M}$ cancel each other. This allows us to obtain a desirable term of the form $J \triangleq -\tilde{u}_x x^{-2} + \lambda_1\alpha_5\omega x^{-1}$. The term $t_2||J||_2^2$ in (3.18) is a quadratic form in ω, where we can exploit the cancellation between $\tilde{u}_x$ and ω to obtain a sharp estimate. See Model 1 for the motivation.

Using the weighted estimate in Lemma A.8 and Lemma A.4 with $f = \omega$ and $g = u$, we get

$$\begin{aligned} t_2||-\tilde{u}_x x^{-2}+\lambda_1\alpha_5\omega x^{-1}||_2^2 &= t_2\Big(||\tilde{u}_x x^{-2}||_2^2 - 2\lambda_1\alpha_5\langle\tilde{u}_x,\omega x^{-3}\rangle + (\lambda_1\alpha_5)^2||\omega x^{-1}||_2^2\Big) \\ &= t_2\Big(||\omega x^{-2}||_2^2 + (\lambda_1\alpha_5)^2||\omega x^{-1}||_2^2\Big) = t_2\Big\langle\omega^2, x^{-4} + (\lambda_1\alpha_5)^2 x^{-2}\Big\rangle. \end{aligned} \tag{3.19}$$

The cancellation is exactly the same as (2.13) in Model 1. For $I_{\mathcal{R}}$, using Young's inequality $ab \le t_{22}a^2 + \frac{1}{4t_{22}}b^2$, (2.9) with $p = 3$ and the weighted estimate in Lemma A.8, we obtain

$$\begin{aligned} I_{\mathcal{R}} &= \langle(\tilde{u} - \frac{1}{5}\tilde{u}_x x)\bar{\theta}_{xx}, \theta_x\psi_n\rangle \le t_{22}||(\tilde{u} - \frac{1}{5}\tilde{u}_x x)x^{-3}||_2^2 + \frac{1}{4t_{22}}||x^3\bar{\theta}_{xx}\psi_n\theta_x||_2^2 \\ &= \frac{t_{22}}{25}||\tilde{u}_x x^{-2}||_2^2 + \frac{1}{4t_{22}}||x^3\bar{\theta}_{xx}\psi_n\theta_x||_2^2 = \frac{t_{22}}{25}||\omega x^{-2}||_2^2 + \frac{1}{4t_{22}}||x^3\bar{\theta}_{xx}\psi_n\theta_x||_2^2. \end{aligned} \tag{3.20}$$

The remainder $I_{\mathcal{R}}$ is much smaller than $I_{\mathcal{M}}$ since we get a small factor $\frac{1}{2p-1} = \frac{1}{5}$ from (2.9). Combining the above estimates, we establish the estimate for $I_n = I_{\mathcal{M}} + I_{\mathcal{R}}$

$$\begin{aligned} I_n \le &\Big\langle\omega^2, t_2 x^{-4} + \frac{t_{22}}{25}x^{-4} + t_2(\lambda_1\alpha_5)^2 x^{-2}\Big\rangle \\ &+\Big\langle\theta_x^2, \frac{1}{4t_2}(\alpha_2 x^{-1} + \alpha_1 x^{-2})^2 + \frac{1}{4t_{22}}(x^3\bar{\theta}_{xx}\psi_n)^2\Big\rangle. \end{aligned} \tag{3.21}$$

Remark 3.3 If we neglect other terms in (3.14) except I_n, a necessary condition for (3.12) is

$$I_n + D_1 + \lambda_1 D_2 \le -c(||\theta_x\psi^{1/2}||_2 + \lambda_1||\omega\varphi^{1/2}||_2^2) \tag{3.22}$$

with $c > 0$, where D_1, D_2 are the damping terms in (3.13). We cannot determine the ratio λ_1 between two norms and t_i in Young's inequality without using the profile $(\bar{\theta}, \bar{\omega})$. For example, if we use equal weights $\lambda_1 = 1, t_2 = t_{22} = \frac{1}{2}$, we cannot apply estimate (3.21) to establish (3.22) even with $c = 0$. Therefore, we introduce several parameters, especially when we apply Young's inequality. At this step, we do not fix λ_1, t_{ij} such that the subproblem (3.22) holds with $c > 0$ as large as possible. In fact, such parameters may not be ideal for (3.12) since the final energy estimate involves other terms in (3.12),(3.14) to be estimated later on. Instead, we identify the ranges $\lambda_1 \in [0.31, 0.33], t_2 \in [5, 5.8], t_{22} \in [13, 14]$, such that a weaker version of (3.22) with $c = 0.01$ holds with the estimate (3.21) on I_n. See Appendix D.1 for rigorous verification. Similarly, we will obtain the ranges of other parameters t_i introduced in later estimates. We will determine the values of λ_1, t_{ij} in these ranges by combining the estimates of I_f, I_n and other terms in (3.14).

The estimates (3.18), (3.19) on the main term is crucial. If we estimate two inner products separately without using the cancellation between $\tilde{u}_x, \omega$ in Lemma A.4 with

$f = \omega$ and $g = u$, we would fail to establish (3.22) even with $c = 0$ since the damping term D_i is relatively small.

Remark 3.4 Several key ideas in the above estimates will be used repeatedly later. Firstly, we will perform decompositions on $\tilde{u}$ into the main term and the remainder similar to (3.17). Secondly, we will use Lemmas A.4, A.5 to estimate the inner product between $\tilde{u}$ and ω similar to (3.19). Thirdly, we will use Lemma A.8 to estimate weighted norms of $\tilde{u}_x, \tilde{u}$ similar to (3.19).

3.6 Estimates of the interaction in the far field I_f

We use ideas and estimates similar to that of I_n to estimate I_f. The main difference is that to estimate the inner product between $\tilde{u}_x$ and ω, instead of using Lemma A.4, we will use Lemma A.5. See estimates (3.18) and (3.23).

Firstly, we choose $c = \frac{3}{7}$ in (2.8) and decompose $\tilde{u}_x(\bar{\theta}_x + \chi\xi_2) + \tilde{u}\bar{\theta}_{xx}$ into the main term $\mathcal{M}$ and the remainder $\mathcal{R}$ as follows

$$\tilde{u}_x(\bar{\theta}_x + \chi\xi_2) + \tilde{u}\bar{\theta}_{xx} = \tilde{u}_x(\bar{\theta}_x + \frac{3}{7}x\bar{\theta}_{xx} + \chi\xi_2) + (\tilde{u} - \frac{3}{7}x\tilde{u}_x)\bar{\theta}_{xx} \triangleq \mathcal{M} + \mathcal{R}.$$

We choose $c = \frac{3}{7}$, which is different from that in (2.8), since we will apply (2.9) with a different power p later. Recall I_f in (3.16). The above formula implies

$$\begin{aligned} I_f &= -\langle \tilde{u}_x(\bar{\theta}_x + \chi\xi_2) + \tilde{u}\bar{\theta}_{xx}, \theta_x\psi_f\rangle + \lambda_1\langle\theta_x, \omega\varphi_f\rangle \\ &= \Big(- \langle \mathcal{M}, \theta_x\psi_f\rangle + \lambda_1\langle\omega, \theta_x\varphi_f\rangle\Big) + \langle -\mathcal{R}, \theta_x\psi_f\rangle \triangleq I_{\mathcal{M}} + I_{\mathcal{R}}. \end{aligned}$$

Recall the weights ψ_f, φ_f in (3.8). Using Young's inequality $a \cdot b \le t_1 a^2 + \frac{1}{4t_1}b^2$ for some $t_1 > 0$ to be determined, we obtain

$$\begin{aligned} I_{\mathcal{M}} &= \langle -\alpha_3\tilde{u}_x x^{-4/3} + \lambda_1\alpha_6\omega x^{-2/3}, \theta_x\rangle = \langle -\alpha_3\tilde{u}_x x^{-1} + \lambda_1\alpha_6\omega x^{-1/3}, \theta_x x^{-1/3}\rangle \\ &\le t_1 || - \alpha_3\tilde{u}_x x^{-1} + \lambda_1\alpha_6\omega x^{-1/3}||_2^2 + \frac{1}{4t_1}||\theta_x x^{-1/3}||_2^2 \triangleq I_{\mathcal{M},1} + I_{\mathcal{M},2}. \end{aligned} \tag{3.23}$$

We design the special form ψ_f in (3.8) to obtain a desirable term of the form $-\alpha_3\tilde{u}_x x^{-1} + \lambda_1\alpha_6\omega x^{-1/3}$. See also Remark 3.2. We further estimate $I_{\mathcal{M},1}$. Applying Lemma A.8 and Lemma A.5, we derive

$$\begin{aligned} I_{\mathcal{M},1} &= t_1(||\alpha_3\tilde{u}_x x^{-1}||_2^2 - 2\alpha_3\lambda_1\alpha_6\langle\tilde{u}_x, \omega x^{-4/3}\rangle + (\lambda_1\alpha_6)^2||\omega x^{-1/3}||_2^2) \\ &= t_1(\alpha_3^2||\omega x^{-1}||_2^2 - \frac{2\alpha_3\lambda_1\alpha_6}{2\sqrt{3}}(||\tilde{u}_x x^{-2/3}||_2^2 - ||\omega x^{-2/3}||_2^2) + (\lambda_1\alpha_6)^2||\omega x^{-1/3}||_2^2) \\ &= t_1\langle\omega^2, \alpha_3^2 x^{-2} + \frac{\alpha_3\lambda_1\alpha_6}{\sqrt{3}}x^{-4/3} + (\lambda_1\alpha_6)^2 x^{-2/3}\rangle - \frac{t_1\alpha_3\lambda_1\alpha_6}{\sqrt{3}}||\tilde{u}_x x^{-2/3}||_2^2. \end{aligned} \tag{3.24}$$

Remark 3.5 The negative sign in $-t_1 2\alpha_3\lambda_1\alpha_6\langle \tilde{u}_x, \omega x^{-4/3}\rangle$ in (3.24) is crucial. Firstly, we can bound the positive term $\frac{\alpha_3\lambda_1\alpha_6 t_1}{\sqrt{3}}||\omega x^{-2/3}||_2$ derived from the identity in Lemma A.5 directly without an overestimate. Secondly, $-\frac{t_1\alpha_3\lambda_1\alpha_6}{\sqrt{3}}||\tilde{u}_x x^{-2/3}||_2^2$ from the same identity provides a good quantity that allows us to control the weighted norm of $\tilde{u}$, $\tilde{u}_x$ with a slowly decaying weight using Lemma A.8.

We introduce D_u to denote the parameter in (3.24)

$$D_u = \frac{t_1\alpha_3\lambda_1\alpha_6}{\sqrt{3}}, \tag{3.25}$$

We use Young's inequality $ab \le t_{12}a^2 + \frac{1}{4t_{12}}b^2$ for some $t_{12} > 0$ and (2.9) with $p = \frac{5}{3}$ to estimate $I_{\mathcal{R}}$ directly

$$\begin{aligned} I_{\mathcal{R}} &= -\langle(\tilde{u} - \frac{3}{7}x\tilde{u}_x), \bar{\theta}_{xx}\psi_f\theta_x\rangle \le t_{12}||(\tilde{u} - \frac{3}{7}\tilde{u}_x x)x^{-5/3}||_2^2 + \frac{1}{4t_{12}}||\theta_x\psi_f\bar{\theta}_{xx}x^{5/3}||_2^2 \\ &= t_{12}\cdot\frac{9}{49}||\tilde{u}_x x^{-2/3}||_2^2 + \frac{1}{4t_{12}}||\theta_x\psi_f\bar{\theta}_{xx}x^{5/3}||_2^2. \end{aligned} \tag{3.26}$$

The remainder $I_{\mathcal{R}}$ is smaller since we get a factor $\frac{1}{2p-1} = \frac{3}{7}$ from (2.9).
Combining the above estimates, we obtain the estimate of $I_f = I_{\mathcal{M},1} + I_{\mathcal{M},2} + I_{\mathcal{R}}$

$$\begin{aligned} I_f \le & t_1\Big\langle\omega^2, \alpha_3^2x^{-2} + \frac{\alpha_3\lambda_1\alpha_6}{\sqrt{3}}x^{-4/3} + (\lambda_1\alpha_6)^2x^{-2/3}\Big\rangle \\ & + \Big\langle\theta_x^2, \frac{1}{4t_1}x^{-2/3} + \frac{1}{4t_{12}}(\psi_f\bar{\theta}_{xx}x^{5/3})^2\Big\rangle - \Big(D_u - \frac{9}{49}t_{12}\Big)||\tilde{u}_x x^{-2/3}||_2^2. \end{aligned} \tag{3.27}$$

Similar to the discussion in Remark 3.3, in order for $I_f + D_1 + D_2 \le -c(||\theta_x\psi^{1/2}||_2 + \lambda_1||\omega\varphi^{1/2}||_2^2)$ with $c = 0.01$, we can choose $t_1 \in [1.2, 1.4]$, $t_{12} \in [0.55, 0.65]$. See Appendix D.1 for the verification.

3.7 Estimates of the interaction with the most singular weight I_s

Recall I_s in (3.16) and $\psi_s = \alpha_4 x^{-4}$ in (3.8). Using Young's inequality $ab \le t_4a^2 + \frac{1}{4t_4}b^2$ for $t_4 > 0$, we yield

$$I_s = \lambda_1\langle\omega, \theta_x\varphi_s\rangle = \lambda_1\alpha_4\langle\omega, \theta_x x^{-4}\rangle \le t_4\langle\omega^2, x^{-3}\rangle + \frac{(\lambda_1\alpha_4)^2}{4t_4}\langle\theta_x^2, x^{-5}\rangle. \tag{3.28}$$

In order for $I_s + D_1 + D_2 \le -c(||\theta_x\psi^{1/2}||_2 + \lambda_1||\omega\varphi^{1/2}||_2^2)$ with $c = 0.01$, we can choose $t_4 \in [3, 5]$. See Appendix D.1 for the verification. We do not combine estimates of I_s with the estimates for the interaction between $\tilde{u}$ and θ_x in Section 3.5 since the weight x^{-4} is too singular. In fact, to apply estimate similar to that in (2.12) in Model 1, the weight for θ_x near 0 is 2 order more singular than that of ω. In this case, it is of order x^{-6} near 0 and more singular than ψ.

3.8 Estimates of the interaction u and ω

Firstly, we rewrite $-\lambda_1\langle\tilde{u}, \bar{\omega}_x\omega\varphi\rangle$ in (3.14) by decomposing $\bar{\omega}_x$ into the main term $\bar{\omega}_x + \chi\xi_3$ and the error term ξ_3

$$I_{u\omega} \triangleq -\lambda_1\langle\tilde{u}, \bar{\omega}_x\omega\varphi\rangle = -\lambda_1\langle\tilde{u}, (\bar{\omega}_x + \chi\xi_3)\omega\varphi\rangle + \lambda_1\langle\tilde{u}, \chi\xi_3\omega\varphi\rangle \triangleq J + I_{r2}. \tag{3.29}$$

We will estimate I_{r2} in Section 3.9 and show that it is very small. See also Remark 3.1.

Difficulty The main difficulty in establishing a sharp estimate for J is the slow decay of the coefficient $(\bar{\omega}_x + \chi\xi_3)\varphi$. A straightforward estimate similar to (3.26) yields $|J| \le \lambda_1||\tilde{u}x^{-p}||_2||\bar{\omega}_x\omega\rho x^p||_2$. In view of the weighted estimate in Lemma A.8, we have effective estimates of $(u - u_x(0)x)x^{-p}$ for exponent $p = 3, 2$ or $\frac{5}{3}$. In order to further control $||\bar{\omega}_x\omega\varphi x^p||_2$ by the weighted L^2 norm $||\omega\varphi^{1/2}||_2$, we cannot choose $p = 3$ or $p = 2$ due to the fast growth of x^p for large $|x|$. On the other hand, if we choose $p = \frac{5}{3}$, the resulting constant $\frac{36}{49}$ in Lemma A.8 is much larger than the constant $\frac{4}{25}, \frac{4}{9}$ corresponding to $p = 3$, $p = 2$.

To overcome this difficulty, we exploit the cancellations between u and ω in both the near field and the far field, which is similar to that in the estimate of I_n, I_f. We decompose the coefficient $(\bar{\omega}_x + \chi\xi_3)\varphi$ in J into the main terms $\mathcal{M}_i$ and the remainder $\mathcal{K}_{u\omega}$

$$\begin{aligned}(\bar{\omega}_x + \chi\xi_3)\varphi &= -\frac{1}{3}e_3\alpha_6 x^{-2} + \tau_1 x^{-4} + \Big((\bar{\omega}_x + \chi\xi_3)\varphi + \frac{1}{3}e_3\alpha_6 x^{-2} - \tau_1 x^{-4}\Big)\\ &\triangleq \mathcal{M}_1 + \mathcal{M}_2 + \mathcal{K}_{u\omega},\end{aligned} \tag{3.30}$$

where e_3, α_6 are defined in (3.7) and (3.8) and $\tau_1 > 0$ is some parameter.

Let us motivate the above decomposition. From the definitions of ξ_3, φ in (3.7)-(3.9) and the discussion therein, we have $\bar{\omega}_x + \chi\xi_3 \approx -\frac{1}{3}e_3 x^{-4/3}$, $\varphi \approx \alpha_6 x^{-2/3}$ for some $e_3, \alpha_6 > 0$ and large $|x|$. Thus, $(\bar{\omega}_x + \chi\xi_3)\varphi$ can be approximated by $-\frac{1}{3}e_3\alpha_6 x^{-2}$ for large $|x|$. Since $\varphi \approx \alpha_4 x^{-4}$ and $\bar{\omega}_x \approx \bar{\omega}_x(0) > 0$ near 0, $(\bar{\omega}_x + \chi\xi_3)\varphi$ is approximated by $\tau_1 x^{-4}$ for some $\tau_1 > 0$ in the near field.

Using the above formula, we can decompose J as follows

$$\begin{aligned}J &= -\lambda_1\langle\tilde{u}, (\bar{\omega}_x + \chi\xi_3)\omega\varphi\rangle = -\lambda_1\langle\tilde{u}, \mathcal{M}_1\omega\rangle - \lambda_1\langle\tilde{u}, \mathcal{M}_2\omega\rangle\\ &\quad -\lambda_1\langle\tilde{u}, \mathcal{K}_{u\omega}\omega\rangle \triangleq I_{\mathcal{M}1} + I_{\mathcal{M}2} + I_{\mathcal{R}}.\end{aligned}$$

To estimate the main terms, we use cancellations in Lemma A.4. Using $\tilde{u} = u - u_x(0)x$ defined in (3.10), $-u_x(0)\langle x, \omega x^{-2}\rangle = \frac{\pi}{2}u_x^2(0)$ and Lemma A.4 with $f = \omega$ and $g = u$, we get

$$I_{\mathcal{M}_1} = \frac{\lambda_1 e_3\alpha_6}{3}\langle\tilde{u}, \omega x^{-2}\rangle = \frac{\lambda_1 e_3\alpha_6}{3}\frac{\pi}{4}u_x(0)^2 - \frac{\lambda_1 e_3\alpha_6}{3}\langle\Lambda\frac{u}{x}, \frac{u}{x}\rangle,$$

where $\Lambda = (-\partial_x^2)^{1/2}$. We denote by $A(u)$ the right hand side of the above equation

$$A(u) \triangleq \frac{\lambda_1 e_3 \alpha_6}{3} \frac{\pi}{4} u_x(0)^2 - \frac{\lambda_1 e_3 \alpha_6}{3} \langle \Lambda \frac{u}{x}, \frac{u}{x} \rangle. \tag{3.31}$$

Since $e_3 \alpha_6 \lambda_1 > 0$ and $\langle \Lambda \frac{u}{x}, \frac{u}{x} \rangle \geq 0$, the second term in $A(u)$ is a good term and we will use it in the weighted H^1 estimate.

Although $I_{\mathcal{M}2}$ is a quadratic form on ω, it does not have a good sign similar to the identities in Lemma A.4. Yet, we can approximate $\tilde{u}$ by $\tilde{u}_x$ using (2.8) and then use the cancellation between $\tilde{u}_x$ and ω. Choosing $c = \frac{1}{5}$ in 2.8 and using the cancellation in Lemma A.4 with $f = \omega$ and $g = u$, we obtain

$$I_{\mathcal{M}2} = -\lambda_1 \tau_1 \langle \tilde{u}, x^{-4} \omega \rangle = -\lambda_1 \tau_1 \langle \tilde{u} - \frac{1}{5} \tilde{u}_x x, \omega x^{-4} \rangle$$
$$-\lambda_1 \tau_1 \langle \frac{\tilde{u}_x}{5}, \omega x^{-3} \rangle = -\lambda_1 \tau_1 \langle \tilde{u} - \frac{1}{5} \tilde{u}_x x, \omega x^{-4} \rangle.$$

The form $\tilde{u} - \frac{1}{5} \tilde{u}_x x$ allows us to gain a small factor $\frac{1}{5}$ using (2.9) with $p = 3$. Using Young's inequality $ab \leq ca^2 + \frac{1}{4c} b^2$, (2.9) with $p = 3$ and Lemma A.8, we obtain

$$\begin{aligned} I_{\mathcal{M}2} &\leq \lambda_1 \tau_1 \Big(t_{34} || (\tilde{u} - \frac{1}{5} \tilde{u}_x) x^{-3} ||_2^2 + \frac{1}{4 t_{34}} || \omega x^{-1} ||_2^2 \Big) \\ &= \lambda_1 \tau_1 \Big(\frac{t_{34}}{25} || \tilde{u}_x x^{-2} ||_2^2 + \frac{1}{4 t_{34}} || \omega x^{-1} ||_2^2 \Big) \\ &= \lambda_1 \tau_1 (\frac{t_{34}}{25} || \omega x^{-2} ||_2^2 + \frac{1}{4 t_{34}} || \omega x^{-1} ||_2^2) = \lambda_1 \tau_1 \Big\langle \omega^2, \frac{t_{34}}{25} x^{-4} + \frac{1}{4 t_{34}} x^{-2} \Big\rangle, \end{aligned} \tag{3.32}$$

for some $t_{34} > 0$. For $t_{31}, t_{32} > 0$ to be defined, we denote

$$S_{u1} = t_{31} x^{-6} + t_{32} x^{-4} + 2 \cdot 10^{-5} x^{-10/3}, \tag{3.33}$$

We estimate $I_{\mathcal{R}}$ directly using Young's inequality and the weighted estimate in Lemma A.8

$$\begin{aligned} I_{\mathcal{R}} &= -\lambda_1 \langle \tilde{u}, \mathcal{K}_{u\omega} \omega \rangle \leq \lambda_1 (|| \tilde{u} S_{u1}^{1/2} ||_2^2 + \frac{1}{4} || S_{u1}^{-1/2} \mathcal{K}_{u\omega} \omega ||_2^2) \\ &\leq \lambda_1 \Big\langle \omega^2, \frac{4 t_{31}}{25} x^{-4} + \frac{4 t_{32}}{9} x^{-2} + \frac{1}{4} \mathcal{K}_{u\omega}^2 S_{u1}^{-1} \Big\rangle + \frac{36 \lambda_1}{49} \cdot 2 \cdot 10^{-5} || \tilde{u}_x x^{-2/3} ||_2^2, \end{aligned} \tag{3.34}$$

where $\mathcal{K}_{u\omega}$ in defined (3.30).

Remark 3.6 From (3.7),(3.8) and (3.9), we have asymptotically $\mathcal{K}_{u\omega} \sim C x^{-4}$ for x close to 0. The slowly decaying part in $\mathcal{K}_{u\omega}$ is given by $f = (\bar{\omega}_x + \chi \xi_3) \alpha_6 x^{-2/3} + \frac{1}{3} e_3 \alpha_6 x^{-2} = (1 - \chi)(\bar{\omega}_x + \frac{1}{3} e_3 x^{-4/3}) \alpha_6 x^{-2/3}$. In the support of $1 - \chi$, since

$-\frac{1}{3}e_3x^{-4/3}$ approximates $\bar{\omega}_x$, f can be approximated by cx^{-2} with some very small constant c. We add $x^{-6}, 2\cdot 10^{-5}x^{-10/3}$ in S_{u1} so that $\mathcal{K}_{u\omega}^2 S_{u1}^{-1}$ can be bounded by φ. We also add the power x^{-4} in S_{u1} to obtain a sharper estimate. See also Remark 3.3 for the discussion on the parameters.

Combining the above estimates on $I_{\mathcal{M}i}, I_{\mathcal{R}}$, we prove

$$\begin{aligned} I_{u\omega} = J + I_{r2} \le \lambda_1\Big\langle \omega^2, \frac{4t_{31}}{25}x^{-4} + \frac{4t_{32}}{9}x^{-2} + \frac{1}{4}\mathcal{K}_{u\omega}^2 S_{u1}^{-1} + \tau_1(\frac{t_{34}}{25}x^{-4} + \frac{1}{4t_{34}}x^{-2})\Big\rangle \\ + A(u) + \frac{72\lambda_1}{49}\cdot 10^{-5}||\tilde{u}_x x^{-2/3}||_2^2 + I_{r2}. \end{aligned} \tag{3.35}$$

The term I_{r2} was not estimated and we keep it on both sides. We can determine the ranges of parameters $t_{31}, t_{32}, t_{34}, \tau_1$ so that $J + D_1 + D_2 \le -0.01(||\theta_x\psi^{1/2}||_2 + \lambda_1||\omega\varphi^{1/2}||_2^2)$.

3.9 Estimates of the I_{r1}, I_{r2}

Recall I_{r1}, I_{r2} in (3.16) and (3.29). Since χ is supported in the far field $|x| \ge \rho_2 > 10^8$ and the profile $(\bar{\omega}, \bar{\theta}_x)$ decays, we can get a small factor in the estimate of these terms. We establish the following estimate in Appendix B.2

$$|I_{r1}| + |I_{r2}| \le \langle G_\theta, \theta_x^2\rangle + \langle G_\omega, \omega^2\rangle + G_c c_\omega^2, \tag{3.36}$$

where G_θ, G_ω, G_c are given by

$$\begin{aligned} G_\theta &= 10^{10}\cdot\frac{(2+\sqrt{3})^2}{4}\chi^2(\xi_1\psi_n + \xi_2\psi_f)^2, \quad G_c = \frac{\lambda_1^2||x\xi_3\chi^{1/2}\varphi^{1/2}||_2^2}{4}\cdot 10^2, \\ G_\omega &= 10^{-10}x^{-4/3} + 10^{-5}x^{-2/3} + \frac{10^5}{4}(\frac{6\lambda_1(2+\sqrt{3})}{5})^2(x^{4/3}\chi\xi_3\varphi)^2 + 10^{-2}\chi\varphi. \end{aligned} \tag{3.37}$$

These functions are very small compared to the weights φ, ψ (3.8)-(3.9). We focus on a typical term G_θ to illustrate the smallness. From (3.7)-(3.8), for large $|x|, \xi_i, \psi_f, \psi$ have decay rate $x^{-2/3}$, ψ_n has a decay rate at least x^{-2}. For $\partial_x^i\bar{\theta}_x$, we recall from the beginning of Section 3.1 that it has decay rate $x^{2\alpha-i}$ with α slightly smaller than $-\frac{1}{3}$. Thus $|\chi(\xi_1\psi_n + \xi_2\psi_f)|^2/\psi$ has decay rate x^{-2}. Since χ is supported in $|x| \ge \rho_2 > 10^8$, we get a small factor $x^{-2}\mathbf{1}_{|x|>\rho_2} < 10^{-16}$, which absorbs the large constant 10^{10} in G_θ. Therefore, G_θ is very small compared to ψ.

3.10 Summary: estimates of $\mathcal{L}_{\theta 1}, \mathcal{L}_{\omega 1}$

Recall $\mathcal{L}_{\theta 1}, \mathcal{L}_{\omega 1}$ in (3.11), the quadratic terms in (3.11), (3.14). Combining (3.13), (3.27),(3.21), (3.28), (3.35) and (3.36), we obtain the estimate on $\mathcal{L}_{\theta 1}, \mathcal{L}_{\omega 1}$

$$\langle \mathcal{L}_{\theta 1}\theta_x, \theta_x\psi\rangle + \lambda_1\langle \mathcal{L}_{\omega 1}\omega, \omega\varphi\rangle \le \langle D_\theta + A_\theta\psi^{-1}, \theta_x^2\psi\rangle + \langle \lambda_1 D_\omega + A_\omega\varphi^{-1}, \omega^2\varphi\rangle$$
$$-\Big(D_u - \frac{9}{49}t_{12} - \frac{72\lambda_1}{49}\cdot 10^{-5}\Big)||\tilde{u}_x x^{-2/3}||_2^2 + A(u) + G_c c_\omega^2, \tag{3.38}$$

where $A(u)$ is defined in (3.31), D_u, t_{12} are given in (C.2), and the A_θ, A_ω terms are the sum of the integrals of ω^2, θ_x^2 in the upper bounds in (3.27),(3.21), (3.28), (3.36) given by

$$\begin{aligned} A_\theta &\triangleq \Big(\frac{1}{4t_1}x^{-2/3} + \frac{1}{4t_{12}}(\psi_f\bar{\theta}_{xx}x^{5/3})^2\Big) + \Big(\frac{1}{4t_2}(\alpha_2 x^{-1} + \alpha_1 x^{-2})^2 + \frac{1}{4t_{22}}(x^3\bar{\theta}_{xx}\psi_n)^2\Big) \\ &\quad + \frac{(\lambda_1\alpha_4)^2}{4t_4}x^{-5} + G_\theta, \\ A_\omega &\triangleq t_1\Big(\alpha_3^2 x^{-2} + \frac{\alpha_3\lambda_1\alpha_6}{\sqrt{3}}x^{-4/3} + (\lambda_1\alpha_6)^2 x^{-2/3}\Big) + \Big(t_2 x^{-4} + \frac{t_{22}}{25}x^{-4} + t_2(\lambda_1\alpha_5)^2 x^{-2}\Big) \\ &\quad + t_4 x^{-3} + \lambda_1\Big(\frac{4t_{31}}{25}x^{-4} + \frac{4t_{32}}{9}x^{-2} + \frac{1}{4}\mathcal{K}_{u\omega}^2 S_{u1}^{-1} + \tau_1\Big(\frac{t_{34}}{25}x^{-4} + \frac{1}{4t_{34}}x^{-2}\Big)\Big) + G_\omega. \end{aligned} \tag{3.39}$$

In the previous estimates, we have obtained the ranges of t_{ij} such that $I + D_1 + D_2 \le -0.01(||\theta_x\psi^{1/2}||_2^2 + \lambda_1||\omega\varphi^{1/2}||_2^2)$ for several terms I in (3.14), e.g. $I = I_f, I_n$. We further determine the approximate values of λ_1, t_{ij} so that

$$D_\theta + A_\theta\psi^{-1} \le -c, \quad \lambda_1 D_\omega + A_\omega\varphi^{-1} \le -\lambda_1 c \tag{3.40}$$

with $c > 0$ as large as possible. The functions in (3.40) depend on the parameters and other explicit functions. The above task is equivalent to solving a constrainted optimization problem by maximizing c, subject to the constraints (3.40) and $\lambda_1, t_{ij} > 0$ within an interval that we have determined.

Estimates (3.38), (3.40) imply the linear stability estimate (3.12) up to the c_ω terms in (3.14), $A(u)$ (3.31) and $G_c c_\omega^2$. In Section 3.11, we further control these c_ω terms. The estimate of these c_ω terms are small. We will perturb λ_1, t_{ij} around their approximate values and finalize the choices of λ_1, t_{ij}. The final values of these parameters are given in (C.2), (C.3).

The main reasons that we can establish (3.40) are the followings. Firstly, we exploit several cancellations using Lemma A.8 and apply sharp weighted estimates in Lemma A.8 to estimate the nonlocal terms. Secondly, we have $I + D_1 + D_2 \le -c(||\theta_x\psi^{1/2}||_2^2 + \lambda_1||\omega\varphi^{1/2}||_2^2)$ for I being the main terms in (3.14), i.e. $I = I_f, I_n$ or I_s. Thirdly, the interactions in I_f, I_n, I_s are mainly supported in different regions. See the discussion after (3.16). Finally, the main term in $I_{u\omega}$ is estimated using several cancellations.

To illustrate that the inequalities in (3.40) can actually be achieved, we plot in Figure 1 the grid point values of the functions $-D_\theta - A_\theta\psi^{-1}$ and $-\lambda_1 D_\omega - A_\omega\varphi^{-1}$ for $x \in [0, 40]$ with the parameters λ_1, t_{ij} given in (C.2), (C.3). It is shown that their grid point values are all positive and uniformly bounded away from 0. In fact, the minimum of the grid point values of $-D_\theta - A_\theta\psi^{-1}$ is above 0.032 and that of $-\lambda_1 D_\omega - A_\omega\phi^{-1}$ is above 0.054.

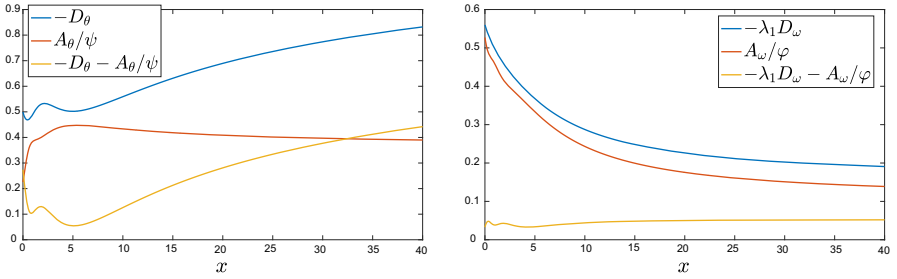

Fig. 1 Left : Grid point values of $-D_\theta$, $A_\theta\psi^{-1}$ and $-D_\theta - A_\theta\psi^{-1}$ for $x \in [0, 40]$. Right: Those of $-\lambda_1 D_\omega$, $A_\omega\phi^{-1}$ and $-\lambda_1 D_\omega - A_\omega\phi^{-1}$ (with $\lambda_1 = 0.32$)

Estimate (3.38) on $\mathcal{L}_{\theta 1}$, $\mathcal{L}_{\omega 1}$ is important and we will use it in Section 5 to establish the weighted H^1 estimates.

3.11 Estimate of the c_ω term

We use the idea in Model 2 in Section 2.3.2 to obtain the damping term for c_ω by deriving the ODEs for c_ω^2 and $\langle\theta_x, x^{-1}\rangle^2$. We introduce some notations

$$d_\theta \triangleq \langle\theta_x, x^{-1}\rangle, \quad \bar{d}_\theta \triangleq \langle\bar{\theta}_x, x^{-1}\rangle, \quad \bar{u}_{\theta,x} \triangleq H\bar{\theta}_x, \quad u_\Delta = \tilde{u} - \frac{1}{5}\tilde{u}_x x. \tag{3.41}$$

3.11.1 Derivation of the ODEs

Recall $c_\omega = u_x(0) = -\frac{2}{\pi}\int_0^{+\infty}\frac{\omega}{x}dx$ from (3.3). Using a derivation similar to that in Model 2 in Section 2.3.2, , we derive the following ODE in Appendix B.3

$$\begin{aligned}\frac{1}{2}\frac{d}{dt}\frac{\pi}{2}c_\omega^2 = &\frac{\pi}{2}(\bar{c}_\omega + \bar{u}_x(0))c_\omega^2 + c_\omega\int_0^\infty\frac{\bar{u}\omega_x + u\bar{\omega}_x}{x}dx\\ &- c_\omega d_\theta - c_\omega\int_0^\infty\frac{F_\omega + N(\omega)}{x}dx.\end{aligned} \tag{3.42}$$

The ODE for d_θ^2 (B.5) is derived similarly in Appendix B.3.1. There is a cancellation between these two ODEs, which is captured by Model 2 in Section 2.3.2. To exploit this cancellation, we combine two ODEs and derive the following ODE in Appendix B.3 with $\lambda_2, \lambda_3 > 0$ to be chosen

$$\frac{1}{2}\frac{d}{dt}(\frac{\lambda_2\pi}{2}c_\omega^2 + \lambda_3 d_\theta^2) = \frac{\pi\lambda_2}{2}(\bar{c}_\omega + \bar{u}_x(0))c_\omega^2 + 2\bar{c}_\omega\lambda_3 d_\theta^2 + \mathcal{T}_0 + \mathcal{R}_{ODE}, \tag{3.43}$$

where $\mathcal{T}_0$ is the sum of the quadratic terms that do not have a fixed sign

$$\begin{aligned}\mathcal{T}_0 = &-(\lambda_2 - \lambda_3\bar{d}_\theta)c_\omega d_\theta + \lambda_2 c_\omega\langle\omega, f_2\rangle - \lambda_3 d_\theta\langle\theta_x, f_6\rangle + \lambda_3 d_\theta\langle\omega, f_4\rangle\\ &+ \lambda_2 c_\omega\langle u_\Delta x^{-1}, f_8\rangle - \lambda_3 d_\theta\langle u_\Delta x^{-1}, f_9\rangle,\end{aligned} \tag{3.44}$$

u_Δ is defined in (3.41), f_i defined in (B.2) are some functions depending on the profile $(\bar\omega, \bar\theta)$, and $\mathcal{R}_{ODE}$ is the sum of the remaining terms in the ODEs given by

$$\mathcal{R}_{ODE} \triangleq -\lambda_2 c_\omega \langle F_\omega + N(\omega), x^{-1}\rangle + \lambda_3 d_\theta \langle F_\theta + N(\theta), x^{-1}\rangle. \tag{3.45}$$

Since the approximate steady state satisfies $\bar c_\omega < 0$, $\bar u_x(0) < 0$, $\frac{\pi\lambda_2}{2}(\bar c_\omega + \bar u_x(0))c_\omega^2$ and $2\bar c_\omega \lambda_3 d_\theta^2$ in (3.43) are damping terms.

3.11.2 Derivation of the $\mathcal{T}_0$ term

Let us explain how we obtain (3.43). The ODEs of c_ω^2, d_θ^2 ((3.42) and (B.5)) involves the integrals of the nonlocal terms u, u_x in the form of $\langle \tilde u, f\rangle$ or $\langle \tilde u_x, g\rangle$ for some functions f, g. To estimate these terms effectively, we use the antisymmetry property of the Hilbert transform in Lemma A.3 to transform these terms into integrals of ω. We first consider $\langle \tilde u_x, g\rangle$ and $\langle u_x, g\rangle$. Using $u_x = H\omega$, $\frac{u_x - u_x(0)}{x} = H(\frac{\omega}{x})$ and Lemma A.3, we get

$$\langle u_x, g\rangle = \langle H\omega, g\rangle = -\langle \omega, Hg\rangle, \quad \langle \tilde u_x, g\rangle = \left\langle H\left(\frac{\omega}{x}\right), xg\right\rangle = -\left\langle \frac{\omega}{x}, H(xg)\right\rangle. \tag{3.46}$$

For $\langle \tilde u, f\rangle$, we first approximate f by p_x for some function p and then perform a decomposition $\tilde u = cx\tilde u_x + (\tilde u - cx\tilde u_x)$. We obtain

$$\begin{aligned}\langle \tilde u, f\rangle &= \langle \tilde u, p_x\rangle + \langle \tilde u, f - p_x\rangle = \langle \tilde u, p_x\rangle + \langle cx\tilde u_x, f - p_x\rangle \\ &+\langle \tilde u - cx\tilde u_x, f - p_x\rangle \triangleq I_1 + I_2 + I_3.\end{aligned}$$

The last term enjoys much better estimate than $\langle \tilde u, f\rangle$ due to (2.9) and the fact that $f - p_x$ is much smaller than f. For I_1, I_2, using integration by parts, we get

$$I_1 + I_2 = \langle \tilde u_x, -p + cx(f - p_x)\rangle.$$

Using (3.46), we can further rewrite the above term as an integral of ω.

In addition, we introduce the function f_i to simplify the integrals of ω, θ_x. These derivations lead to the $\mathcal{T}_0$ term. We refer the details to Appendix B.3.

We remain to estimate the c_ω terms in (3.11) in the weighted L^2 estimates and f_3, f_7 that are defined in (B.2). We combine $\mathcal{T}_0$ and these c_ω terms, and define

$$\begin{aligned}\mathcal{T} &\triangleq \mathcal{T}_0 + c_\omega\langle \bar\theta_x - x\bar\theta_{xx},\ \theta_x\psi\rangle + \lambda_1 c_\omega\langle \bar\omega - x\bar\omega_x, \omega\varphi\rangle \\ &= \mathcal{T}_0 + c_\omega\langle \omega, f_3\rangle + c_\omega\langle \theta_x, f_7\rangle.\end{aligned} \tag{3.47}$$

In the weighted L^2 estimates, it remains to estimate $\mathcal{T}$. Though each term in $\mathcal{T}$ can be estimated by the weighted L^2 norms of ω, θ_x and $c_\omega^2, \langle \theta_x, x^{-1}\rangle^2$ using the Cauchy-Schwarz inequality, these straightforward estimates do not lead to sharp estimates since these Cauchy-Schwarz inequalities do not achieve (or are close to) equalities for the same functions. We use the optimal-constant argument in [11] to obtain a sharp estimate on $\mathcal{T}$.

3.11.3 Sharp estimates on $\mathcal{T}$

For positive $T_1, T_2, T_3 \in C(\mathbb{R}_+)$ and positive parameter $s_1, s_2 > 0$ to be determined, we consider the following inequality with sharp constant C_{opt}

$$\mathcal{T} \le C_{opt}(||\omega T_1^{1/2}||_2^2 + ||\theta_x T_2^{1/2}||_2^2 + ||\frac{u_\Delta}{x} T_3^{1/2}||_2^2 + s_1 c_\omega^2 + s_2 d_\theta^2), \quad (3.48)$$

where u_Δ is defined in (3.41). We define several functions

$$\begin{aligned} &X = \omega T_1^{1/2}, \quad Y = \theta_x T_2^{1/2}, \quad Z = u_\Delta x^{-1} T_3^{1/2}, \\ &g_1 = -\frac{2}{\pi} x^{-1} T_1^{-1/2}, \ g_2 = f_2 T_1^{-1/2}, \ g_3 = f_3 T_1^{-1/2}, \ g_4 = f_4 T_1^{-1/2}, \\ &g_5 = x^{-1} T_2^{-1/2}, \ g_6 = f_6 T_2^{-1/2}, \ g_7 = f_7 T_2^{-1/2}, \ g_8 = f_8 T_3^{-1/2}, \ g_9 = f_9 T_3^{-1/2}. \end{aligned} \quad (3.49)$$

Notice that each term in (3.44) and (3.47) can be seen as the projection of X, Y, Z onto some function g_i. For example, c_ω, d_θ can be written as follows

$$c_\omega = u_x(0) = -\frac{2}{\pi} \int_0^\infty \frac{\omega}{x} dx = \langle X, g_1 \rangle, \quad d_\theta = \int_0^\infty \frac{\theta_x}{x} dx = \langle Y, g_5 \rangle.$$

Using the definition of $\mathcal{T}$ in (3.44), (3.47) and the functions in (3.49), we rewrite (3.48) as

$$\begin{aligned} \mathcal{T} =& \langle X, g_1 \rangle \langle X, g_3 \rangle + \langle X, g_1 \rangle \langle Y, g_7 \rangle \\ &- (\lambda_2 - \lambda_3 \bar{d}_\theta) \langle X, g_1 \rangle \langle Y, g_5 \rangle + \lambda_2 \langle X, g_1 \rangle \langle X, g_2 \rangle \\ &- \lambda_3 \langle Y, g_5 \rangle \langle Y, g_6 \rangle + \lambda_3 \langle Y, g_5 \rangle \langle X, g_4 \rangle + \\ &\lambda_2 \langle X, g_1 \rangle \langle Z, g_8 \rangle - \lambda_3 \langle Y, g_5 \rangle \langle Z, g_9 \rangle \\ \le& C_{opt}(||X||_2^2 + ||Y||_2^2 + ||Z||_2^2 + s_1 \langle X, g_1 \rangle^2 + s_2 \langle Y, g_5 \rangle^2). \end{aligned} \quad (3.50)$$

We project X, Y, Z onto the following finite dimensional spaces

$$\begin{aligned} &X \in \text{span}\{g_1, g_2, g_3, g_4\} \triangleq \Sigma_1, \quad Y \in \text{span}\{g_5, g_6, g_7\} \triangleq \Sigma_2, \\ &Z \in \text{span}\{g_8, g_9\} \triangleq \Sigma_3, \end{aligned} \quad (3.51)$$

which only makes the right hand side of (3.50) smaller. Then (3.50) completely reduces to an optimization problem on the finite dimensional space. Using the optimal-constant argument in [11], we obtain

$$C_{opt} = \lambda_{\max}(D^{-1/2} M_s D^{-1/2}),$$

where D, M_s defined in (B.14) are symmetric matrices with entries determined by the inner products among g_i. In particular, C_{opt} can be computed rigorously and we present the details in Appendix B.5.

3.12 Summary of the estimates

Recall the c_ω terms in (3.11), the operators in (3.5). Combining (3.38), (3.44) and (3.47), we yield

$$\begin{aligned}\langle \mathcal{L}_\theta \theta_x, \theta_x \psi\rangle + \lambda_1 \langle \mathcal{L}_\omega \omega, \omega\varphi\rangle + \mathcal{T}_0 &= \langle \mathcal{L}_{\theta 1} \theta_x, \theta_x \psi\rangle + \lambda_1 \langle \mathcal{L}_{\omega 1} \omega, \omega\varphi\rangle + \mathcal{T} \\ &\le \langle D_\theta + A_\theta \psi^{-1}, \theta_x^2 \psi\rangle + \langle \lambda_1 D_\omega + A_\omega \varphi^{-1}, \omega^2 \varphi\rangle \\ &- \Big(D_u - \frac{9}{49} t_{12} - \frac{72\lambda_1}{49} \cdot 10^{-5}\Big) ||\tilde{u}_x x^{-2/3}||_2^2 + \mathcal{T} + A(u) + G_c c_\omega^2 \triangleq J.\end{aligned} \tag{3.52}$$

We use the remaining damping of $\omega, \theta_x, \tilde{u}_x$ and the argument in Section 3.11.3 to control $\mathcal{T}$. In (B.16), Appendix B.6, we define $T_i > 0, s_i > 0$ that are used to compute the upper bound of $C_{opt} < 1$ in (3.48). These functions and scalars are essentially determined by four parameters $\lambda_2, \lambda_3, \kappa, t_{61} > 0$. Using the estimate (3.48), we obtain

$$\mathcal{T} \le ||\omega T_1^{1/2}||_2^2 + ||\theta_x T_2^{1/2}||_2^2 + ||\frac{u_\Delta}{x} T_3^{1/2}||_2^2 + s_1 c_\omega^2 + s_2 d_\theta^2. \tag{3.53}$$

The u_Δ term can be further bounded by $||\tilde{u}_x x^{-2/3}||_2$ and $||\omega x^{-2}||_2$ similar to (3.34), which is established in (B.19) in Appendix B.6. Plugging (B.19) and (3.53) in (3.52), we obtain

$$\begin{aligned}J \le &-\kappa ||\theta_x \psi^{1/2}||_2^2 - \kappa\lambda_1 ||\omega\varphi^{1/2}||_2^2 + (s_1 + G_c) c_\omega^2 \\ &+ s_2 d_\theta^2 - 10^{-6} ||\tilde{u}_x x^{-2/3}||_2^2 + A(u),\end{aligned} \tag{3.54}$$

for $\kappa > 0$ determined in Appendix C. The details are elementary and presented in Appendix B.6. For $\lambda_2, \lambda_3 > 0$ given in (C.3), we define the weighted L^2 energy

$$E_1^2(\theta_x, \omega) = ||\theta_x \psi^{1/2}||_2^2 + \lambda_1 ||\omega\psi^{1/2}||_2^2 + \lambda_2 \frac{\pi}{2} \cdot \frac{4}{\pi^2} \langle \omega, x^{-1}\rangle^2 + \lambda_3 \langle \theta_x, x^{-1}\rangle^2. \tag{3.55}$$

Note that $\frac{2}{\pi}\langle \omega, x^{-1}\rangle = -u_x(0) = -c_\omega$ (3.3). Recall the relations of different operators in (3.5). Combining the equations (3.11), (3.43) and using the estimates (3.52) and (3.54), we establish

$$\begin{aligned}\frac{1}{2}\frac{d}{dt} E_1^2(\theta, \omega) &= \langle \mathcal{L}_\theta \theta_x, \theta_x \psi\rangle + \lambda_1 \langle \mathcal{L}_\omega \omega, \omega\varphi\rangle + \mathcal{T}_0 \\ &+ \frac{\pi\lambda_2}{2} (\bar{c}_\omega + \bar{u}_x(0)) c_\omega^2 + 2\bar{c}_\omega \lambda_3 d_\theta^2 + \mathcal{R}_{L^2} \\ &\le -\kappa ||\theta_x \psi^{1/2}||_2^2 - \kappa\lambda_1 ||\omega\varphi^{1/2}||_2^2 - 10^{-6} ||\tilde{u}_x x^{-2/3}||_2^2 + A(u) \\ &+ \Big(\frac{\pi\lambda_2}{2} (\bar{c}_\omega + \bar{u}_x(0)) + s_1 + G_c\Big) c_\omega^2 + (2\bar{c}_\omega \lambda_3 + s_2) d_\theta^2 + \mathcal{R}_{L^2},\end{aligned}$$

where $\mathcal{R}_{L^2}$ is given by

$$\mathcal{R}_{L^2} \triangleq N_1 + F_1 + \lambda_1 N_2 + \lambda_1 F_2 + \mathcal{R}_{ODE} \tag{3.56}$$

and N_i, F_i are defined in (3.11) and $\mathcal{R}_{ODE}$ in (3.45). Recall $A(u)$ in (3.31), $c_\omega = u_x(0)$. Using the definitions of s_i in (B.16), we get

$$\frac{\pi\lambda_2}{2}(\bar{c}_\omega + \bar{u}_x(0)) + s_1 + G_c + \frac{\pi\lambda_1 e_3\alpha_6}{12} = -r_{c_\omega}, \quad s_2 + 2\bar{c}_\omega\lambda_3 = -\kappa\lambda_3,$$

for $r_{c_\omega}, \kappa > 0$ determined in Appendix C. Hence, we obtain

$$\begin{aligned} &A(u) + \Big(\frac{\pi\lambda_2}{2}(\bar{c}_\omega + \bar{u}_x(0)) + s_1 + G_c\Big)c_\omega^2 + (2\bar{c}_\omega\lambda_3 + s_2)d_\theta^2 \\ &\quad = -r_{c_\omega}c_\omega^2 - \kappa\lambda_3 d_\theta^2 - \frac{\lambda_1 e_3\alpha_6}{3}\langle\Lambda\frac{u}{x}, \frac{u}{x}\rangle. \end{aligned}$$

Therefore, we obtain

$$\begin{aligned} \frac{1}{2}\frac{d}{dt}E_1^2(\theta,\omega) \le\ & -\kappa||\theta_x\psi^{1/2}||_2^2 - \kappa\lambda_1||\omega\varphi^{1/2}||_2^2 \\ & - 10^{-6}||\tilde{u}_x x^{-2/3}||_2^2 - \frac{\lambda_1 e_3\alpha_6}{3}\langle\Lambda\frac{u}{x}, \frac{u}{x}\rangle \\ & - r_{c_\omega}c_\omega^2 - \kappa\lambda_3 d_\theta^2 + \mathcal{R}_{L^2} \triangleq Q + \mathcal{R}_{L^2}, \end{aligned} \tag{3.57}$$

These parameters satisfy $r_{c_\omega} \ge \frac{\pi}{2}\kappa\lambda_2$. Thus (3.57) implies

$$\frac{1}{2}\frac{d}{dt}E_1^2(\theta,\omega) \le -\kappa E_1^2(\theta,\omega) + \mathcal{R}_{L^2}, \tag{3.58}$$

and we establish the linear stability. See also (3.12). Compared to (3.58), (3.57) contains extra damping terms $-||\tilde{u}_x x^{-2/3}||_2^2, -\langle\Lambda\frac{u}{x}, \frac{u}{x}\rangle$ and $-(r_{c_\omega} - \frac{\pi}{2}\kappa\lambda_2)c_\omega^2$. We choose $r_{c_\omega} > \kappa\frac{\pi}{2}\lambda_2$ and keep these terms in (3.57) mainly to obtain sharper constants in our later weighted H^1 estimates.

3.13 From linear stability to nonlinear stability with rigorous verification

In this subsection, we describe some main ideas how to go from linear stability to nonlinear stability with computer-assisted proof.

(1) As we discuss at the beginning of Section 2, the most challenging and essential part in the proof is the weighted L^2 linear stability analysis established in Section 3, since there is *no* small parameter and the linearized equations (2.7) are complicated.

(2) The weighted L^2 linear stability estimates can be seen as a-priori estimates on the perturbation, and we proceed to perform higher order energy estimates in a similar manner and establish the nonlinear energy estimate for some energy $E(t)$ of

the perturbation

$$\frac{d}{dt}E^2 \le CE^3 - \lambda E^2 + \varepsilon E. \tag{3.59}$$

Here, $-\lambda E^2$ with $\lambda > 0$ comes from the linear stability, CE^3 with some constant $C(\bar{\omega}, \bar{\theta}) > 0$ controls the nonlinear terms, and ε is the weighted norm of the residual error of the approximate steady state. See more details in Section 5. To close the bootstrap argument $E(t) < E^*$ with some threshold $E^* > 0$, a sufficient condition is that $\varepsilon < \varepsilon^* = \lambda^2/(4C)$, which provides an upper bound on the required accuracy of the approximate steady state.

The essential parts of the estimates in (1), (2) are established based on the grid point values of $(\bar{\omega}, \bar{\theta})$ constructed using a moderate fine mesh. These parts do not involve the lengthy rigorous verification in the Supplementary Material [10]. These estimates already provide a strong evidence of nonlinear stability.

A significant difference from this step and step (1) is that we have a small parameter ε. As long as ε is sufficiently small, thanks to the damping term $-\lambda E^2$ established in step (1), we can afford a large constant $C(\bar{\omega}, \bar{\theta})$ in the estimate of the nonlinear terms and close the nonlinear estimates. We can complete all the nonlinear estimates in this step.

(3) We follow the general approach in [11] to construct an approximate steady state with residual error below a required level ε^*. To achieve the desired accuracy, the construction is typically done by solving (2.2) for a sufficiently long time using a fine mesh. The difficulty of the construction depends on the target accuracy ε^*, and we refer to Section 4 for more discussion on the new difficulty and the construction of the approximate steady state for the HL model. Here, the mesh size plays a role similar to a small parameter that we can use. In practice, the profile $(\bar{\omega}_1, \bar{\theta}_1)$ constructed using a moderate fine mesh Ω_1 is close to the one (ω_2, θ_2) constructed using a finer mesh Ω_2 with higher accuracy. As a result, the constants $C(\bar{\omega}, \bar{\theta})$ and λ that we estimate in (3.59) using different approximate steady states (ω_i, θ_i) are nearly the same. This refinement procedure allows us to obtain an approximate steady state, based on which we close the nonlinear estimates (3.59). We refer more discussion of this philosophy to [11].

(4) Finally, we follow the standard procedure to perform rigorous verification on the estimates to pass from the grid point value to its continuous counterpart. Estimates that require rigorous verification with computer assistance are recorded in Appendix D. In the verification step, we can evaluate the approximate steady state on a much finer mesh Ω_3 with many more grid points so that they almost capture the whole behavior of the solution. Then, we use the regularity of the solution to pass from finite grid points to the whole real line. In this procedure, the mesh size in Ω_3 plays a role similar to a small parameter that we can exploit. In practice, to perform the rigorous verification, we evaluate the solution computed in a mesh with about 5000 grid points using a much denser mesh with more than $5 \cdot 10^5$ grid points.

In summary, in steps (2)-(4), we can take advantage of a small parameter which can be either the small error or the small mesh size, while there is no small parameter

in step (1). Though these three steps could be technical, they are relatively standard from the viewpoint of analysis.

We remark that the approach of computer-assisted proof has played an important role in the analysis of many PDE problems, especially in computing explicit tight bounds of complicated (singular) integrals [4, 19, 34] or bounding the norms of linear operators [1, 30]. We refer to [33] for an excellent survey on computer-assisted proofs in establishing rigorous analysis for PDEs, which also explains the use of interval arithmetics that guarantees rigorous computer-assisted verifications. Examples of highly nontrivial results established by the use of interval arithmetics can be found in, for example, [31, 35, 51, 67]. Our approach to establish stability analysis with computer assistance is different from existing computer-assisted approach, e.g. [3], where the stability is established by numerically tracking the spectrum of a given operator and quantifying the spectral gap. The key difference between their approach and ours is that we *do not* use direct computation to quantify the spectral gap of the linearized operator. One of the main reasons is that the linearized operator in our case is not compact due to the Hilbert transform, and the non-compact component cannot be treated as a small perturbation. Thus we cannot approximate the linearized operator by a finite rank operator that can be further analyzed using matrix computation.

4 On the approximate steady state

The proof of the main Theorem 2 heavily relies on an approximate steady state solution $(\bar{\theta}, \bar{\omega}, \bar{c}_l, \bar{c}_\omega)$ to the dynamic rescaling equations (2.2), which is smooth enough, e.g. $\bar{\omega}, \bar{\theta}_x \in C^3$. Moreover, as discussed in Section 3.13, the residual error of the approximate steady state must be small enough in order to close the nonlinear estimates. In particular, the residual error ε requirement depends on the stability gap λ via the inequality $\varepsilon < \lambda^2/(4C)$.

For comparison, we refer the reader to our previous work on proving the finite-time, approximate self-similar blowup of the 1D De Gregorio model via a similar computer-aided strategy [11], where the corresponding approximate steady state is constructed numerically on a compact domain $[-10, 10]$. The stability gap that the authors proved in that work is relatively large (around 0.3), and thus the point-wise error requirement on the residual can be relaxed to 10^{-6}.

For the HL model, however, the stability gap $\lambda \approx \kappa = 0.03$ (see (C.3)) that we can prove in the linear stability analysis (3.58) is much smaller, which leads to a much stronger requirement on the residual error. More precisely, we need to bound the residual in a weighted norm by 5.5×10^{-7} with weights (3.9) that are singular of order $x^{-k}, k \geq 4$ near 0 and decay slowly for large x. This effectively requires the point-wise values of the residual to be as small as 10^{-10}. To achieve this goal, it is not sufficient to simply follow the method in [11], mainly due to the following reasons:

(1) The steady state solution to (2.2) is supported on the whole real line and has a slowly decaying tail in the far field (see below). If we approximate the steady state on a finite domain $[-L, L]$, we need to use an unreasonably large L (roughly $L \geq 10^{30}$) for the tail part beyond $[-L, L]$ to be considered as a negligible

error, since truncating the tail leads to an error of order $L^{c_\omega/c_l} \approx L^{-1/3}$. It is then impractical to achieve a uniformly small residual by only using mesh-based algorithms such as spline interpolations.

(2) Numerically computing the Hilbert transform of a function supported on the whole real line $\mathbb{R}$ is sensitively subject to round-off errors. For example, when computing u from an odd function ω via the Hilbert transform, we need to evaluate the convolution kernel $\log(|y-x|/|y+x|)$, which will be mistaken as 0 by a computer program using double-precision if $|x/y| < 10^{-16}$. Such round-off errors, when accumulated over the whole mesh, are unacceptable in our case since we have a very high accuracy requirement for the computation of the approximate steady state solution.

To design a practical method of obtaining a sufficiently accurate construction, we must have some a priori knowledge on the behavior of a steady state $(\omega_\infty, \theta_\infty, c_{l,\infty}, c_{\omega,\infty})$. Assume that the velocity u_∞ grows (if it grows) only sub-linearly in the far field, i.e. $u_\infty(x)/x, u_{\infty,x}(x) \to 0$ as $x \to \infty$. Substituting this ansatz into the steady state equation of θ_x in (2.2) yields

$$\frac{\theta_{\infty,xx}}{\theta_{\infty,x}} \sim \frac{2c_{\omega,\infty}}{c_{l,\infty}} \cdot x^{-1}, \quad \text{which implies} \quad \theta_{\infty,x} \sim x^{2c_{\omega,\infty}/c_{l,\infty}}.$$

Furthermore, using these results to the steady state equation of ω in (2.2) yields

$$\frac{\omega_{\infty,x}}{\omega_\infty} \sim \frac{c_{\omega,\infty}}{c_{l,\infty}} \cdot x^{-1}, \quad \text{which implies} \quad \omega_\infty \sim x^{c_{\omega,\infty}/c_{l,\infty}}.$$

From our preliminary numerical simulation, we have $c_{\omega,\infty}/c_{l,\infty}$ close to $-1/3$. This straightforward argument implies that ω_∞ and $\theta_{\infty,x}$ should behave asymptotically like $x^{c_{\omega,\infty}/c_{l,\infty}}$, $x^{2c_{\omega,\infty}/c_{l,\infty}}$ as $x \to +\infty$, respectively, which in turn justifies the sub-linear growth of u_∞.

Guided by these observations, we will construct our approximate steady state as the combination of two parts:

$$\bar{\omega} = \omega_b + \omega_p, \quad \bar{\theta} = \theta_b + \theta_p. \tag{4.1}$$

We will call (ω_b, θ_b) the explicit part and (ω_p, θ_p) the perturbation part. The explicit part (ω_b, θ_b) is constructed analytically to approximate the asymptotic tail behavior of the steady state for $x \geq L$, and satisfies $\omega_b, \theta_{b,x} \in C^5$ and $\omega_b \sim x^\alpha$, $\theta_{x,b} \sim x^{2\alpha}$ with $\alpha \approx \bar{c}_\omega/\bar{c}_l < -\frac{1}{3}$. The construction of ω_b and its Hilbert transform relies on the following crucial identity

$$H(\mathrm{sgn}(x)|x|^{-a}) = -\cot\frac{\pi a}{2} \cdot |x|^{-a}, \quad a \in (0, 1), \tag{4.2}$$

which is proved in the proof of Lemma A.5 in the Appendix. It indicates that the leading order behavior of Hf for large x is given by $-\cot\frac{\pi a}{2} \cdot |x|^{-a}$, if f is odd with a decay rate $|x|^{-a}$. By perturbing $\mathrm{sgn}(x)|x|^{-a}$ and (4.2), we construct $\omega_b \in C^5$ and

obtain the leading order behavior of $H\omega_b$ for large x. This is one of the main reasons that we can compute the Hilbert transform of a function with slow decay accurately and overcome large round-off error in its computation. The perturbation part (ω_p, θ_p) is constructed numerically using a quintic spline interpolation and methods similar to those in [11] in the domain $[-L, L]$ for some reasonably large L (around 10^{16}). By our construction, they satisfy that $\omega_p, \theta_{p,x} \in C_c^3$. Since achieving a small residual error is critical to our proof, a large portion of the Supplementary Material [10] is devoted to the construction (Section 10) and error estimates of the approximate steady state (Section 11-15) with the above decomposition, especially the ω_b part.

4.1 Connection to the approximate steady state of the 2D Boussinesq in $\mathbb{R}^2_+$

To generalize the current framework to the 2D Boussinesq equations, an important step is to construct an approximate steady state with a sufficiently residual error. The construction of the approximate steady state of the HL model provides important guidelines on this. The steady state equations of the dynamic rescaling formulation of the 2D Boussinesq, see e.g. [7], read

$$\begin{aligned}&(c_l x + \mathbf{u}) \cdot \nabla \omega = c_\omega \omega + \theta_x,\\ &(c_l x + \mathbf{u}) \cdot \nabla \theta = (c_l + 2c_\omega)\theta, \quad \mathbf{u} = \nabla^\perp (-\Delta)^{-1}\omega.\end{aligned}$$

Denote $r = |x|$. Assume that the velocity u grows sub-linearly in the far field : $\frac{u(x)}{r} \to 0$ as $r \to \infty$ and the scaling factors satisfy $c_l > 0, c_\omega < 0$. Note that $x \cdot \nabla = r\partial_r$. Passing to the polar coordinate $(r, \beta), r = |x|, \beta = \arctan \frac{x_2}{x_1}$ and dropping the lower order terms, we yield

$$c_l r \partial_r \omega(r, \beta) = c_\omega \omega + \theta_x + l.o.t., \quad c_l r \partial_r \theta(r, \beta) = (2c_\omega + c_l)\theta + l.o.t.$$

Using an argument similar to the above argument for the HL model, we obtain

$$\omega(r, \beta) \sim p(\beta) r^\alpha, \quad \theta(r, \beta) \sim q(\beta) r^{1+2\alpha}, \quad \alpha = \frac{c_\omega}{c_l} < 0.$$

We remark that θ_x has a decay rate $r^{2\alpha}$ faster than that of ω. The computation in [55] suggests that $\alpha \approx -\frac{1}{3}$. Thus, the profile (if it exists) for the 2D Boussinesq does not have a fast decay, and we also encounter the difficulties similar to (1) and (2). In particular, the 2D analog of difficulty (2) is to obtain the stream function $\psi = (-\Delta)^{-1}\omega$ accurately in $\mathbb{R}^2_+$. To design a practical method that overcomes these difficulties, it is important to perform a decomposition similar to (4.1), where $\omega_p, \nabla\theta_p$ have compact support and ω_b, θ_b capture the tail behavior of the steady state. For the 2D Boussinesq, ω_b, θ_b become semi-analytic since the angular part $p(\beta), q(\beta)$ cannot be determined a-priori. To overcome the difficulty of solving the stream function in the far field, we seek a generalization of (4.2). We consider the ansatz $\psi = r^{2+\alpha} f(\beta)$ and solve

$$-\Delta(r^{2+\alpha} f(\beta)) = r^\alpha p(\beta)$$

with boundary condition $f(0) = f(\pi/2) = 0$ due to the Dirichlet boundary condition and the odd symmetry for the solution ω. In the polar coordinate, the above equation is equivalent to

$$(-\partial_\beta^2 - (2+\alpha)^2) f(\beta) = p(\beta), \quad f(0) = f(\pi/2) = 0.$$

Solving the above equation is significantly simpler than solving $-\Delta\psi = \omega$ in $\mathbb{R}^2_+$ since it is one-dimensional and in a compact domain. The above two formulas are a generalization of (4.2) that connects the leading order far field behavior of ω with that of the velocity. We believe that the above decomposition is crucial to construct the approximate steady state with sufficiently small residual error for the 2D Boussinesq equations. The supplementary material on the analysis of the decomposition (4.1) for the HL model can be seen as a preparation for the more complicated decomposition in the 2D Boussineq equations.

5 Nonlinear stability and finite time blowup

In this section, we further establish nonlinear stability analysis of (3.6).

5.1 Weighted H^1 estimate

In order to obtain nonlinear stability, we first establish the weighted H^1 estimate similar to

$$\begin{aligned}\frac{1}{2}\frac{d}{dt}(||D_x\theta_x\psi^{1/2}||_2^2 + \lambda_1||D_x\omega\varphi^{1/2}||_2^2) \le -c(||D_x\theta_x\psi^{1/2}||_2^2 \\ + \lambda_1||D_x\omega\varphi^{1/2}||_2^2) + CE_1^2(\theta,\omega) + \mathcal{R}_{H^1}\end{aligned} \tag{5.1}$$

for some $c, C > 0$, where $D_x = x\partial_x$, E_1 is defined in (3.55) and $\mathcal{R}_{H^1}$ are the error terms and nonlinear terms in the weighted H^1 estimate to be introduced.

In the work of Elgindi-Ghoul-Masmoudi [26], they made a good observation that the weighted H^1 estimates of the equation studied in [26] can be established by performing weighted L^2 estimates of $x\partial_x f$ with the same weight as that in the weighted L^2 estimate, since the commutator between the linearized operator and $x\partial_x$ is of lower order. Inspired by this observation, we perform weighted L^2 estimates on $x\partial_x\theta_x$ and $x\partial_x\omega$. However, one important difference between our problem and that considered in [26] is that the commutator between the linearized operator in (3.6) and $x\partial_x$ is not of lower order.

Denote $D_x = x\partial_x$. Similar weighted derivatives have been used in [7, 24, 26] for stability analysis. We derive the equations for $D_x\theta_x$, $D_x\omega$. Taking D_x on both side of

(3.6), we get

$$\begin{aligned}\partial_t D_x\theta_x &= \mathcal{L}_{\theta 1}(D_x\theta_x, D_x\omega) + c_\omega D_x(\bar{\theta}_x - x\bar{\theta}_{xx})\\ &\quad + [D_x, \mathcal{L}_{\theta 1}](\theta_x, \omega) + D_x F_\theta + D_x N(\theta),\\ \partial_t D_x\omega &= \mathcal{L}_{\omega 1}(D_x\theta_x, D_x\omega) + c_\omega D_x(\bar{\omega} - x\bar{\omega}_x)\\ &\quad + [D_x, \mathcal{L}_{\omega 1}](\theta_x, \omega) + D_x F_\theta + D_x N(\theta),\end{aligned} \tag{5.2}$$

where $[D_x, \mathcal{L}](f, g) \triangleq D_x\mathcal{L}(f, g) - \mathcal{L}(D_x f, D_x g)$. In the Appendix B.4, we obtain the following formulas for the commutators

$$\begin{aligned}[D_x, \mathcal{L}_{\theta 1}](\theta_x, \omega) &= -(\bar{u}_x - \frac{\bar{u}}{x})D_x\theta_x - D_x\bar{u}_x\theta_x - D_x\tilde{u}\bar{\theta}_{xx} - \tilde{u}(\bar{\theta}_{xx} + D_x\bar{\theta}_{xx}),\\ [D_x, \mathcal{L}_{\omega 1}](\theta_x, \omega) &= -(\bar{u}_x - \frac{\bar{u}}{x})D_x\omega - \tilde{u}(\bar{\omega}_x + D_x\bar{\omega}_x),\end{aligned} \tag{5.3}$$

where $\tilde{u}, \tilde{u}_x$ are defined in (3.10).

Performing the weighted H^1 estimates, we get

$$\begin{aligned}&\frac{1}{2}\frac{d}{dt}\Big(\langle D_x\theta_x, D_x\theta_x\psi\rangle + \lambda_1\langle D_x\omega, D_x\omega\varphi\rangle\Big)\\ &\qquad = \Big(\langle \mathcal{L}_{\theta 1}(D_x\theta, D_x\omega), D_x\theta_x\psi\rangle + \lambda_1\langle \mathcal{L}_{\omega 1}(D_x\theta, D_x\omega), D_x\omega\varphi\rangle\Big)\\ &\qquad + \Big(\langle [D_x, \mathcal{L}_{\theta 1}](\theta_x, \omega), D_x\theta_x\psi\rangle + \lambda_1\langle [D_x, \mathcal{L}_{\omega 1}](\theta_x, \omega), D_x\omega\varphi\rangle\Big)\\ &\qquad + \Big(\langle c_\omega D_x(\bar{\theta}_x - x\bar{\theta}_{xx}), D_x\theta_x\psi\rangle\\ &\qquad + \lambda_1\langle c_\omega D_x(\bar{\omega} - x\bar{\omega}_x), D_x\omega\varphi\rangle\Big) + \mathcal{R}_{H^1}\\ &\qquad \triangleq Q_1 + Q_2 + Q_3 + \mathcal{R}_{H^1},\end{aligned} \tag{5.4}$$

where $\mathcal{R}_{H^1}$ is the remaining term in the weighted H^1 estimate

$$\begin{aligned}\mathcal{R}_{H^1} &= \langle D_x N(\theta), D_x\theta_x\psi\rangle + \lambda_1\langle D_x N(\omega), D_x\omega\varphi\rangle\\ &+\langle D_x F_\theta, D_x\theta_x\psi\rangle + \lambda_1\langle D_x F_\omega, D_x\omega\varphi\rangle.\end{aligned} \tag{5.5}$$

5.1.1 Estimate of Q_1

Applying the estimate of $\mathcal{L}_{\theta,1}, \mathcal{L}_{\omega 1}$ in (3.38) to $(D_x\theta_x, D_x\omega)$, we obtain

$$\begin{aligned}Q_1 &\le \langle D_\theta + A_\theta\psi^{-1}, (D_x\theta_x)^2\psi\rangle + \langle \lambda_1 D_\omega + A_\omega\varphi^{-1}, (D_x\omega)^2\varphi\rangle\\ &\quad + A(-\Lambda^{-1}(D_x\omega)) + G_c\cdot(H D_x\omega(0))^2,\end{aligned} \tag{5.6}$$

where G_c is defined in (3.37), and we have dropped the term related to $||\tilde{u}_x x^{-2/3}||_2^2$ in (3.38) since $D_u - \frac{9}{49}t_{12} - \frac{72\lambda_1}{49}\cdot 10^{-5} > 0$. In addition, we have replaced $u = -\Lambda^{-1}\omega$

in $A(u)$ in (3.38) by $-\Lambda^{-1}(D_x\omega)$ and replaced $c_\omega = H\omega(0)$ by $HD_x\omega(0)$. Recall the definition of $A(u)$ in (3.31). Since $\Lambda = H\partial_x$ and $H \circ H = -Id$, we yield

$$\partial_x(-\Lambda^{-1}D_x\omega)(0) = HD_x\omega(0) = -\frac{1}{\pi}\int_{\mathbb{R}} \omega_x dx = 0,$$

which implies

$$G_c \cdot (H(D_x\omega)(0))^2 = 0, \quad A(-\Lambda^{-1}D_x\omega) \le 0. \tag{5.7}$$

We treat Q_1 as the damping terms in the weighted H^1 estimate since from (D.5), we have

$$D_\theta + A_\theta \psi^{-1} \le -\kappa, \quad \lambda_1 D_\omega + A_\omega \varphi^{-1} \le -\lambda_1\kappa, \quad \kappa > 0. \tag{5.8}$$

5.1.2 Estimate of Q_2

Recall the commutators in (5.3). The profile satisfies $\bar{u}_x - \frac{\bar{u}}{x} > 0$ and thus $-(\bar{u}_x - \frac{\bar{u}}{x})f$ with $f = D_x\theta_x, D_x\omega$ is a damping term in the $D_x\theta_x$ or $D_x\omega$ equation. We do not estimate these terms.

For the term $D_x\bar{u}_x\theta_x$ in (5.3), using integration by parts, we get

$$-\langle D_x\bar{u}_x\theta_x, D_x\theta_x\psi\rangle = -\langle x^2\bar{u}_{xx}\psi, \frac{1}{2}\partial_x(\theta_x)^2\rangle = \frac{1}{2}\langle (x^2\bar{u}_{xx}\psi)_x, \theta_x^2\psi\rangle.$$

The approximate steady state satisfies the following inequality

$$(x^2\bar{u}_{xx}\psi)_x \le 0.02\psi, \tag{5.9}$$

which will be verified rigorously by the methods in the Supplementary Material [10]. We record it in (D.8), Appendix D. Using (5.9), we obtain

$$-\langle D_x\bar{u}_x\theta_x, D_x\theta_x\psi\rangle \le \varepsilon_1 ||\theta_x\psi^{1/2}||_2^2, \quad \varepsilon_1 = 0.01. \tag{5.10}$$

The nonlocal terms in (5.3) are of lower order than $D_x\omega$ and we estimate then directly. We introduce some weights

$$\begin{aligned} S_{u2} &= t_{71}x^{-6} + t_{72}x^{-4} + 2\cdot 10^{-6}x^{-10/3}, \\ S_{u3} &= t_{81}x^{-6} + t_{82}x^{-4} + 2\cdot 10^{-6}x^{-10/3}, \end{aligned} \tag{5.11}$$

for some parameters $t_{ij} > 0$ to be determined. Using Young's inequality, we get

$$\begin{aligned} &|\langle D_x\tilde{u}\bar{\theta}_{xx}, D_x\theta_x\psi\rangle| + |\langle \tilde{u}(\bar{\theta}_{xx} + D_x\bar{\theta}_{xx}), D_x\theta_x\psi\rangle| \\ &\le ||D_x\tilde{u}S_{u2}^{1/2}||_2^2 + \frac{1}{4}||S_{u2}^{-1/2}\bar{\theta}_{xx}D_x\theta_x\psi||_2^2 + ||\tilde{u}S_{u3}^{1/2}||_2^2 \\ &+ \frac{1}{4}||S_{u3}^{-1/2}(\bar{\theta}_{xx} + D_x\bar{\theta}_{xx})D_x\theta_x\psi||_2^2. \end{aligned} \tag{5.12}$$

We introduce the weights S_{u2}, S_{u3} for a reason similar to that of S_{u1} in Remark 3.6. Recall $D_x\tilde{u} = \tilde{u}_x$ and $\tilde{u}$, $\tilde{u}_x$ in (3.10). Using the weighted estimates in Lemma A.8 yields

$$\begin{aligned} &||D_x\tilde{u}S_{u2}^{1/2}||_2^2 + ||\tilde{u}S_{u3}^{1/2}||_2^2 \\ \leq &\Big\langle \omega^2, (t_{71} + \frac{4t_{81}}{25})x^{-4} + (t_{72} + \frac{4t_{82}}{9})x^{-2} \Big\rangle + (1 + \frac{36}{49}) \cdot 2 \cdot 10^{-6}||\tilde{u}_x x^{-2/3}||_2^2. \end{aligned} \tag{5.13}$$

In (5.13), we do not estimate $||\tilde{u}_x x^{-2/3}||_2^2$ in $||D_x\tilde{u}S_{u2}^{1/2}||_2$ and keep it on both sides.

Remark 5.1 We will choose large enough parameters t_{ij} in S_{u2}, S_{u3} (5.11) so that the weighted L^2 norm of $D_x\theta_x$ terms in (5.12) are relative small compared to the damping term of $D_x\theta_x$ in the weighted H^1 estimate (5.4), e.g. Q_1 in (5.6). See also (5.8). The weighted L^2 norm of ω and $||\tilde{u}_x x^{-2/3}||_2$ in (5.13) will be bounded using the damping terms in the weighted L^2 estimate (3.57). The same argument applies to controlling the weighted L^2 norm of $D_x\omega$ term in (5.18).

Next, we estimate the $\tilde{u}((\bar{\omega}_x + D_x\bar{\omega})$ term in (5.3). The idea is similar to that in Section 3.8. We perform the following decomposition

$$\begin{aligned} -\lambda_1\langle\tilde{u}(\bar{\omega}_x + D_x\bar{\omega}_x), D_x\omega\varphi\rangle &= -\lambda_1\langle\tilde{u}(\bar{\omega}_x + D_x\bar{\omega}_x - \frac{1}{3}\chi\xi_3), D_x\omega\varphi\rangle \\ &\quad - \frac{1}{3}\lambda_1\langle\tilde{u}\chi\xi_3, D_x\omega\varphi\rangle \\ &\triangleq J + I_{r3}. \end{aligned} \tag{5.14}$$

The estimate of I_{r3} is similar to (3.36) and we obtain the following estimate in Appendix B.2

$$|I_{r3}| \leq \langle G_{\omega 2}, \omega^2\rangle + \langle G_{\omega 3}, (D_x\omega)^2\rangle + G_{c2}c_\omega^2, \tag{5.15}$$

where $G_{\omega 2}$, $G_{\omega 3}$ and G_{c2} are given by

$$\begin{aligned} G_{\omega 2} &= \frac{1}{4\cdot 10^6}(\frac{2\lambda_1(2+\sqrt{3})}{5})^2 x^{-2/3}, \quad G_{c2} = \frac{\lambda_1^2||x\xi_3\chi^{1/2}\varphi^{1/2}||_2^2}{36} \cdot 10^3, \\ G_{\omega 3} &= 10^6(x^{4/3}\chi\xi_3\varphi)^2 + 10^{-3}\chi\varphi. \end{aligned} \tag{5.16}$$

These functions are small due to the same reason that we describe in Section 3.9.

For J, we perform a decomposition

$$\begin{aligned} J = &-\lambda_1\Big\langle\tilde{u}, \Big((\bar{\omega}_x + D_x\bar{\omega}_x - \frac{1}{3}\chi\xi_3)\varphi - \frac{e_3\alpha_6}{9}x^{-2}\Big)D_x\omega\Big\rangle \\ &-\frac{\lambda_1 e_3\alpha_6}{9}\langle\tilde{u}, D_x\omega x^{-2}\rangle \triangleq I_1 + I_2 \end{aligned}$$

Note that $\tilde{u} = u - u_x(0)x$ and $\int_0^\infty x D_x\omega x^{-2}dx = \int_0^\infty \omega_x dx = 0$. Using Lemma A.4 with $f = \omega$ and $g = u$, we get

$$I_2 = -\frac{\lambda_1 e_3\alpha_6}{9}\Big(\langle u, D_x\omega x^{-2}\rangle - u_x(0)\int_0^\infty x D_x\omega x^{-2}dx\Big) = -\frac{\lambda_1 e_3\alpha_6}{9}\langle u, \omega_x x^{-1}\rangle$$
$$= \frac{\lambda_1 e_3\alpha_6}{9}\langle \Lambda\frac{u}{x}, \frac{u}{x}\rangle,$$

which can be controlled using the damping term in (3.57). Denote

$$S_{u4} = t_{91}x^{-6} + t_{92}x^{-4} + 5\cdot 10^{-4}x^{-10/3},$$
$$\mathcal{K}_{u\omega 2} = (\bar{\omega}_x + D_x\bar{\omega}_x - \frac{1}{3}\chi\xi_3)\varphi - \frac{e_3\alpha_6}{9}x^{-2}. \tag{5.17}$$

For I_1, using Young's inequality and the weighted estimate in Lemma A.8, we get

$$\begin{aligned} |I_1| &\le \lambda_1\langle S_{u4}, \tilde{u}^2\rangle + \frac{\lambda_1}{4}\langle \mathcal{K}_{u\omega 2}^2 S_{u4}^{-1}, (D_x\omega)^2\rangle \\ &\le \lambda_1\langle \omega^2, \frac{4t_{91}}{25}x^{-4} + \frac{4t_{92}}{9}x^{-2}\rangle + \frac{36\lambda_1}{49}\cdot 5\cdot 10^{-4}||\tilde{u}_x x^{-2/3}||_2^2 \\ &+ \frac{\lambda_1}{4}\langle \mathcal{K}_{u\omega 2}^2 S_{u4}^{-1}, (D_x\omega)^2\rangle. \end{aligned} \tag{5.18}$$

We introduce the weight S_{u4} for a reason similar to that of S_{u1} in Remark 3.6. The $||\tilde{u}_x x^{-2/3}||_2^2$ term is further controlled by the corresponding damping term in (3.57).

Combining the above estimates on the commutators in (5.3), we obtain

$$\begin{aligned} Q_2 \le& \langle -(\bar{u}_x - \frac{\bar{u}}{x}) + B_\theta\psi^{-1}, (D_x\theta_x)^2\psi\rangle + \langle -\lambda_1(\bar{u}_x - \frac{\bar{u}}{x}) + B_\omega\varphi^{-1}, (D_x\omega)^2\varphi\rangle \\ &+ \varepsilon_1||\theta_x\psi^{1/2}||_2^2 \\ &+ \langle A_{\omega 2}, \omega^2\rangle + \frac{\lambda_1 e_3\alpha_6}{9}\langle \Lambda\frac{u}{x}, \frac{u}{x}\rangle + \Big((1+\frac{36}{49})\cdot 2\cdot 10^{-6} \\ &+ \frac{36\lambda_1}{49}\cdot 5\cdot 10^{-4}\Big)||\tilde{u}_x x^{-2/3}||_2^2 + G_{c2}c_\omega^2, \end{aligned} \tag{5.19}$$

where G_{c2} is defined in (5.16). The term $(\bar{u}_x - \frac{\bar{u}}{x})$ comes from the commutators (5.3) and we do not estimate them in Q_2 in (5.4). The terms B_θ, B_ω, $A_{\omega 2}$ are the sum of the coefficients in the integrals of $(D_x\theta_x)^2$, $(D_w\omega)^2$, ω^2 in the above estimates

$$\begin{aligned} &B_\theta \triangleq \frac{1}{4}S_{u2}^{-1}(\bar{\theta}_{xx}\psi)^2 + \frac{1}{4}S_{u3}^{-1}\left(\bar{\theta}_{xx} + D_x\bar{\theta}_{xx}\right)^2\psi^2, \quad B_\omega \triangleq \frac{\lambda_1}{4}\mathcal{K}_{u\omega 2}^2 S_{u4}^{-1} + G_{\omega 3}, \\ &A_{\omega 2} \triangleq \left(t_{71} + \frac{4t_{81}}{25}\right)x^{-4} + \left(t_{72} + \frac{4t_{82}}{9}\right)x^{-2} + \lambda_1\left(\frac{4t_{91}}{25}x^{-4} + \frac{4t_{92}}{9}x^{-2}\right) + G_{\omega 2}. \end{aligned} \tag{5.20}$$

5.1.3 Estimate of Q_3

Recall the c_ω terms in (5.2). Denote by K_1, K_2 the following L^2 norms

$$K_1 \triangleq ||\partial_x(x^3\bar{\theta}_{xxx}\psi)\psi^{-1/2}||_2, \quad K_2 \triangleq ||\partial_x(x^3\bar{\omega}_{xx}\varphi)\varphi^{-1/2}||_2. \tag{5.21}$$

Using integration by parts and the Cauchy-Schwarz inequality, we obtain

$$\begin{aligned}|c_\omega\langle D_x(\bar{\theta}_x - x\bar{\theta}_{xx}), D_x\theta_x\psi\rangle| =& |c_\omega\langle -x^2\bar{\theta}_{xxx}\cdot(x\psi),\ \partial_x\theta_x\rangle| = |c_\omega\langle\partial_x(x^3\bar{\theta}_{xxx}\psi), \theta_x\rangle| \\ \le& |c_\omega|\cdot||\partial_x(x^3\bar{\theta}_{xxx}\psi)\psi^{-1/2}||_2||\theta_x\psi^{1/2}||_2 \\ *=& K_1|c_\omega|\cdot||\theta_x\psi^{1/2}||_2,\end{aligned}$$

where we have used $x\partial_x(f - x\partial_x f) = -x^2 f_{xx}$, $f = \bar{\theta}_x$ in the first equality. Similarly, we have

$$\begin{aligned}&\lambda_1|c_\omega\langle D_x(\bar{\omega} - x\bar{\omega}_x), D_x\omega\varphi\rangle| \le \lambda_1|c_\omega|\cdot||\partial_x(x^3\bar{\omega}_{xx}\varphi)\varphi^{-1/2}||_2||\omega\varphi^{1/2}||_2 \\ &= \lambda_1 K_2|c_\omega|\cdot||\omega\varphi^{1/2}||_2.\end{aligned}$$

Using Young's inequality, we obtain

$$\begin{aligned}Q_3 \le& K_1|c_\omega|\cdot||\theta_x\psi^{1/2}||_2 + \lambda_1 K_2|c_\omega|\cdot||\omega\varphi^{1/2}||_2 \\ \le& \gamma_1||\theta_x\psi^{1/2}||_2^2 + \gamma_2||\omega\varphi^{1/2}||_2^2 + c_\omega^2\Big(\frac{K_1^2}{4\gamma_1} + \frac{(\lambda_1 K_2)^2}{4\gamma_2}\Big),\end{aligned} \tag{5.22}$$

where $\gamma_1, \gamma_2 > 0$ are chosen in (C.4).

5.1.4 Summary of the estimates

We determine the parameters t_{ij} in the estimates in Sections 5.1.1-5.1.3 and choose κ_2 so that

$$\begin{aligned}&D_{\theta_2} + B_\theta\psi^{-1} \le -\kappa_2, \quad D_{\omega 2} + B_\omega\varphi^{-1} \le -\kappa_2\lambda_1, \\ &D_{\theta 2} \triangleq D_\theta + A_\theta\psi^{-1} - (\bar{u}_x - \frac{\bar{u}}{x}), \quad D_{\omega 2} \triangleq \lambda_1 D_\omega + A_\omega\varphi^{-1} - \lambda_1(\bar{u}_x - \frac{\bar{u}}{x}).\end{aligned} \tag{5.23}$$

The terms $D_{\theta 2}$, $D_{\omega 2}$ are the coefficients of the damping terms in the weighted H^1 estimate (5.4) and are already determined in the weighted L^2 estimates. The terms $B_\theta\psi^{-1}$, $B_\omega\varphi^{-1}$ defined in (5.20) are the coefficients in the weighted L^2 norm of $D_x\theta_x$, $D_x\omega$ in (5.12), (5.18). The motivation of (5.23) is that we use the damping terms to control the weighted L^2 norms of $D_x\theta_x$, $D_x\omega$ in the estimates of Q_i. The idea is the same as that in Remark 5.1.

We first choose $\kappa_2 < \kappa = 0.03$ in Appendix C, where κ is related to (3.58). This choice is motivated by our estimate (5.28). The dependences of $A_{\omega 2}$, B_θ, B_ω on t_{ij} are given in (5.20), (5.11), (5.17). Inequalities in (5.23) can be seen as constraints on t_{ij}.

We choose t_{ij} subject to the constraints (5.23) such that $||A_{\omega 2}\varphi^{-1}||_\infty$ is as small as possible. This enables us to obtain sharper constant a_{H^1} in the weighted H^1 estimate (5.25). After t_{ij} are determined, we verify (5.23) and

$$||A_{\omega 2}\varphi^{-1}||_\infty \le a_{H^1}, \tag{5.24}$$

using the methods in the Supplementary Material [10], and record them in (D.9), Appendix D, where a_{H^1} is given in (C.4).

Combining (5.6), (5.7), (5.10), (5.19), (5.22) and (5.23), we prove

$$\begin{aligned}
&\frac{1}{2}\frac{d}{dt}(||(D_x\theta_x)\psi^{1/2}||_2^2+\lambda_1||(D_x\omega)\varphi^{1/2}||_2^2) \le -\kappa_2||(D_x\theta_x)\psi^{1/2}||_2^2-\kappa_2\lambda_1||(D_x\omega)\varphi^{1/2}||_2^2\\
&+(\varepsilon_1+\gamma_1)||\theta_x\psi^{1/2}||_2^2+(a_{H^1}+\gamma_2)||\omega\varphi^{1/2}||_2^2+\Big(G_{c2}+\frac{K_1^2}{4\gamma_1}+\frac{(\lambda_1K_2)^2}{4\gamma_2}\Big)c_\omega^2\\
&+\frac{\lambda_1e_3\alpha_6}{9}\langle\Lambda\frac{u}{x},\frac{u}{x}\rangle+\Big((1+\frac{36}{49})\cdot 2\cdot 10^{-6}+\frac{36\lambda_1}{49}\cdot 5\cdot 10^{-4}\Big)||\tilde{u}_x x^{-2/3}||_2^2+\mathcal{R}_{H^1}.
\end{aligned} \tag{5.25}$$

Recall the weighted L^2 energy E_1 in (3.55). For some $\lambda_4>0$, we construct the energy

$$\begin{aligned}
&E^2(\theta_x,\omega)=E_1^2(\theta_x,\omega)+\lambda_4(||D_x\theta_x\psi^{1/2}||_2^2+\lambda_1||D_x\omega\varphi^{1/2}||_2^2)\\
=&||\theta_x\psi^{1/2}||_2^2+\lambda_1||\omega\psi^{1/2}||_2^2+\lambda_2\frac{\pi}{2}c_\omega^2+\lambda_3d_\theta^2\\
&+\lambda_4(||D_x\theta_x\psi^{1/2}||_2^2+\lambda_1||D_x\omega\varphi^{1/2}||_2^2).
\end{aligned} \tag{5.26}$$

Note that c_ω, $||\theta_x\psi^{1/2}||_2$, $||\omega\varphi^{1/2}||_2$ in (5.25) can be bounded by the energy E_1 in (3.55). The terms $\langle\Lambda\frac{u}{x},\frac{u}{x}\rangle$ and $||\tilde{u}_x x^{-2/3}||_2^2$ can be bounded by their damping terms in (3.57). To motivate later estimates and the choice of several parameters, we neglect these two terms. Then (5.25) implies (5.1) with $c=\kappa_2$ and some $C>0$. Combining (3.58) and (5.1), we get

$$\begin{aligned}
&\frac{1}{2}\frac{d}{dt}E^2(\theta_x,\omega)\le-(\kappa-\lambda_4C)E_1^2-\kappa_2(||D_x\theta_x\psi^{1/2}||_2^2+\lambda_1||D_x\omega\varphi^{1/2}||_2^2)+\mathcal{R}_{L^2}\\
&+\lambda_4\mathcal{R}_{H^1},
\end{aligned} \tag{5.27}$$

where $\kappa=0.03$. We first choose $\kappa_2<\kappa$ and then λ_4 small enough, such that

$$\kappa-\lambda_4C\ge\kappa_2. \tag{5.28}$$

Then we obtain the linear stability of (3.6) in the energy norm E.

5.2 Nonlinear stability

Combining (3.57) and (5.25), we derive

$$\begin{aligned}\frac{1}{2}\frac{d}{dt}E^2(\theta_x,\omega) \le & -\kappa||\theta_x\psi^{1/2}||_2^2-\kappa\lambda_1||\omega\varphi^{1/2}||_2^2-r_{c_\omega}c_\omega^2-\kappa\lambda_3 d_\theta^2\\ & -\lambda_4\kappa_2||(D_x\theta_x)\psi^{1/2}||_2^2-\lambda_4\kappa_2\lambda_1||(D_x\omega)\varphi^{1/2}||_2^2+\lambda_4(\varepsilon_1+\gamma_1)||\theta_x\psi^{1/2}||_2^2\\ & +\lambda_4(a_{H^1}+\gamma_2)||\omega\varphi^{1/2}||_2^2+\lambda_4\Big(G_{c2}+\frac{K_1^2}{4\gamma_1}+\frac{(\lambda_1K_2)^2}{4\gamma_2}\Big)c_\omega^2\\ & +\left(\frac{\lambda_1e_3\alpha_6}{9}\lambda_4-\frac{\lambda_1e_3\alpha_6}{3}\right)\left\langle\Lambda\frac{u}{x},\frac{u}{x}\right\rangle\\ & +\Big(\Big((1+\frac{36}{49})\cdot 2\cdot 10^{-6}+\frac{36\lambda_1}{49}\cdot 5\cdot 10^{-4}\Big)\lambda_4-10^{-6}\Big)||\tilde{u}_x x^{-2/3}||_2^2\\ & +\mathcal{R}_{L^2}+\lambda_4\mathcal{R}_{H^1}.\end{aligned}$$

Since $\kappa_2<\kappa$, we choose small $\lambda_4>0$ in Appendix C so that

$$\begin{aligned}&\lambda_4\cdot\frac{\lambda_1e_3\alpha_6}{9}<\frac{\lambda_1e_3\alpha_6}{3},\quad \Big((1+\frac{36}{49})\cdot 2\cdot 10^{-6}+\frac{36\lambda_1}{49}\cdot 5\cdot 10^{-4}\Big)\lambda_4<10^{-6},\\ &r_{c_\omega}-\lambda_4\Big(\frac{K_1^2}{4\gamma_1}+\frac{(\lambda_1K_2)^2}{4\gamma_2}\Big)-\lambda_4G_{c2}>\kappa_2\cdot\frac{\pi\lambda_2}{2},\\ &\kappa-\lambda_4\gamma_1-\lambda_4\varepsilon_1\ge\kappa_2,\quad \kappa\lambda_1-\lambda_4\gamma_2-\lambda_4a_{H^1}\ge\kappa_2\lambda_1,\quad \kappa\lambda_3\ge\kappa_2\lambda_3,\end{aligned}\tag{5.29}$$

where K_1, K_2 are defined in (5.21). The above inequalities will be verified rigorously by the methods in the Supplementary Material [10]. Note that $r_{c_\omega}>\frac{\pi}{2}\lambda_2\kappa$ and $\kappa_2<\kappa$. The above conditions are essentially the same as (5.28). We keep the damping term $\langle\Lambda\frac{u}{x},\frac{u}{x}\rangle$ and $||\tilde{u}_x x^{-2/3}||_2^2$ in (3.57) to control the corresponding terms in (5.25). Plugging the above estimates and (5.29) into the differential inequality, we yield

$$\begin{aligned}\frac{1}{2}\frac{d}{dt}E^2(\theta_x,\omega)\le & -\kappa_2||\theta_x\psi^{1/2}||_2^2-\kappa_2\lambda_1||\omega\varphi^{1/2}||_2^2-\kappa_2\frac{\pi\lambda_2}{2}c_\omega^2-\kappa_2\lambda_3d_\theta^2\\ & -\lambda_4\kappa_2||(D_x\theta_x)\psi^{1/2}||_2^2-\lambda_4\kappa_2\lambda_1||(D_x\omega)\varphi^{1/2}||_2^2+\mathcal{R}_{L^2}+\lambda_4\mathcal{R}_{H^1}\\ \le & -\kappa_2E^2(\theta_x,\omega)+\mathcal{R}_{L^2}+\lambda_4\mathcal{R}_{H^1}\triangleq-\kappa_2E^2(\theta_x,\omega)+\mathcal{R},\end{aligned}\tag{5.30}$$

where $\mathcal{R}=\mathcal{R}_{L^2}+\lambda_4\mathcal{R}_{H^1}$ and $\kappa_2=0.024$ is given in (C.4).

5.2.1 Outline of the estimates of the nonlinear and error terms

Recall the definitions of $\mathcal{R}_{L^2}$ and $\mathcal{R}_{H^1}$ in (3.56) and (5.5). The nonlinear terms in $\mathcal{R}_{L^2}$, $\mathcal{R}_{H^1}$, e.g. $\langle D_xN(\theta),D_x\theta_x\psi\rangle$, depend cubically on θ_x,ω. In the Supplementary Material [10], we use the energy $E(\theta_x,\omega)$ and interpolation to control $||u_x||_\infty$ and $||\theta_x||_\infty$. Using these L^∞ estimates, we further estimate the nonlinear terms in $\mathcal{R}$. For

example, a typical nonlinear term in $\mathcal{R}$ can be estimated as follows

$$\begin{aligned}|\langle u\theta_{xx}, \theta_x\psi\rangle| &= \frac{1}{2}|\langle u\psi, \partial_x(\theta_x)^2\rangle| = \frac{1}{2}|\langle (u\psi)_x, \theta_x^2\rangle| = \frac{1}{2}|\langle u_x\psi + u\psi_x, \theta_x^2\rangle| \\ &\leq \frac{1}{2}(||u_x||_{L^\infty} + ||\frac{u}{x}||_\infty||\frac{x\psi_x}{\psi}||_{L^\infty})||\theta_x\psi^{1/2}||_2^2 \\ &\leq \frac{1}{2}||u_x||_{L^\infty}\left(1 + ||\frac{x\psi_x}{\psi}||_{L^\infty}\right)||\theta_x\psi^{1/2}||_2^2,\end{aligned}$$

where we have used $|\frac{u}{x}| \leq ||u_x||_\infty$ in the last inequality since $u(0) = 0$. The above upper bound can be further bounded by $E^3(\theta_x, \omega)$.

The error terms in $\mathcal{R}_{L^2}, \mathcal{R}_{H^1}$, e.g. $F_1 = \langle F_\theta, \theta_x\psi\rangle$, depend linearly on θ_x, ω. We estimate these terms using the Cauchy-Schwarz inequality. A typical term F_1 can be estimated as follows

$$|F_1| \leq ||F_\theta\psi^{1/2}||_2||\theta_x\psi^{1/2}||_2.$$

The error term $||F_\theta\psi^{1/2}||_2$ is small and $||\theta_x\psi^{1/2}||_2$ can be further bounded by $E(\theta_x, \omega)$.

In the Supplementary Material [10], we work out the constants in these estimates and establish the following estimates

$$\mathcal{R} = \mathcal{R}_{L^2} + \lambda_4\mathcal{R}_{L^2} \leq 36E^3 + \varepsilon E, \quad \varepsilon = 5.5 \cdot 10^{-7}.$$

5.2.2 Nonlinear stability and finite time blowup

Plugging the above estimate on $\mathcal{R}$ in (5.30), we establish the nonlinear estimate

$$\frac{1}{2}\frac{d}{dt}E^2(\theta_x, \omega) \leq -\kappa_2 E(\theta_x, \omega)^2 + 36E(\theta_x, \omega)^3 + \varepsilon E(\theta_x, \omega),$$

where $\kappa_2 = 0.024$ is given in (C.4). We choose the threshold $E_* = 2.5 \cdot 10^{-5}$ in the Bootstrap argument. Since

$$-\kappa_2 E_*^2 + 36E_*^3 + \varepsilon E_* < 0,$$

the above differential inequality implies that if $E(0) < E_*$, the bootstrap assumption

$$E(\theta_x(t), \omega(t)) < E_* \tag{5.31}$$

holds for all $t > 0$. Consequently, we can choose odd initial perturbations θ_x, ω which satisfy $\omega_x(0) = \theta_{xx}(0) = 0$, $E(\theta_x, \omega) < E_*$ and modify the far field of $\bar{\theta}, \bar{\omega}$ so that $\bar{\omega} + \omega, \theta_x + \bar{\theta}_x \in C_c^\infty$. The bootstrap result implies that for all time $t > 0$, the solution $\omega(t) + \bar{\omega}, \theta_x(t) + \bar{\theta}_x, c_l(t) + \bar{c}_l, c_\omega(t) + \bar{c}_\omega$ remain close to $\bar{\omega}, \bar{\theta}_x, \bar{c}_l, \bar{c}_\omega$, respectively. Using the rescaling argument in Section 2, we obtain finite time blowup of the HL model.

5.3 Convergence to the steady state

We use the time-differentiation argument in [11] to establish convergence. The initial perturbations (θ_x, ω) satisfy the properties in the previous Section. Since the linearized operators and the error terms in (3.6) are time-independent, differentiating (3.6) in t, we get

$$\partial_t(\theta_x)_t = \mathcal{L}_\theta((\theta_x)_t, \omega_t) + \partial_t N(\theta), \quad \partial_t(\omega)_t = \mathcal{L}_\omega((\theta_x)_t, \omega_t) + \partial_t N(\omega).$$

Applying the estimates of $\mathcal{L}_\theta, \mathcal{L}_\omega$ in Section 3 and (3.58) to $(\theta_x)_t, \omega_t$, we obtain

$$\frac{1}{2}\frac{d}{dt}E_1((\theta_x)_t, \omega_t)^2 \le -\kappa E_1((\theta_x)_t, \omega_t)^2 + \mathcal{R}_2,$$

where the energy notation E_1 is defined in (3.55) and $\mathcal{R}_2$ is given by

$$\begin{aligned} &E_1((\theta_x)_t, \omega_t) = ||(\theta_x)_t\psi^{1/2}||_2^2 + \lambda_1||\omega_t\psi^{1/2}||_2^2 + \lambda_2\frac{\pi}{2}(\partial_t c_\omega)^2 + \lambda_3(\partial_t d_\theta)^2,\\ &\mathcal{R}_2 = \langle\partial_t N(\theta), (\theta_x)_t\psi\rangle + \lambda_1\langle\partial_t N(\omega), \omega_t\varphi\rangle\\ &- \lambda_2\partial_t c_\omega\langle\partial_t N(\omega), x^{-1}\rangle + \lambda_3\partial_t d_\theta\langle\partial_t N(\theta), x^{-1}\rangle. \end{aligned}$$

The term $\partial_t c_\omega$ in the above estimates is from

$$H\omega_t(0) = \partial_t H\omega(0) = \partial_t c_\omega.$$

Similarly, we obtain the term $\partial_t d_\theta$. Using the a-priori estimate $E(\theta_x, \omega) < E_*$ in (5.31) and the energy $E_1((\theta_x)_t, \omega_t)$, we can further estimate $\mathcal{R}_2$. In the Supplementary Material [10], we prove

$$\frac{1}{2}\frac{d}{dt}E_1((\theta_x)_t, \omega_t)^2 \le -0.02E_1((\theta_x)_t, \omega_t)^2. \tag{5.32}$$

Using this estimate and the argument in [11], we prove that the solution $\omega + \bar{\omega}, \theta_x + \bar{\theta}_x$ converge to the steady state $\omega_\infty, \theta_{\infty,x}$ in $L^2(\varphi), L^2(\psi)$ and $c_l(t), c_\omega(t)$ converge to $c_{l,\infty}, c_{\omega,\infty}$ exponentially fast. Moreover, the steady state admits regularity $(D_x)^i(\omega_\infty - \bar{\omega}) \in L^2(\varphi), (D_x)^i(\theta_{x,\infty} - \bar{\theta}_x) \in L^2(\psi)$ for $i = 0, 1$. We obtain θ_∞ from $\theta_{\infty,x}$ by imposing $\theta_\infty(0) = 0$ and integration.

Recall the energy E in (5.26). Since

$$\lambda_2\pi/2 > 3 > 1.5^2, \quad E > (\lambda_2\pi/2)^{1/2}|c_\omega| \ge 1.5|c_\omega|$$

(see (C.3)), using the convergence result, the a-priori estimate (5.31) and (3.3), we obtain

$$E(\theta_{x,\infty} - \bar{\theta}_x, \omega_\infty - \bar{\omega}) \le E_*, \quad c_{l,\infty} = \bar{c}_l = 3, \quad |c_{\omega,\infty} - \bar{c}_\omega| \le \frac{2}{3}E_* = \frac{5}{3}\cdot 10^{-5}. \tag{5.33}$$

Recall $\bar{c}_\omega < -1.0004$ from the beginning of Section 3.1. Thus, $c_{\omega,\infty} < -1$ and we conclude that the blowup is focusing and asymptotically self-similar with blowup scaling $\lambda = \frac{c_{l,\infty}}{-c_{\omega,\infty}}$ satisfying

$$|\lambda - \bar{\lambda}| \le |\frac{c_{l,\infty}}{c_{\omega,\infty}} - \frac{\bar{c}_l}{\bar{c}_\omega}| + |\frac{\bar{c}_l}{\bar{c}_\omega} + \bar{\lambda}| < 3|\bar{c}_\omega - c_{\omega,\infty}|$$
$$+10^{-5} < 6 \cdot 10^{-5}, \quad \bar{\lambda} = 2.99870,$$

where $\bar{\lambda}$ is the determined by the first 6 digits of $-\bar{c}_l/\bar{c}_\omega$.

5.4 Uniqueness of the self-similar profiles

Suppose that (ω_1, θ_1) and (ω_2, θ_2) are two initial perturbations which are small in the energy norm $E(\omega_i, \theta_{i,x}) < E_*$. The associated solution $(\omega_i, \theta_{i,x})$ solves (3.6)

$$\partial_t \theta_{i,x} = \mathcal{L}_\theta(\theta_{i,x}, \omega_i) + F_\theta + N(\theta_i), \quad \partial_t \omega_i = \mathcal{L}_\omega(\theta_{i,x}, \omega_i) + F_\omega + N(\omega_i).$$

Denote

$$\delta\omega \triangleq \omega_1 - \omega_2, \quad \delta\theta \triangleq \theta_1 - \theta_2,$$
$$\delta N_\theta = N(\theta_1) - N(\theta_2), \quad \delta N_\omega = N(\omega_1) - N(\omega_2). \tag{5.34}$$

A key observation is that the forcing terms F_θ, F_ω do not depend on (ω_i, θ_i). Thus, we derive

$$\partial_t \delta\theta_x = \mathcal{L}_\theta(\delta\theta_x, \delta\omega) + \delta N_\theta, \quad \partial_t \delta\omega = \mathcal{L}_\omega(\delta\theta_x, \delta\omega) + \delta N_\omega.$$

Applying the estimates of $\mathcal{L}_\theta$, $\mathcal{L}_\omega$ in Section 3 and (3.58), we get

$$\frac{1}{2}\frac{d}{dt} E_1(\delta\theta_x, \delta\omega)^2 \le -\kappa E_1(\delta\theta_x, \delta\omega)^2 + \mathcal{R}_3$$

where the energy notation E_1 is defined in (3.55) and $\mathcal{R}_3$ is given by

$$\mathcal{R}_3 = \langle \delta N_\theta, \delta\theta_x \psi \rangle + \lambda_1 \langle \delta N_\omega, \delta\omega\varphi \rangle - \lambda_2 c_\omega(\delta\omega) \cdot \langle \delta N_\omega, x^{-1} \rangle$$
$$+\lambda_3 d_\theta(\delta\theta_x) \cdot \langle \delta N_\theta, x^{-1} \rangle.$$

The above formulations are very similar to that in Section 5.3. Formally, the difference operator δ is similar to the time differentiation ∂_t. In the Supplementary Material [10], we show that $(\delta\theta_x, \delta\omega)$ enjoys the same estimates as that of $(\partial_t\theta_x, \omega_t)$ in (5.32)

$$\frac{1}{2}\frac{d}{dt} E_1(\delta\theta_x, \delta\omega)^2 \le -0.02 E_1(\delta\theta_x, \delta\omega)^2. \tag{5.35}$$

As a result, $E_1(\delta\theta_x, \delta\omega)$ converges to 0 exponentially fast and the two solutions $(\omega_i + \bar{\omega}_i, \theta_i + \bar{\theta}_i), i = 1, 2$ converge to steady states $(\omega_{i,\infty}, \theta_{i,\infty})$ with the same ω_∞ and $\theta_{\infty,x}$. Since $\theta_{i,\infty}(0) = 0$, two steady states are the same.

5.5 Numerical evidence of stronger uniqueness

The above discussion argues that the steady state is unique at least within a small energy norm ball. However, our numerical computation suggests that the steady state of the dynamical rescaling equations (2.2),(2.3) is unique (up to rescaling) for a much larger class of smooth initial data ω, θ with $\theta(0) = 0$ that satisfy the following conditions:

(1) odd symmetry: $\omega(x)$ and $\theta_x(x)$ are odd functions of x;
(2) non-degeneracy condition: $\omega_x(0) > 0$ and $\theta_{xx}(0) > 0$;
(3) sign condition: $\omega(x), \theta_x(x) > 0$ for $x > 0$.

In fact, these conditions are consistent with the initial data considered by Luo-Hou in [54, 55] restricted on the boundary. They are preserved by the equations as long as the solution exists. Moreover, this class of initial data leads to finite time blowup of the HL model [12].

Here we present the convergence study for the dynamic rescaling equations for four sets of initial data that belong to the function class described above. The four initial data of ω are given by $\omega^{(i)}(x) = a_i f_i(b_i x), i = 1, 2, 3, 4$, where

$$f_1(x) = \frac{x}{1+x^2}, \quad f_2(x) = \frac{xe^{-(x/10)^2}}{1+x^2}, \quad f_3(x) = \frac{x}{1+x^4}, \quad f_4 = \frac{x(1-x^2)^2}{(1+x^2)^3},$$

and the parameters a_i, b_i are chosen to normalize the initial data such that they satisfy the same normalization conditions:

$$\omega_x^{(i)}(0) = 1 \quad \text{and} \quad u_x^{(i)}(0) = -2.5, \quad i = 1, 2, 3, 4.$$

The initial data of θ_x are chosen correspondingly as

$$\theta_x^{(i)} = (c_l x + u^{(i)})\omega_x^{(i)} - c_\omega \omega^{(i)}, \quad i = 1, 2, 3, 4,$$

so that the initial residual of the ω equation is everywhere 0. The initial value of the scaling parameters are set to be $c_l = 3$ and $c_\omega = -1$, respecting our preliminary numerical result that $\bar{c}_l/\bar{c}_\omega \approx -3$. Note that all these initial data of ω, θ_x are far away from the approximate steady (with proper rescaling) with $O(1)$ distance in the the energy norm that is used in our analysis. In particular, we have $\omega^{(1)}(x) = O(x^{-1})$, $\omega^{(2)}(x) = O(x^{-1}e^{-(x/10)^2})$, $\omega^{(3)}(x) = O(x^{-3})$ for $x \to +\infty$, while the approximate steady should satisfy $\bar{\omega}(x) = O(x^{\bar{c}_\omega/\bar{c}_l})$ where $\bar{c}_\omega/\bar{c}_l$ is approximately $-1/3$ according to our numerical results. Moreover, $\omega^{(4)}(x)$ has two peaks, while $\bar{\omega}(x)$ only has one. Figure 2(a) plots the four initial data of ω for $x \in [0, 40]$.

With each set of these initial data, we numerically solve the dynamic rescaling equations (2.2) subject to the normalization conditions (2.3) using the algorithm

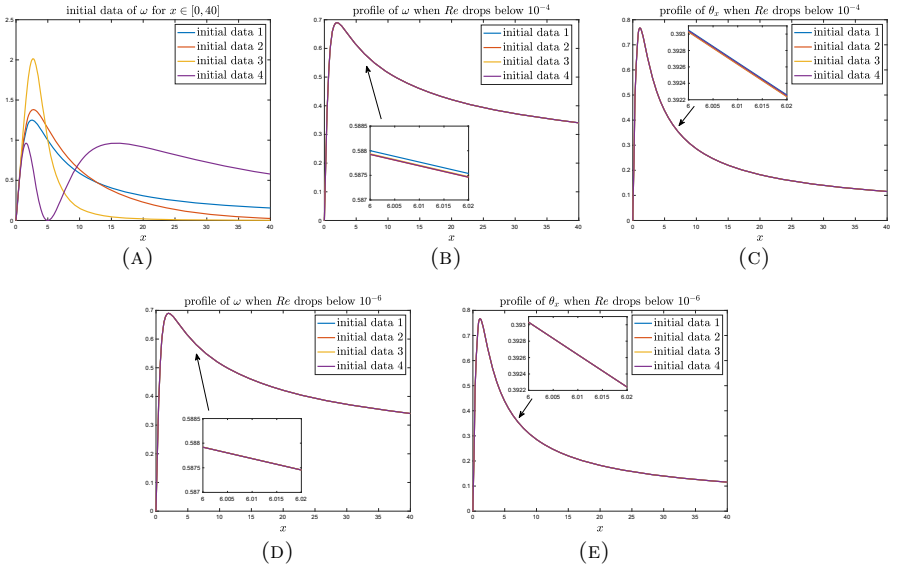

Fig. 2 (A) Four different initial data of ω; (B)(C) Profiles of ω and θ_x when Re drops below 10^{-4} the first time. (D)(E) Profiles of ω and θ_x when Re drops below 10^{-6} the first time

described in Section 10 of the Supplementary Material [10] (by modifying the initial values of the part ω_p and $(\theta_x)_p$). We verify the uniqueness of the steady state by comparing the profiles of ω at the first time the maximum grid-point residual $Re := \max_i\{|F_\omega(x_i)|, |F_{\theta_x}(x_i)|\}$ drops below some small number ϵ. Here the residuals F_ω and F_{θ_x} are defined as

$$F_\omega = -(c_l x + u)\omega_x + c_\omega + v, \quad F_{\theta_x} = -(c_l x + u)\theta_{xx} + (2c_\omega - u_x)\theta_x. \tag{5.36}$$

Figure 2 (b) and (c) plot the solutions of ω when $Re \leq 10^{-4}$ and when $Re \leq 10^{-6}$, respectively. We can see that the profiles of ω from different initial data are barely distinguishable when the residual is smaller than 10^{-4}; they become even closer to each other when the residual is even smaller. This implies that the solutions in the four cases of computation should converge to the same steady state.

6 Hölder regularity of the blowup solution

To estimate the C^γ norm with $\gamma = \frac{c_{\theta,\infty}}{c_{l,\infty}}$ of the solution θ, we will use the following estimate

$$\begin{aligned}\frac{|f(y) - f(x)|}{|x - y|^\gamma} &= |x - y|^{-\gamma} \left| \int_x^y f_x(z)dz \right| \lesssim |x - y|^{-\gamma} \int_x^y z^{\gamma-1}dz \cdot ||f_x x^{1-\gamma}||_\infty \\ &\lesssim |x - y|^{-\gamma}(y^\gamma - x^\gamma) \cdot ||f_x x^{1-\gamma}||_\infty \lesssim ||f_x x^{1-\gamma}||_\infty. \end{aligned} \tag{6.1}$$

for any $0 \le x < y$. The difficulty lies in the decay estimate of θ_x since the previous a-priori estimates only imply that θ_x decays with rate slower than $x^{\gamma-1}$. The decay rate $x^{\gamma-1}$ is sharp since it is exactly the decay rate of the self-similar profile $\theta_{\infty,x}$, which will be established in Section 6.1. In Section 6.2, we establish the decay estimates of the perturbation. In Section 6.3, we estimate the Hölder norm of the solution.

Notations In this Section, we use the notation $A \lesssim B$ if there exists some finite constant $C > 0$, such that $A \le CB$. The constant C *can* depend on the norms of the approximate steady state $(\bar{\theta}, \bar{\omega})$ and the self-similar profile $(\theta_\infty, \omega_\infty)$ constructed in Section 5.3, e.g. $||\theta_x||_\infty$, $||\bar{\theta}_x||_\infty$, as long as these norms are finite. These constants do not play an important role in characterizing several exponents and thus we do not need to track them.

6.1 Decay estimates of the self-similar profile

Recall that we have constructed the self-similar profile $(\theta_\infty, \omega_\infty)$ in Section 5.3. Using the estimate (5.33),we obtain

$$\begin{aligned} &|u_\infty(x)| \lesssim |x|^{5/6}, \quad |c_{l,\infty}x + u_\infty(x)| \ge 0.3|x|, \quad u_{\infty,x} \in L^\infty, \\ &\theta_\infty(1) \neq 0, \quad \theta_{x,\infty} \in L^\infty, \end{aligned} \tag{6.2}$$

whose proofs are referred to Section 10 in the Supplementary Material [10]. Recall that the profile $(\theta_\infty, \omega_\infty)$ solves

$$(c_{l,\infty}x + u_\infty)\theta_{\infty,x} = c_{\theta,\infty}\theta_\infty, \quad u_{\infty,x} = H\omega_\infty. \tag{6.3}$$

Solving the ODE on θ_∞, we obtain

$$\begin{aligned} &\theta_\infty(x) = \theta_\infty(1)\exp(J(x)), \quad J(x) \triangleq \int_1^x \frac{c_{\theta,\infty}}{c_{l,\infty}y + u_\infty(y)}dy, \\ &\theta_{\infty,x} = \frac{c_{\theta,\infty}\theta_\infty(x)}{c_{l,\infty}x + u_\infty(x)}. \end{aligned} \tag{6.4}$$

Denote $\gamma = \frac{c_{\theta,\infty}}{c_{l,\infty}}$. Using the estimates on u_∞ in (6.2), we obtain $|J(x) - \gamma\log(x)| \lesssim 1$. Thus, for some constant $C_1 > 0$ depending on the profile, we get

$$\lim_{x\to\infty} \theta_\infty(x)x^{-\gamma} = C_1\theta_\infty(1) \neq 0.$$

Plugging the above limit and (6.2) in the formula of $\theta_{\infty,x}$ in (6.4), we yield

$$\lim_{x\to\infty} \theta_{x,\infty}x^{1-\gamma} = \lim_{x\to\infty} \frac{c_{\theta,\infty}x}{c_{l,\infty}x + u_\infty(x)} \cdot \theta_\infty(x)x^{-\gamma} = C_1\gamma\theta_\infty(1). \tag{6.5}$$

Combining the above estimate and $\theta_{\infty,x} \in L^\infty$ from (6.2), we prove

$$||\theta_{\infty,x}x^{1-\gamma}||_\infty \lesssim 1. \tag{6.6}$$

Differentiating (6.3) and using $c_{\theta,\infty} = c_{l,\infty} + 2c_{\omega,\infty}$, we get

$$(c_{l,\infty}x + u_\infty)\theta_{\infty,xx} = (c_{\theta,\infty} - c_{l,\infty} - u_{\infty,x})\theta_{\infty,x} = (2c_{\omega,\infty} - u_{\infty,x})\theta_{\infty,x}. \tag{6.7}$$

Using (6.2), we further obtain

$$\left|\frac{x\theta_{\infty,xx}}{\theta_{\infty,x}}\right| = \left|\frac{(2c_{\omega,\infty} - u_{\infty,x})x}{c_{l,\infty}x + u_\infty}\right| \lesssim \left|\frac{x}{c_{l,\infty}x + u_\infty}\right| \lesssim 1. \tag{6.8}$$

6.2 Decay estimates of the perturbation

Note that we have constructed $(\theta_\infty, \omega_\infty)$ in Section 5.3 with estimate (5.33). We treat them as known functions. Similar to (3.1), (3.2), linearizing the θ_x equation around the self-similar profile, we get

$$\begin{aligned}\partial_t\theta_x + (c_{l,\infty}x + u_\infty + u)\theta_{xx} &= (2c_{\omega,\infty} - u_{\infty,x})\theta_x + (2c_\omega - u_x)\theta_{\infty,x}\\ &\quad -u\theta_{\infty,xx} + (2c_\omega - u_x)\theta_x,\end{aligned}$$

with normalization conditions

$$c_\omega = u_x(0), \quad c_l = 0, \quad c_\theta = c_l + 2c_\omega. \tag{6.9}$$

Here, the nonlinear terms are given by $u\theta_{xx}$, $(2c_\omega - u_x)\theta_x$, and the error term is 0 since we linearize the equation around the exact steady state. To obtain the decay estimates of θ_x with a decay rate $O(|x|^{\gamma-1})$, we choose ρ with a growth rate $O(|x|^{1-\gamma})$ and perform L^∞ estimate on $\theta_x\rho$, which will imply $|\theta_x| \le |\rho^{-1}| \lesssim |x|^{\gamma-1}$ for large x. We derive the equation for $\theta_x\rho$ as follows

$$\begin{aligned}\partial_t(\theta_x\rho) + (c_{l,\infty}x + u_\infty + u)(\theta_x\rho)_x &= I(\rho)\theta_x\rho + J,\\ I(\rho) &\triangleq 2c_{\omega,\infty} - u_{\infty,x} + (c_{l,\infty}x + u_\infty)\rho_x\rho^{-1},\\ J &\triangleq (2c_\omega - u_x)\theta_{\infty,x}\rho - u\theta_{\infty,xx}\rho + u\theta_x\rho_x + (2c_\omega - u_x)\theta_x\rho.\end{aligned} \tag{6.10}$$

For a typical function ρ with a growth rate $O(|x|^{\gamma-1})$, e.g. $\rho = \mathrm{sgn}(x)|x|^{\gamma-1}$, since u_∞ has sublinear growth (6.2), for large $x > 0$, we get

$$\begin{aligned}I(\rho) &= 2c_{\omega,\infty} + c_{l,\infty}x(x^{1-\gamma})_x x^{\gamma-1} + l.o.t.\\ &= 2c_{\omega,\infty} + c_{l,\infty}(1-\gamma) + l.o.t. = l.o.t.,\end{aligned}$$

where we have $c_{l,\infty}(1-\gamma) = c_{l,\infty} - c_{\theta,\infty} = -2c_{\omega,\infty}$ to obtain the last equality. Thus, we expect that $I(\rho)$ is not uniformly negative, i.e. $I(\rho) \le -c$ for some $c > 0$, and we do not obtain a damping term in the L^∞ estimate of $\theta_x\rho$, which is different from the weighted L^2 and H^1 estimates in Sections 3, 5. In some sense, the decay rate $O(|x|^{\gamma-1})$ is critical. An ideal choice of ρ with the desired growth rate is $\theta_{\infty,x}^{-1}$, since

we have (6.5) and $I(\rho)$ term in (6.10) vanishes :

$$I(\rho) = 2c_{\omega,\infty} - u_{\infty,x} - \frac{(c_{l,\infty}x + u_\infty)\theta_{\infty,xx}}{\theta_{\infty,x}}$$
$$= \frac{(2c_{\omega,\infty} - u_{\infty,x})\theta_{\infty,x} - (c_{l,\infty}x + u_\infty)\theta_{\infty,xx}}{\theta_{\infty,x}} = 0,$$

where we have used (6.7) to obtain the last equality.

Recall $c_\omega = u_x(t,0)$. Using $\rho = \theta_{\infty,x}^{-1}$, $|\frac{x\theta_{\infty,xx}}{\theta_{\infty,x}}| \lesssim 1$ in (6.8) and $|\frac{u}{x}| \lesssim ||u_x||_\infty$, we get

$$|J| = \left|(2c_\omega - u_x)\frac{\theta_{\infty,x}}{\theta_{\infty,x}} - u\frac{\theta_{\infty,xx}}{\theta_{\infty,x}} - u\theta_x\frac{\theta_{\infty,xx}}{\theta_{\infty,x}^2} + (2c_\omega - u_x)\theta_x\rho\right|$$
$$\lesssim ||u_x||_\infty(1 + ||\theta_x\rho||_\infty).$$

For $\theta_x(\cdot,0)\rho \in L^\infty$, performing L^∞ estimates in (6.10), we yield

$$\frac{d}{dt}||\theta_x\rho||_\infty \lesssim ||u_x||_\infty(1 + ||\theta_x\rho||_\infty). \tag{6.11}$$

Next, we control $||u_x||_\infty$. Recall the energy E in (5.26) and the a-priori estimates in (5.31),(5.33)

$$E(\theta_{x,\infty} + \theta_x - \bar{\theta}_x, \omega_\infty + \omega - \bar{\omega}) \le E_*, \quad E(\theta_{x,\infty} - \bar{\theta}_x, \omega_\infty - \bar{\omega}) \le E_*.$$

Using the triangle inequality, for any $t \ge 0$, we get

$$||\theta_x\psi^{1/2}||_2 + ||D_x\theta_x\psi^{1/2}||_2 + ||\omega\varphi^{1/2}||_2 + ||D_x\omega\varphi^{1/2}||_2$$
$$+|c_\omega(\omega)| + |d_\theta(\theta_x)| \lesssim 1. \tag{6.12}$$

Denote $\kappa_3 = 0.02$. Applying (5.35) to two solutions $(\theta_\infty, \omega_\infty)$ and $(\theta_\infty + \theta, \omega_\infty + \omega)$, we get

$$||\theta_x(t)\psi^{1/2}||_2 + ||\omega(t)\varphi^{1/2}||_2 + |c_\omega(t)| \lesssim E_1(\theta_x(t), \omega(t))$$
$$\le e^{-\kappa_3 t}E_1(\theta_x(0), \omega(0) \lesssim e^{-\kappa_3 t}, \tag{6.13}$$

where we have used (6.12) to obtain the last inequality. Since $H(D_x\omega)(0) = 0$, using Lemma A.1, we get $H(D_x\omega) = D_xH\omega = xu_{xx}$. From (3.8) and (3.9), we have $x^{-4/3} + x^{-2/3} \lesssim \varphi$. Applying Lemma A.6 to $f = D_x\omega$ and $f = \omega$ (note that $H(D_x\omega)(0) = 0$), we obtain

$$||u_x||_\infty^2 \lesssim \int_{\mathbb{R}} |u_{xx}u_x|dx = \int_{\mathbb{R}} |H(D_x\omega)\cdot H\omega x^{-1}|dx$$
$$\lesssim ||H(D_x\omega)x^{-2/3}||_2||H\omega x^{-1/3}||_2$$
$$\lesssim ||D_x\omega x^{-2/3}||_2||\omega x^{-1/3}||_2 \lesssim ||D_x\omega\varphi^{1/2}||_2||\omega\varphi^{1/2}||_2 \lesssim e^{-\kappa_3 t/2}. \tag{6.14}$$

Plugging the above estimate in (6.11), we yield

$$\frac{d}{dt}||\theta_x\rho||_\infty \lesssim e^{-\kappa_3 t/4}(1+||\theta_x\rho||_\infty).$$

Since $\kappa_3 > 0$, solving the differential inequality and using $|x^{1-\gamma}| \lesssim |\theta_{x,\infty}^{-1}|$ from (6.6), we prove

$$\sup_{t\geq 0}||\theta_x(t)\rho||_\infty \lesssim 1, \quad \sup_{t\geq 0}||\theta_x(t)x^{1-\gamma}||_\infty \lesssim \sup_{t\geq 0}||\theta_x(t)\theta_{x,\infty}^{-1}||_\infty \lesssim 1,$$

Since θ is even, using (6.1), (6.6) and the above estimate, we prove

$$\sup_{t\geq 0}||\theta_\infty + \theta(t)||_{C^\gamma} \lesssim 1. \tag{6.15}$$

Remark 6.1 Since we do not have a damping term in the L^∞ estimate (6.11), the exponential convergence estimates in (6.13), (6.14) play a crucial role in obtaining (6.15).

6.3 Hölder regularity

Denote $\hat{\theta} = \theta_\infty + \theta$ and by θ_{phy} the solution with initial data $\hat{\theta}(0,\cdot)$ in the physical space. Recall the rescaling relation and the normalization conditions (6.9)

$$\begin{aligned}
C_\omega(\tau) &= \exp(\int_0^\tau c_\omega(s) + c_{\omega,\infty} ds), \quad t(\tau) = \int_0^\tau C_\omega(s) ds,\\
C_\theta(\tau) &= \exp(\int_0^\tau c_\theta(s) + c_{\theta,\infty} ds), \quad C_l(\tau) = \exp(-\int_0^\tau (c_l(s) + c_{l,\infty}) ds),\\
\hat{\theta}(x,\tau) &= C_\theta(\tau)\theta_{phy}(C_l(\tau)x, t(\tau)), \quad c_\theta = 2c_\omega, \quad c_l = 0.
\end{aligned} \tag{6.16}$$

From assumptions $\hat{\theta}_x(0)|x|^{1-\gamma} \in L^\infty$ in (d) in Theorem 2, $E(\hat{\theta}_x(0) - \bar{\theta}_x, \hat{\omega}(0) - \bar{\omega}) \lesssim 1$, and estimates (6.5) and $E(\theta_{\infty,x} - \bar{\theta}_x, \omega_\infty - \bar{\omega}) \lesssim 1$, it is not difficult to obtain that $\theta_x\rho \in L^\infty$. Thus, $\theta, \hat{\theta}$ enjoys the energy estimates in Section 6.2. Using (6.13), (6.15), (6.16) and $\gamma c_{l,\infty} = c_{\theta,\infty}$, we prove

$$\sup_{\tau\geq 0}||\theta_{phy}(t(\tau))||_{C^\gamma} = \sup_{\tau\geq 0}||\hat{\theta}(\tau)||_{C^\gamma} C_\theta^{-1} C_l^{-\gamma} = \sup_{\tau\geq 0}||\hat{\theta}(\tau)||_{C^\gamma} \exp(\int_0^\tau -2c_\omega d\tau) \lesssim 1.$$

6.3.1 Blowup in higher Hölder norm

We show that for any $\beta > \gamma$, the C^β norm of the solution blows up. Since $1 \lesssim \psi(x)$ for $x \in [0,1]$, using (6.13) and Cauchy-Schwarz inequality, we get

$$|\theta(1)-\theta(0)| = |\int_0^1 \theta_x(y)dy| \lesssim \Big(\int_0^1 \theta_x(y)^2 dy\Big)^{1/2} \lesssim ||\theta_x \psi^{1/2}||_2 \lesssim e^{-\kappa_3 \tau}. \tag{6.17}$$

Recall the formulas in (6.16). Denote $T = t(\infty)$. Since $|c_\omega(\tau)|$ decays exponentially (6.13) and $c_{\omega,\infty} < -\frac{1}{2}$, we obtain

$$\begin{aligned} &C_\omega(\tau) \gtrsim e^{c_{\omega,\infty}\tau}, \quad C_\theta(\tau)^{-1} \gtrsim e^{-c_{\theta,\infty}\tau}, \quad C_l(\tau)^{-1} \gtrsim e^{c_{l,\infty}\tau}, \\ &T - t(\tau) = \int_\tau^\infty C_\omega(s)ds \gtrsim \int_\tau^\infty e^{c_{\omega,\infty}s} ds \gtrsim e^{c_{\omega,\infty}\tau}. \end{aligned}$$

Recall $\gamma c_{l,\infty} = c_{\theta,\infty} = c_{l,\infty} + 2c_{\omega,\infty}$. Denote $\delta = -\frac{\beta c_{l,\infty} - c_{\theta,\infty}}{c_{\omega,\infty}} = \frac{2(\beta-\gamma)}{1-\gamma} > 0$. We have

$$S \triangleq \liminf_{\tau\to\infty} ||\theta_{phy}(x,\tau)||_{C^\beta} (T-t(\tau))^\delta \gtrsim \liminf_{\tau\to\infty} ||\hat{\theta}(x,\tau)||_{C^\beta} C_\theta^{-1} C_l^{-\beta} \exp(\delta c_{\omega,\infty}\tau).$$

Note that $\theta_\infty(0) = 0$. Using (6.17), we have $||\hat{\theta}(\tau)||_{C^\beta} \geq |\hat{\theta}(\tau,1) - \hat{\theta}(\tau,0)| \geq |\theta_\infty(1)| - C\exp(-\kappa_3\tau)$. Using this estimate, $\delta = -\frac{\beta c_{l,\infty} - c_{\theta,\infty}}{c_{\omega,\infty}}$ and (6.2), we establish

$$S \gtrsim \liminf_{\tau\to\infty} |\theta_\infty(1)| \exp((-c_{\theta,\infty} + \beta c_{l,\infty} + \delta c_{\omega,\infty})\tau) \gtrsim |\theta_\infty(1)| > 0.$$

We conclude the proof of result (d) in Theorem 2.

Remark 6.2 The exponential convergence in (6.13) is crucial for us to obtain the unique Hölder exponent γ that characterizes the regularity of the singular solution and the sharp blowup rate. It enables us to essentially treat the perturbation as 0.

7 Connection between the HL model and the 2D Boussinesq equations in $\mathbb{R}^+_2$

In this section, we discuss the connection between the leading order system of the HL model and that of the 2D Boussinesq equations in $\mathbb{R}^+_2$ with low regularity initial data.

7.1 The leading order system for the 2D Boussinesq equations

The 2D Boussinesq equations in $\mathbb{R}^+_2$ read

$$\begin{aligned} \omega_t + \mathbf{u}\cdot\nabla\omega &= \theta_x, \\ \theta_t + \mathbf{u}\cdot\nabla\theta &= 0, \end{aligned} \tag{7.1}$$

where the velocity field $\mathbf{u} = (u, v)^T : \mathbb{R}^2_+ \times [0, T) \to \mathbb{R}^2_+$ is determined via the Biot-Savart law

$$-\Delta\psi = \omega, \quad u = -\psi_y, \quad v = \psi_x,$$

with no flow boundary condition $\psi(x, 0) = 0 \quad x \in \mathbb{R}$.

Consider the polar coordinate (r, β) in $\mathbb{R}^+_2 : r = (x^2 + y^2)^{1/2}$, $\beta = \arctan(y/x)$. For $\alpha > 0$, denote

$$R = r^\alpha, \quad \Omega(R, \beta) = \omega(x, y), \quad \eta(R, \beta) = \theta_x(x, y), \quad \xi(R, \beta) = \theta_y(x, y).$$

In [7], the following leading order system of (7.1) is derived based on the framework developed in [24] under the assumption that $\omega, \nabla\theta$ are in some Hölder space C^α with sufficient small α

$$\Omega_t = \eta, \quad \eta_t = \frac{2}{\pi\alpha} L_{12}(\Omega)\eta, \quad L_{12}(\Omega) = \int_R^\infty \int_0^{\pi/2} \frac{\Omega(s, \beta)\sin(2\beta)}{s} ds d\beta. \tag{7.2}$$

An important observation made in [7] is that for certain class of C^α data, θ is anisotropic in the sense that $|\theta_y| \lesssim \alpha|\theta_x|$. Moreover, this property is preserved dynamically. Therefore, the θ_y variable does not appear in the leading order system. Define the following operators

$$Pf(R) = \int_0^{\pi/2} f(R, \beta)\sin(2\beta) d\beta, \quad Sf(R) = \frac{2}{\pi\alpha} \int_R^\infty f(S)\frac{dS}{S}. \tag{7.3}$$

By definition, we have

$$\frac{2}{\pi\alpha} L_{12}(\Omega) = \frac{2}{\pi\alpha} \int_R^\infty P\Omega(s)\frac{ds}{s} = S(P\Omega). \tag{7.4}$$

Since $L_{12}(\Omega)$ does not depend on β, we apply the operator P to both sides of (7.2) to obtain

$$\partial_P \Omega = P\eta, \quad \partial_t P\eta = \frac{2}{\pi\alpha} L_{12}(\Omega) P\eta = S(P\Omega) \cdot P\eta. \tag{7.5}$$

The above system is an 1D coupled system on $P\Omega$, $P\eta$. Once $P\Omega$, $P\eta$ are determined, we can obtain an explicit solution of (7.2).

7.2 The leading order system for the HL model

We use the observation made in [28] that the advection can be substantially weakened by choosing C^α data with sufficiently small α. Suppose that $\omega, \theta_x \in C^\alpha$ with small

α. Then the advection terms in the system of (ω, θ_x) in the HL model become lower order terms

$$\omega_t = \theta_x + l.o.t., \quad (\theta_x)_t = -u_x\theta_x + l.o.t., \quad u_x = H\omega. \tag{7.6}$$

The above system is already very similar to (7.2) by taking $\Omega = \omega, \eta = \theta_x$. We further perform a simplification for the Hilbert transform. We impose extra assumptions that ω, θ_x are odd, which are preserved dynamically. Due to these symmetries, it suffices to consider the HL model on $\mathbb{R}_+$. For $x > 0$, symmetrizing the kernel, we get

$$\begin{aligned} H\omega(x) &= \frac{1}{\pi}\int_{\mathbb{R}_+} \omega(y)\left(\frac{1}{x-y} - \frac{1}{x+y}\right)dy = \frac{1}{\pi}\int_{\mathbb{R}_+} \omega(y)\frac{2y}{x^2-y^2}dy \\ &= \frac{1}{\pi}\int_{\mathbb{R}_+} \omega(y)\frac{2}{(x/y)^2-1}\frac{dy}{y}. \end{aligned}$$

We learn the following formal derivation of the leading order part of general singular integral operator from Dr. Elgindi. [1] Denote

$$X = x^\alpha, \quad Y = y^\alpha, \quad \Omega(X) = \omega(x), \quad \eta(X) = \theta_x(x). \tag{7.7}$$

Using the above change of variables and $\frac{dy}{y} = \frac{1}{\alpha}\frac{dY}{Y}$, we get

$$H\omega(x) = \frac{1}{\alpha\pi}\int_{\mathbb{R}_+} \omega(Y^{1/\alpha})\frac{2}{(\frac{X}{Y})^{1/\alpha}-1}\frac{dY}{Y} = \frac{1}{\alpha\pi}\int_{\mathbb{R}_+} \Omega(Y)K_\alpha(X,Y)\frac{dY}{Y},$$

where $K_\alpha(X,Y) = \frac{2}{(\frac{X}{Y})^{1/\alpha}-1}$. Next, we consider the leading order part of $K_\alpha(X,Y)$ as $\alpha \to 0^+$. Note that

$$\lim_{\alpha\to 0^+}(\frac{X}{Y})^{1/\alpha} = 0, \text{ for } X < Y, \quad \lim_{\alpha\to 0^+}(\frac{X}{Y})^{1/\alpha} = \infty, \text{ for } X > Y.$$

Hence, for $X \neq Y$ and $X, Y > 0$, we get

$$\lim_{\alpha\to 0^+} K_\alpha(X,Y) = -2\cdot \mathbf{1}_{Y>X}.$$

Therefore, formally, we get

$$H\omega(x) = -\frac{2}{\alpha\pi}\int_X^\infty \omega(Y)\frac{dY}{Y} + l.o.t. = -S\Omega(X) + l.o.t., \tag{7.8}$$

[1] Similar derivation was presented in the One World PDE Seminar "Singularity formation in incompressible fluids" by Dr. Elgindi. https://www.youtube.com/watch?v=29zUjm7xFlI&feature=youtu.be

where the operator S is defined in (7.3). Now, plugging the above formula in (7.6), dropping the lower order terms in (7.6) and applying the notations (7.7), we derive another leading order system for the HL model

$$\partial_t \Omega(X) = \eta(X), \quad \partial_t \eta(X) = S\Omega(X) \cdot \eta(X). \tag{7.9}$$

The above system is exactly the same as that in (7.5). We remark that the lower order term in the simplification (7.8) needs to be estimated rigorously. In general, the system (7.6) is more complicated than (7.9) since the Hilbert transform is nonlocal and is a singular operator, while we can obtain a local relation between Sf and f by taking derivative $\partial_X(Sf)(X) = -\frac{2}{\pi\alpha}\frac{f(X)}{X}$.

Note that $\mathbf{1}_{X<Y} = \mathbf{1}_{x<y}$. Undoing the change of variables in (7.7), we get

$$\begin{aligned} S\Omega(X) &= \frac{2}{\pi\alpha}\int_{\mathbb{R}_+} \mathbf{1}_{x<y}\Omega(Y)\frac{dY}{Y} = \frac{2}{\alpha\pi}\int_{\mathbb{R}_+} \mathbf{1}_{x<y}\omega(y)\cdot\alpha\frac{dy}{y} \\ &= \frac{2}{\pi}\int_x^\infty \omega(y)\frac{dy}{y}. \end{aligned} \tag{7.10}$$

The operator on the right hand side is closely related to the Choi-Kiselev-Yao (CKY) simplification of the Hilbert transform [13]. Therefore, the leading order system (7.9) can be seen as the CKY's simplification of (7.6) without the lower order terms.

8 Concluding remarks

In this paper, we proved that the HL model develops a finite time focusing asymptotically self-similar blowup from smooth initial data with compact support and finite energy. Moreover, we showed that the solution of the dynamic rescaling equations converges to an exact steady state exponentially fast in time and the self-similar blowup profile is unique within a small energy ball. We also presented strong numerical evidence to demonstrate the uniqueness of the self-similar profile for a much larger class of initial data that satisfy certain symmetry and sign conditions consistent with the initial data considered by Luo-Hou in [54, 55]. The possibility of having a unique self-similar profile for a large class of initial data is very interesting and quite surprising if it can be justified rigorously.

One of the main difficulties in our stability analysis is to control a number of nonlocal terms with a relatively small damping coefficient. This is also the essential difficulty in generalizing the method of analysis presented in this work to prove the finite time blowup of the 2D Boussinesq equations or 3D axisymmetric Euler equations with smooth initial data and boundary. To establish linear stability, we designed singular weight functions carefully, applied several sharp weighted functional inequalities to control the nonlocal terms, and took into account cancellation among various nonlocal terms.

Our ultimate goal is to prove rigorously the Luo-Hou blowup scenario for the 2D Boussinesq equations and 3D Euler equations with smooth initial data and boundary.

Our numerical study suggested that the real parts of the eigenvalues of the discrete linearized operator for the 2D Boussinesq equations with smooth initial data and boundary are all negative and bounded away from 0 by a finite spectral gap. See also Section 3.4 in Dr. Pengfei Liu's Ph.D. thesis [53] for an illustration of the eigenvalue distribution of the discretized linearized operator. Moreover, our numerical study shows that $|\theta_y|$ is an order of magnitude smaller than $|\theta_x|$. This seems to imply that the main driving mechanism for singularity formation is due to the coupling between ω and θ_x, which is captured by our analysis for the HL model.

The framework of analysis that we established for the HL model provides a promising approach to studying the singularity formation of the 2D Boussinesq equations and 3D axisymmetric Euler equations with smooth initial data and boundary. We can follow the general strategy developed in this paper by (1) extracting the damping effect from the local terms, (2) treating the advection terms as perturbation to vortex stretching, and (3) controlling the nonlocal terms by developing sharp functional inequalities on the Biot-Savart law and exploiting cancellation among them to control the nonlocal terms by using the damping effects from the local terms. Compared with the HL model, we will encounter some additional difficulties associated with the advection away from the boundary, and need to estimate more complicated Biot-Savart law in 2D Boussinesq and 3D Euler equations. We will explore a more effective functional space, e.g. weighted L^p or weighted C^α space, to establish the stability analysis. Such space offers the advantage of weakening the effect of the advection in the stability analysis and extracting larger damping effect from the local terms in the linearized equations. Moreover, it still allows us to estimate the Biot-Savart law effectively.

Guided by the singularity analysis presented in this paper, we have recently made some encouraging progress towards the ultimate goal of proving finite time self-similar blowup of the 2D Boussinesq equations and 3D Euler equations with smooth initial data and boundary. We will report our results in our future work.

Supplementary Information The online version contains supplementary material available at https://doi.org/10.1007/s40818-022-00140-7.

Acknowledgements The research was in part supported by NSF Grants DMS-1907977 and DMS-1912654. D. Huang would like to acknowledge the generous support from the Choi Family Postdoc Gift Fund.

Appendix A. Properties of the Hilbert transform

Throughout this section, we assume that ω is smooth and decays sufficiently fast. The general case can be obtained by approximation. The properties of the Hilbert transform in Lemmas A.1-A.3 are well known, see e.g. [6, 11, 23].

Lemma A.1 *Assume that ω is odd. We have*

$$H\omega(x) - H\omega(0) = xH\left(\frac{\omega}{x}\right).$$

Lemma A.2 *Assume that ω is odd and $\omega_x(0) = 0$. For $p = 1, 2$, we have*

$$(u_x - u_x(0))x^{-p} = H(\omega x^{-p}). \tag{A.1}$$

Consequently, the L^2 isometry property of the Hilbert transform implies

$$||(u_x - u_x(0))x^{-p}||_2^2 = ||\omega x^{-p}||_2^2.$$

Recall the inner product $\langle f, g\rangle = \int_0^\infty fgdx$ (see (2.5))and $\Lambda = (-D)^{1/2} = H\partial_x$.

Lemma A.3 *For $f \in L^p, g \in L^q$ with $\frac{1}{p} + \frac{1}{q} = 1$ and $1 < p < \infty$, we have*

$$\langle Hf, g\rangle = -\langle f, Hg\rangle. \tag{A.2}$$

Lemma A.4 *Denote $\Lambda = (-\partial_x^2)^{1/2}$. Assume that f is odd and $g_x = Hf, g(0) = 0$. We have*

$$\langle Hf - Hf(0), fx^{-3}\rangle = 0, \quad \langle g, f_x x^{-1}\rangle = -\Big\langle \Lambda\frac{g}{x}, \frac{g}{x}\Big\rangle,$$
$$\langle g, fx^{-2}\rangle = -\Big\langle \Lambda\frac{g}{x}, \frac{g}{x}\Big\rangle - \frac{\pi}{4}g_x(0)^2.$$

Identities similar to those in Lemma A.4 have been used in [2, 6, 11, 26]. We refer the proof of Lemma A.4 to the arXiv version of this paper [8].

Lemma A.5 *Assume that $\omega \in L^2(|x|^{-4/3} + |x|^{-2/3})$ is odd and $u_x = H\omega$. We have*

$$\int_{\mathbb{R}} \frac{(u_x(x) - u_x(0))^2}{|x|^{4/3}} = \int_{\mathbb{R}} \Big(\frac{w^2}{|x|^{4/3}} + 2\sqrt{3}\cdot \mathrm{sgn}(x)\frac{\omega(u_x(x) - u_x(0))}{|x|^{4/3}}\Big)dx.$$

It seems that the identity (4.2) $H(|x|^{-\alpha}) = \tan\left(\frac{\alpha\pi}{2}\right) sgn(x)|x|^{-\alpha}$, which will be used in the proof of Lemma A.5, is difficult to locate in the literature. We thus give a proof.

Proof Firstly, we compute $H(|x|^{-\alpha})$. For $\alpha \in (0, 1)$, we have $H(|x|^{-\alpha}) = C_\alpha sgn(x)|x|^{-\alpha}$, for some constant C_α. We determine C_α by applying Lemma A.3 to

$$f = |x|^{-\alpha}, \quad Hf = C_\alpha sgn(x)|x|^{-\alpha}, \quad g = -\frac{x}{1+x^2}, \quad Hg = \frac{1}{1+x^2},$$

which implies

$$C_\alpha \int_0^\infty \frac{x^{1-\alpha}}{1+x^2}dx = \int_0^\infty \frac{1}{x^\alpha(1+x^2)}dx.$$

The integrals can be evaluated using the Beta function $\mathrm{B}(x, y)$ and $\mathrm{B}(\beta, 1-\beta) = \frac{\pi}{\sin(\beta\pi)}$ for $\beta \in (0, 1)$. In particular, we get

$$C_\alpha = \frac{\mathrm{B}(\frac{\alpha+1}{2}, \frac{1-\alpha}{2})}{\mathrm{B}(\frac{2-\alpha}{2}, \frac{\alpha}{2})} = \frac{\pi/\sin((\alpha+1)\pi/2)}{\pi/\sin((2-\alpha)\pi/2)} = \tan\left(\frac{\alpha\pi}{2}\right).$$

Choosing $\alpha = 1/3$, we get

$$H(|x|^{-1/3}) = \frac{1}{\sqrt{3}} sgn(x)|x|^{-1/3}, \quad H(sgn(x)|x|^{-1/3}) = -\sqrt{3}|x|^{-1/3}. \quad \text{(A.4)}$$

Recall that ω is odd. We assume that ω is in the Schwartz space. Applying the Cotlar identity, see e.g. [11, 23],

$$(HF)^2 = F^2 + 2H(F \cdot HF),$$

we yield

$$\begin{aligned} I \triangleq \int_{\mathbb{R}} \frac{(u_x(x) - u_x(0))^2}{|x|^{4/3}} &= \int_{\mathbb{R}} |x|^{2/3} \left(H\left(\frac{\omega}{x}\right)\right)^2 dx \\ &= \int_{\mathbb{R}} \left\{ |x|^{2/3} \left(\frac{\omega}{x}\right)^2 + 2|x|^{2/3} H\left(\frac{\omega}{x} H\left(\frac{\omega}{x}\right)\right) \right\} dx. \end{aligned}$$

Since the Hilbert transform is antisymmetric (Lemma A.3), we get $H(\omega H(\frac{\omega}{x})) = -\frac{1}{\pi}\int_{\mathbb{R}} \frac{\omega}{x} H(\frac{\omega}{x}) dx = 0$. Using Lemma A.1, we obtain

$$|x|^{2/3} H\Big(\frac{\omega}{x} H(\frac{\omega}{x})\Big) = |x|^{2/3} \frac{1}{x} H\Big(\omega H(\frac{\omega}{x})\Big) = \mathrm{sgn}(x)|x|^{-1/3} H\Big(\omega H(\frac{\omega}{x})\Big).$$

Thus, applying Lemma A.3, then (A.4) and $H(\frac{\omega}{x}) = \frac{u_x - u_x(0)}{x}$ in Lemma A.1, we prove

$$\begin{aligned} I &= \int_{\mathbb{R}} \left\{ \frac{\omega^2}{|x|^{4/3}} - 2H\left(sgn(x)|x|^{-1/3}\right) \omega H\left(\frac{\omega}{x}\right) \right\} dx \\ &= \int_{\mathbb{R}} \left\{ \frac{\omega^2}{|x|^{4/3}} + 2\sqrt{3}|x|^{-1/3} \omega H\left(\frac{\omega}{x}\right) \right\} dx \\ &= \int_{\mathbb{R}} \left\{ \frac{\omega^2}{|x|^{4/3}} + 2\sqrt{3}|x|^{-1/3} \omega \frac{u_x - u_x(0)}{x} \right\} dx \\ &= \int_{\mathbb{R}} \Big(\frac{\omega^2}{|x|^{4/3}} + 2\sqrt{3} sgn(x) \frac{\omega(u_x(x) - u_x(0))}{|x|^{4/3}} \Big) dx. \end{aligned}$$

To prove the Lemma for general odd $\omega \in L^2(|x|^{-4/3} + |x|^{-2/3})$, or equivalently $\frac{\omega}{x} \in L^2(|x|^{2/3} + |x|^{4/3})$, we approximate $\frac{\omega}{x}$ by the Schwartz function and use the fact that $|x|^{2/3}$ is an A_2 weight [23]. □

The weighted estimates in Lemma A.6 were established in [18].

Lemma A.6 *For $f \in L^2(x^{-4/3} + x^{-2/3})$, we have*

$$||(Hf - Hf(0))x^{-2/3}||_2 \le \cot\frac{\pi}{12}||fx^{-2/3}||_2 = (2+\sqrt{3})||fx^{-2/3}||_2,$$
$$||Hfx^{-1/3}||_2 \le \cot\frac{\pi}{12}||fx^{-1/3}||_2 = (2+\sqrt{3})||fx^{-1/3}||_2.$$

The estimate in the following Lemma is the Hardy inequality [36].

Lemma A.7 *Assume that u is odd. Then for $p > \frac{3}{2}$, we have*

$$\int_0^{+\infty} \frac{(u(x) - u_x(0)x)^2}{x^{2p}} \le \frac{4}{(2p-1)^2}\int_0^{+\infty} \frac{(u_x(x) - u_x(0))^2}{x^{2p-2}}.$$

Lemma A.8 *Assume that ω is odd and $\omega \in L^2(x^{-4} + x^{-2/3})$. Let $u_x = H\omega$. For any $\alpha, \beta, \gamma \ge 0$, we have*

$$||(u_x - u_x(0))(\alpha x^{-4} + \beta x^{-2})^{1/2}||_2^2 = ||\omega(\alpha x^{-4} + \beta x^{-2})^{1/2}||_2^2$$
$$\Big|\Big|(u - u_x(0)x)\Big(\frac{\alpha}{x^6} + \frac{\beta}{x^4} + \frac{\gamma}{x^{10/3}}\Big)^{1/2}\Big|\Big|_2^2 \le \Big|\Big|\omega\Big(\frac{4\alpha}{25x^4} + \frac{4\beta}{9x^2}\Big)^{1/2}\Big|\Big|_2^2 + \frac{36\gamma}{49}||(u_x - u_x(0))x^{-2/3}||_2^2.$$

The first identity follows from Lemma A.2. Applying Lemma A.7 with $p = 3, 2, \frac{5}{3}$ and then Lemma A.2 to the power x^{-4}, x^{-2} yield the second inequality. The constants $\frac{4}{25}, \frac{4}{9}, \frac{36}{49}$ are determined by $\frac{4}{(2p-1)^2}$ with $p = 3, 2, \frac{5}{3}$.

Appendix B. Derivations and estimates in the linear stability analysis

B.1 Derivation of (2.9)

For $p \in [1, 3]$, using integration by parts yields

$$||(\tilde{u} - \frac{1}{2p-1}\tilde{u}_x x)x^{-p}||_2^2 = \int_{\mathbb{R}_+}\Big(\frac{1}{(2p-1)^2}\frac{\tilde{u}_x^2}{x^{2p-2}} - \frac{2}{2p-1}\frac{\tilde{u}\tilde{u}_x}{x^{2p-1}} + \frac{\tilde{u}^2}{x^{2p}}\Big)dx$$
$$= \int_{\mathbb{R}_+}\Big(\frac{1}{(2p-1)^2}\frac{\tilde{u}_x^2}{x^{2p-2}} + \frac{1}{2p-1}(\partial_x x^{-(2p-1)})\tilde{u}^2 + \frac{\tilde{u}^2}{x^{2p}}\Big)dx$$
$$= \frac{1}{(2p-1)^2}\int_{\mathbb{R}_+}\frac{\tilde{u}_x^2}{x^{2p-2}}dx.$$

B.2. Estimate of I_{r1}, I_{r2}, I_{r3}

We construct the cutoff function χ in (3.8) as follows

$$\chi(x) = \frac{2}{\pi}\arctan((\frac{x-l_1}{l_2})^3)\mathbf{1}_{x\geq l_1}\ , \quad l_1 = 5\cdot 10^8, \quad l_2 = 10l_1.$$

Recall I_{r1}, I_{r2} in (3.16), (3.29) and (5.14)

$$\begin{aligned} I_{r1} &= \langle \tilde{u}_x \chi(\xi_1\psi_n + \xi_2\psi_f), \theta_x\rangle, \quad I_{r2} = \lambda_1\langle \tilde{u}, \chi\xi_3\omega\varphi\rangle, \\ I_{r3} &= -\frac{1}{3}\lambda_1\langle \tilde{u}\chi\xi_3, D_x\omega\varphi\rangle. \end{aligned} \tag{B.1}$$

Recall from the beginning of Section 3.1 that $\bar{\omega}, \bar{\theta}_x, \bar{\omega}_x, \bar{\theta}_{xx}$ have decay rates $x^{\alpha}, x^{2\alpha}, x^{\alpha-1}, x^{2\alpha-1}$, respectively, with α slightly smaller than $-\frac{1}{3}$. Using the formulas of ξ_i in (3.7) and $\varphi_f, \varphi_n, \psi$ in (3.8), (3.9), we obtain the decay rates $\chi(\xi_1\psi_n + \xi_2\psi_f) \sim C_1 x^{-4/3}$, $\chi\xi_3\varphi \sim C_2 x^{-2}$ for sufficiently large x, where C_1, C_2 are some constants.

Recall $\tilde{u}_x = u_x - u_x(0)$. Using the Cauchy-Schwarz inequality and Lemmas A.6, we obtain

$$\begin{aligned} |I_{r1}| &\leq ||\tilde{u}_x x^{-2/3}||_2 ||\chi(\xi_1\psi_n + \xi_2\psi_f)\theta_x||_2 \\ &\leq (2+\sqrt{3})||\omega x^{-2/3}||_2 ||\chi(\xi_1\psi_n + \xi_2\psi_f)\theta_x||_2. \end{aligned}$$

For I_{r2}, we first decompose it as follows using $\tilde{u} = u - u_x(0)x$

$$I_{r2} = \lambda_1\langle u, \chi\xi_3\omega\varphi\rangle - u_x(0)\lambda_1\langle x, \chi\xi_3\omega\varphi\rangle \triangleq J_1 + J_2.$$

Using the Cauchy-Schwarz inequality, Lemma A.7 with $p = \frac{4}{3}$ and Lemma A.6, we get

$$\begin{aligned} |J_1| &\leq \lambda_1 ||u x^{-4/3}||_2 ||x^{4/3}\chi\xi_3\omega\varphi||_2 \leq \frac{6\lambda_1}{5}||u_x x^{-1/3}||_2 ||x^{4/3}\chi\xi_3\omega\varphi||_2 \\ &\leq \frac{6\lambda_1(2+\sqrt{3})}{5}||\omega x^{-1/3}||_2 ||x^{4/3}\chi\xi_3\omega\varphi||_2. \end{aligned}$$

Recall $c_\omega = u_x(0)$. For J_2, using Cauchy-Schwarz inequality, we yield

$$|J_2| \leq \lambda_1 |c_\omega| \cdot ||\chi^{1/2}\omega\varphi^{1/2}||_2 ||x\xi_3\chi^{1/2}\varphi^{1/2}||_2.$$

In the above estimates of I_{r1}, if we further bound $||\chi(\xi_1\psi_n + \xi_2\psi_f)\theta_x||_2$ by the weighted L^2 norm $||\theta_x\psi^{1/2}||_2$, we obtain a small factor $\rho_2^{-1/3}$ since χ is supported in $|x| \geq \rho_2$ and the profile has decay. See also the above discussion on the decay rates. Similarly, we get a small factor in the estimates of J_1, J_2 from $||x^{4/3}\chi\xi_3\omega\varphi||_2$, $||x^{4/3}\chi\xi_3\omega\varphi||_2$, respectively.

Using Young's inequality $ab \le ta^2 + \frac{1}{4t}b^2$, we obtain

$$
\begin{aligned}
|I_{r1}| + |I_{r2}| \le\ & t_{51}||\omega x^{-2/3}||_2^2 + \frac{(2+\sqrt{3})^2}{4t_{51}}||\chi(\xi_1\psi_n + \xi_2\psi_f)\theta_x||_2^2 + t_{52}||\omega x^{-1/3}||_2^2 \\
& + \frac{1}{4t_{52}}\left(\frac{6\lambda_1(2+\sqrt{3})}{5}\right)^2 ||x^{4/3}\chi\xi_3\omega\varphi||_2^2 \\
& + t_{53}||\chi^{1/2}\omega\varphi^{1/2}||_2^2 + \frac{\lambda_1^2||x\xi_3\chi^{1/2}\varphi^{1/2}||_2^2}{4t_{53}}c_\omega^2,
\end{aligned}
$$

where $t_{51} = 10^{-10}, t_{52} = 10^{-5}, t_{53} = 10^{-2}$. We choose these weights t_{5i} so that the terms ta^2, $\frac{1}{4t}b^2$ in Young's inequality are comparable. It follows the estimate (3.36).

Note that replacing ω in I_{r2} in (B.1) by $-\frac{1}{3}D_x\omega$, we obtain I_{r3}. Therefore, applying the same estimate as that of I_{r2} to I_{r3}, we yield

$$
\begin{aligned}
|I_{r3}| \le\ & \frac{2\lambda_1(2+\sqrt{3})}{5}||\omega x^{-1/3}||_2||x^{4/3}\chi\xi_3 D_x\omega\varphi||_2 \\
& + \frac{\lambda_1}{3}|c_\omega| \cdot ||\chi^{1/2}D_x\omega\varphi^{1/2}||_2||x\xi_3\chi^{1/2}\varphi^{1/2}||_2.
\end{aligned}
$$

Using Young's inequality $ab \le ta^2 + \frac{1}{4t}b^2$, we establish

$$
\begin{aligned}
|I_{r3}| \le\ & t_{94}||x^{4/3}\chi\xi_3 D_x\omega\varphi||_2^2 \\
& + \frac{1}{4t_{94}}\left(\frac{2\lambda_1(2+\sqrt{3})}{5}\right)^2 ||\omega x^{-1/3}||_2^2 + t_{95}||\chi^{1/2}D_x\omega\varphi^{1/2}||_2^2 \\
& + \frac{\lambda_1^2||x\xi_3\chi^{1/2}\varphi^{1/2}||_2^2}{36t_{95}}c_\omega^2.
\end{aligned}
$$

where $t_{94} = 10^6, t_{95} = 10^{-3}$. We choose these weights t_{94}, t_{95} so that the terms ta^2, $\frac{1}{4t}b^2$ in Young's inequality are comparable. It follows (5.15).

B.3 Derivations of the ODE (3.43) in Section 3.11

We use the following functions in the derivations

$$
\begin{aligned}
& f_2 \triangleq \frac{1}{4}\frac{\bar{u}_x}{x} - \frac{1}{5}\left(\frac{3}{4}\bar{u}_{xx} + \frac{1}{4}\frac{\bar{u}_x}{x}\right) - \frac{\bar{u}_x}{x} + \frac{\bar{u}}{x^2}, \quad f_3 \triangleq \lambda_1(\bar{\omega} - x\bar{\omega}_x)\varphi, \\
& f_4 \triangleq \frac{3}{5}\frac{\bar{u}_{\theta,x}}{x} + \frac{1}{5}\left(\frac{3}{5}\bar{u}_{\theta,xx} + \frac{2}{5}\frac{\bar{u}_{\theta,x}}{x}\right), \quad f_6 \triangleq \frac{\bar{u}}{x^2}, \\
& f_7 \triangleq (\bar{\theta}_x - x\bar{\theta}_{xx})\psi, \quad f_8 \triangleq \frac{3}{4}\bar{\omega}_x + \frac{1}{4}\frac{\bar{\omega}}{x}, \quad f_9 \triangleq \frac{3}{5}\bar{\theta}_{xx} + \frac{2}{5}\frac{\bar{\theta}_x}{x}.
\end{aligned} \tag{B.2}
$$

B.3.1. Derivations of the ODE for c_ω^2, d_θ^2 and (3.43)

Recall $c_\omega = u_x(0) = -\frac{2}{\pi}\int_0^{+\infty}\frac{\omega}{x}dx$ from (3.3). Multiplying the equation of ω in (3.1) by $-\frac{1}{x}$ and then taking the integral from $0, +\infty$ yield

$$\begin{aligned}\frac{d}{dt}\frac{\pi}{2}c_\omega =& \frac{d}{dt}\int_0^{+\infty}\frac{\omega}{-x}dx = \int_0^\infty \frac{(\bar{c}_l x+\bar{u})\omega_x + u\bar{\omega}_x}{x}dx - \int_0^\infty \frac{\theta_x}{x}dx\\ &+\int_0^\infty \frac{\bar{c}_\omega\omega + c_\omega\bar{\omega}}{-x}dx - \int_0^\infty \frac{F_\omega + N(\omega)}{x}dx\\ =&\int_0^\infty \frac{\bar{u}\omega_x + u\bar{\omega}_x}{x}dx - d_\theta + \frac{\pi}{2}(\bar{c}_\omega + \bar{u}_x(0))c_\omega - \int_0^\infty \frac{F_\omega + N(\omega)}{x}dx,\end{aligned}$$

where we have used the notation d_θ in (3.41) and $\int_0^\infty \frac{f}{-x} = \frac{\pi}{2}Hf(0)$ with $f = \omega, \bar{\omega}$ in the last identity. Multiplying c_ω on both sides, we yield

$$\begin{aligned}\frac{1}{2}\frac{d}{dt}\frac{\pi}{2}c_\omega^2 =& \frac{\pi}{2}(\bar{c}_\omega + \bar{u}_x(0))c_\omega^2 + c_\omega\int_0^\infty \frac{\bar{u}\omega_x + u\bar{\omega}_x}{x}dx - c_\omega d_\theta\\ &- c_\omega\int_0^\infty \frac{F_\omega + N(\omega)}{x}dx.\end{aligned} \tag{B.3}$$

which is exactly (3.42).

We derive the ODE for d_θ using the θ equation in (3.1). Since $\int_{\mathbb{R}_+}\frac{\bar{c}_l x\theta_{xx}}{x}dx = 0$, we get

$$\begin{aligned}\frac{d}{dt}d_\theta =& 2\bar{c}_\omega\int_{\mathbb{R}_+}\frac{\theta_x}{x} + 2c_\omega\int_{\mathbb{R}_+}\frac{\bar{\theta}_x}{x} - \int_0^\infty \frac{\bar{u}_x\theta_x + \bar{u}\theta_{xx}}{x}dx - \int_0^\infty \frac{u\bar{\theta}_{xx} + u_x\bar{\theta}_x}{x}dx\\ &+\int_0^\infty \frac{F_\theta + N(\theta)}{x}dx \triangleq I_1 + I_2 + I_3 + I_4 + I_5.\end{aligned} \tag{B.4}$$

We use the notation $\langle\cdot,\cdot\rangle$ in (2.5) to simplify the integral. For I_3, using integration by parts, we obtain

$$I_3 = -\langle(\bar{u}\theta_x)_x, x^{-1}\rangle = \langle\bar{u}\theta_x, \partial_x x^{-1}\rangle = -\langle\bar{u}\theta_x, x^{-2}\rangle.$$

Similarly, for I_4, we get

$$I_4 = -\langle u\bar{\theta}_x, x^{-2}\rangle.$$

Recall $c_\omega = u_x(0)$. We rewrite the above term using the decomposition $u = \tilde{u} + u_x(0)x$ (3.10)

$$I_4 = -\langle(\tilde{u} + u_x(0)x)\bar{\theta}_x, x^{-2}\rangle = -\langle\tilde{u}\bar{\theta}_x, x^{-2}\rangle - c_\omega\bar{d}_\theta.$$

where we have used the notation $\bar{d}_\theta$ defined in (3.41). Using (3.41), we can simplify I_1, I_2 as

$$I_1 = 2\bar{c}_\omega d_\theta, \quad I_2 = 2c_\omega \bar{d}_\theta.$$

The $c_\omega d_\theta$ term in I_2 and I_4 are canceled partially. Using these computations and multiplying both sides of (B.4) by d_θ yields

$$\begin{aligned}\frac{1}{2}\frac{d}{dt}d_\theta^2 = 2\bar{c}_\omega d_\theta^2 + c_\omega \bar{d}_\theta d_\theta - d_\theta \int_0^\infty \frac{\bar{u}\theta_x}{x^2}dx - d_\theta \int_0^\infty \frac{\tilde{u}\bar{\theta}_x}{x^2}dx \\ + d_\theta \int_0^\infty \frac{F_\theta + N(\theta)}{x}dx.\end{aligned} \tag{B.5}$$

Since $\bar{d}_\theta > 0$, the term $c_\omega d_\theta$ in (B.5) and (B.3) have cancellation.

The quadratic parts on the right hand sides in (B.3), (B.5) involve the following terms remained to estimate

$$J_1 = \langle \bar{u}, \omega_x x^{-1}\rangle,\ J_2 = \langle u, \bar{\omega}_x x^{-1}\rangle,\ J_3 = \langle \bar{u}, \theta_x x^{-2}\rangle,\ J_4 = \langle \tilde{u}, \bar{\theta}_x x^{-2}\rangle. \tag{B.6}$$

We use the idea in Section 3.11.2 to rewrite the integrals of u as the integrals of ω and of $\tilde{u} - \frac{1}{5}\tilde{u}_x x = u_\Delta$ (see (3.41)). We use the functions f_i defined (B.2) to simplify the integrals of θ_x, ω. In Appendix B.3.2, we rewrite J_i as follows

$$\begin{aligned}J_1 + J_2 &= \langle \omega, f_2\rangle + \langle u_\Delta x^{-1}, f_5\rangle, \\ J_3 &= \langle \theta_x, f_6\rangle, \quad J_4 = \langle u_\Delta x^{-1}, f_9\rangle - \langle \omega, f_4\rangle.\end{aligned} \tag{B.7}$$

For some parameters $\lambda_2, \lambda_3 > 0$ to be determined, combining (B.3) and (B.5), we yield

$$\begin{aligned}\frac{1}{2}\frac{d}{dt}\left(\frac{\lambda_2\pi}{2}c_\omega^2 + \lambda_3 d_\theta^2\right) = \frac{\pi\lambda_2}{2}\left(\bar{c}_\omega + \bar{u}_x(0)\right)c_\omega^2 + \lambda_2 c_\omega (J_1 + J_2) \\ - \lambda_2 c_\omega d_\theta - \lambda_2 c_\omega \langle F_\omega + N(\omega), x^{-1}\rangle \\ + 2\bar{c}_\omega \lambda_3 d_\theta^2 + \lambda_3 c_\omega \bar{d}_\theta d_\theta \\ - \lambda_3 d_\theta J_3 - \lambda_3 d_\theta J_4 + \lambda_3 d_\theta \langle F_\theta + N(\theta), x^{-1}\rangle.\end{aligned}$$

Plugging (B.7) in the above ODE, we derive (3.43).

B.3.2 Derivations of (B.7) in the ODEs

Recall the integrals J_i from (B.6). We use the idea in Section 3.11.2 to derive the formulas in (B.7).

Recall $\tilde{u} = u - u_x(0)x$ from (3.10). Firstly, we consider J_2. Since $\int_0^\infty \bar{\omega}_x dx = 0$, we have

$$J_2 = \langle u - u_x(0)x, \bar{\omega}_x x^{-1}\rangle = \langle \tilde{u}, \bar{\omega}_x x^{-1}\rangle.$$

We approximate the far field of $\bar{\omega}_x x^{-1}$ by $\frac{1}{4}(\frac{\bar{\omega}}{x})_x$ and derive

$$J_2 = \Big\langle \tilde{u}, \frac{\bar{\omega}_x}{x} - \frac{1}{4}(\frac{\bar{\omega}}{x})_x \Big\rangle + \frac{1}{4}\Big\langle \tilde{u}, (\frac{\bar{\omega}}{x})_x \Big\rangle \triangleq J_{21} + J_{22}.$$

Applying integration by parts, (A.1) and (A.2) yields

$$J_{22} = -\frac{1}{4}\langle \tilde{u}_x, \bar{\omega} x^{-1}\rangle = -\frac{1}{4}\Big\langle H\left(\frac{\omega}{x}\right), \bar{\omega}\Big\rangle = \frac{1}{4}\Big\langle \frac{\omega}{x}, H\bar{\omega}\Big\rangle = \frac{1}{4}\Big\langle \frac{\omega}{x}, \bar{u}_x\Big\rangle.$$

In J_{21}, the coeifficient

$$\frac{\bar{\omega}_x}{x} - \frac{1}{4}(\frac{\bar{\omega}}{x})_x = \frac{3}{4}\frac{\bar{\omega}_x}{x} + \frac{1}{4}\frac{\bar{\omega}}{x^2}$$

decays much faster than $\bar{\omega}_x x^{-1}$ for large x. We approximate $\tilde{u}$ by $\frac{1}{5}\tilde{u}_x x$

$$\begin{aligned} J_{21} &= \Big\langle \tilde{u}, \frac{3}{4}\frac{\bar{\omega}_x}{x} + \frac{1}{4}\frac{\bar{\omega}}{x^2}\Big\rangle = \Big\langle \tilde{u} - \frac{1}{5}\tilde{u}_x x, \frac{3}{4}\frac{\bar{\omega}_x}{x} + \frac{1}{4}\frac{\bar{\omega}}{x^2}\Big\rangle \\ &+ \frac{1}{5}\Big\langle \tilde{u}_x x, \frac{3}{4}\frac{\bar{\omega}_x}{x} + \frac{1}{4}\frac{\bar{\omega}}{x^2}\Big\rangle \triangleq I_1 + I_2. \end{aligned}$$

Using a direct computation and then applying (A.1) and (A.2), we get

$$\begin{aligned} I_2 &= \frac{1}{5}(\frac{3}{4}\langle \tilde{u}_x, \bar{\omega}_x\rangle + \frac{1}{4}\langle \frac{\tilde{u}_x}{x}, \bar{\omega}\rangle) = \frac{1}{5}(\frac{3}{4}\langle u_x, \bar{\omega}_x\rangle + \frac{1}{4}\langle H\left(\frac{\omega}{x}\right), \bar{\omega}\rangle) \\ &= \frac{1}{5}(-\frac{3}{4}\langle \omega, H\bar{\omega}_x\rangle - \frac{1}{4}\langle \frac{\omega}{x}, H\bar{\omega}\rangle) = -\frac{1}{5}\langle \omega, \frac{3}{4}\bar{u}_{xx} + \frac{1}{4}\frac{\bar{u}_x}{x}\rangle, \end{aligned}$$

where we have used $\int_0^\infty u_x(0)\bar{\omega}_x dx = 0$ in the second identity. Using the notation and function in (3.41), (B.2), we can simplify I_1 as

$$I_1 = \langle u_\Delta x^{-1}, f_8\rangle.$$

Combining the above calculations on J_{22}, I_1, I_2, we obtain

$$J_2 = I_1 + I_2 + J_{22} = \Big\langle \omega, \frac{1}{4}\frac{\bar{u}_x}{x} - \frac{1}{5}(\frac{3}{4}\bar{u}_{xx} + \frac{1}{4}\frac{\bar{u}_x}{x})\Big\rangle + \Big\langle \frac{u_\Delta}{x}, f_8\Big\rangle.$$

For J_1 in (B.6), using integration by parts, we obtain

$$J_1 = \langle \bar{u}x^{-1}, \omega_x\rangle = -\langle \partial_x(\bar{u}x^{-1}), \omega\rangle = \langle -\frac{\bar{u}_x}{x} + \frac{\bar{u}}{x^2}, \omega\rangle.$$

We can simplify $J_1 + J_2$ using the function f_2 in (B.2)

$$J_1 + J_2 = \langle \omega, f_2\rangle + \langle u_\Delta x^{-1}, f_5\rangle. \tag{B.8}$$

For J_3, using f_6 defined in (B.2), we get

$$J_3 = \langle \theta_x, \bar{u}x^{-2} \rangle = \langle \theta_x, f_6 \rangle. \tag{B.9}$$

For J_4 in (B.6), we use a similar computation to obtain

$$\begin{aligned} J_4 &= \langle \tilde{u}, \bar{\theta}_x x^{-2} \rangle = \Big\langle \tilde{u}, \frac{\bar{\theta}_x}{x^2} + \frac{3}{5}\Big(\frac{\bar{\theta}_x}{x}\Big)_x \Big\rangle - \frac{3}{5}\Big\langle \tilde{u}, \Big(\frac{\bar{\theta}_x}{x}\Big)_x \Big\rangle = \langle \tilde{u}, \frac{3}{5}\frac{\bar{\theta}_{xx}}{x} + \frac{2}{5}\frac{\bar{\theta}_x}{x^2} \rangle - \frac{3}{5}\Big\langle \tilde{u}, (\frac{\bar{\theta}_x}{x})_x \Big\rangle \\ &= \Big\langle \tilde{u} - \frac{1}{5}\tilde{u}_x x, \frac{3}{5}\frac{\bar{\theta}_{xx}}{x} + \frac{2}{5}\frac{\bar{\theta}_x}{x^2} \Big\rangle + \frac{1}{5}\Big\langle \tilde{u}_x x, \frac{3}{5}\frac{\bar{\theta}_{xx}}{x} + \frac{2}{5}\frac{\bar{\theta}_x}{x^2} \Big\rangle - \frac{3}{5}\Big\langle \tilde{u}, (\frac{\bar{\theta}_x}{x})_x \Big\rangle \triangleq J_{41} + J_{42} + J_{43}. \end{aligned}$$

For J_{41}, using the notations in (3.41) and (B.2), we obtain

$$J_{41} = \langle u_\Delta x^{-1}, f_9 \rangle.$$

For J_{42}, J_{43}, using Lemmas A.2 and A.3, we derive

$$\begin{aligned} J_{42} &= \frac{1}{5}\Big\langle \tilde{u}_x, \frac{3}{5}\bar{\theta}_{xx} + \frac{2}{5}\frac{\bar{\theta}_x}{x} \Big\rangle = \frac{1}{5}\left(\frac{3}{5}\Big\langle H\omega - H\omega(0), \bar{\theta}_{xx} \Big\rangle + \frac{2}{5}\Big\langle H\left(\frac{\omega}{x}\right), \bar{\theta}_x \Big\rangle \right) \\ &= -\frac{1}{5}\left(\frac{3}{5}\langle \omega, H\bar{\theta}_{xx} \rangle + \frac{2}{5}\langle \frac{\omega}{x}, H\bar{\theta}_x \rangle \right), \\ J_{43} &= \frac{3}{5}\Big\langle \tilde{u}_x, \frac{\bar{\theta}_x}{x} \Big\rangle = \frac{3}{5}\Big\langle H(\frac{\omega}{x}), \bar{\theta}_x \Big\rangle = -\frac{3}{5}\Big\langle \frac{\omega}{x}, H\bar{\theta}_x \Big\rangle. \end{aligned}$$

Combining the above computations and using the notations $\bar{u}_{\theta,x}$, f_4 defined in (3.41), (B.2), we yield

$$\begin{aligned} J_4 &= J_{41} + J_{42} + J_{43} = \langle u_\Delta x^{-1}, f_9 \rangle - \Big\langle \omega, \frac{3}{5}\frac{\bar{u}_{\theta,x}}{x} + \frac{1}{5}\left(\frac{3}{5}\bar{u}_{\theta,xx} + \frac{2}{5}\frac{\bar{u}_{\theta,x}}{x} \right) \Big\rangle \\ &= \langle u_\Delta x^{-1}, f_9 \rangle - \langle \omega, f_4 \rangle. \end{aligned}$$

The formulas in (B.8), (B.9) and the above formula imply (B.7).

B.4 Derivations of the commutators in (5.3)

Recall $D_x = x\partial_x$ and the operators in (3.5). We choose $f = \theta_x$, $g = \omega$ in (3.5). We use the notation $u_x = H\omega$. Then $u = -\Lambda^{-1}\omega$.

Firsrly, we compute the commutator related to the transport term. Using $(\bar{c}_l x + \bar{u})\partial_x = (\bar{c}_l + \frac{\bar{u}}{x})D_x$, for $p = \omega$ or θ_x, we yield

$$\begin{aligned} -[D_x, (\bar{c}_l x + \bar{u})\,\partial_x]p &= -[D_x, \left(\bar{c}_l + \frac{\bar{u}}{x}\right) D_x] \\ p &= -D_x\left(\left(\bar{c}_l + \frac{\bar{u}}{x}\right) D_x p \right) + \left(\bar{c}_l + \frac{\bar{u}}{x}\right) D_x(D_x p) \end{aligned}$$

$$= -D_x\left(\bar{c}_l + \frac{\bar{u}}{x}\right) D_x p = -\left(\bar{u}_x - \frac{\bar{u}}{x}\right) D_x p. \quad \text{(B.10)}$$

Next, we compute the velocity corresponding to $D_x\omega$. Using Lemma A.1, we get

$$H(D_x\omega) - H(D_x\omega)(0) = xH(\omega_x) = x\partial_x H\omega = xu_{xx}.$$

Note that $H(D_x\omega)(0) = -\frac{1}{\pi}\int_{\mathbb{R}} \omega_x dx = 0$. We obtain $D_x u_x = xu_{xx} = H(D_x\omega)$. From

$$(xu_x - u)_x = xu_{xx} = H(D_x\omega), \quad (xu_x - u)(0) = 0,$$

we obtain that $xu_x - x$ is the velocity corresponding to $D_x\omega$. Therefore, we have

$$\begin{aligned} H\omega = u_x, \quad -\Lambda^{-1}\omega = u, \quad H(D_x\omega)(0) = 0, \\ H(D_x\omega) = xu_{xx}, \quad -\Lambda^{-1}(D_x\omega) = xu_x - u. \end{aligned}$$

Using these formulas, for $q = \bar{\omega}_x$ or $\bar{\theta}_{xx}$ we obtain

$$\begin{aligned} &D_x\Big(-(-\Lambda^{-1}\omega - H\omega(0)x)q\Big) - \Big(-(-\Lambda^{-1}D_x\omega - HD_x\omega(0)x)q\Big) \\ &\quad = D_x(-(u - u_x(0)x)q) + (xu_x - u)q \\ &\quad = -(u - u_x(0)x)D_x q + (-(xu_x - u_x(0)x))q + (xu_x - u) \\ &q = -(u - u_x(0)x)(D_x q + q). \end{aligned} \quad \text{(B.11)}$$

Similarly, we have

$$\begin{aligned} &D_x\Big(-(H\omega - H\omega(0)x)q\Big) - (-(HD_x\omega - HD_x\omega(0))q) \\ &\quad = D_x(-(u_x - u_x(0))q) + xu_{xx}q \\ &\quad = -D_x u_x q - (u_x - u_x(0))D_x q + xu_{xx}q = -(u_x - u_x(0))D_x q. \end{aligned} \quad \text{(B.12)}$$

Since $\bar{c}_\omega\omega$, θ_x in $\mathcal{L}_{\omega 1}$ (3.5) vanish in the commutator, applying (B.10) with $p = \omega$ and (B.11) with $q = \bar{\omega}_x$ yields the formula for $[D_x, \mathcal{L}_{\omega 1}]$ in (5.3). Note that

$$D_x((2\bar{c}_\omega - \bar{u}_x)\theta_x) - (2\bar{c}_\omega - \bar{u}_x)D_x\theta_x = -D_x\bar{u}_x\theta_x.$$

Combining this computation, (B.10) with $p = \theta_x$, (B.11) with $q = \bar{\theta}_{xx}$ and (B.12) with $q = \bar{\theta}_x$, we derive the formula for $[D_x, \mathcal{L}_{\theta 1}]$ in (5.3).

B.5 Derivation and computing C_{opt} in Section 3.11.3

Recall the inequality (3.50), the functions in (3.49) and the spaces Σ_i in (3.51). We use the argument similar to that in [11] to derive and compute C_{opt}.

In Section 3.11.3, we have reduced (3.50) to an optimization problem on the finite dimensional space $\Sigma_1 \oplus \Sigma_2 \oplus \Sigma_3$ with $X \in \Sigma_1$, $Y \in \Sigma_2$, $Z \in \Sigma_3$. Here, we have a direct sum of spaces since there is no inner product among X, Y, Z. Let $\{\mathbf{e}_1, \mathbf{e}_2, \mathbf{e}_3, \mathbf{e}_4\}$ be an orthonormal basis (ONB) of Σ_1 with $\mathbf{e}_1 = \frac{g_1}{||g_1||_2^2}$; $\{\mathbf{e}_5, \mathbf{e}_6, \mathbf{e}_7\}$ be that of Σ_2 with $\mathbf{e}_2 = \frac{g_5}{||g_5||_2^2}$; $\{\mathbf{e}_8, \mathbf{e}_9\}$ be that of Σ_3. Then $\{\mathbf{e}_i\}_{i=1}^9$ is an ONB of $\Sigma \triangleq \Sigma_1 \oplus \Sigma_2 \oplus \Sigma_3$.

Let $v_i \in \mathbb{R}^9$ be the coordinate of g_i in Σ under the basis $\{\mathbf{e}_i\}_{i=1}^9$ and $p = (x, y, z) \in \mathbb{R}^4 \times \mathbb{R}^3 \times \mathbb{R}^2$ be that of $X + Y + Z$. The vectors v_i and p are column vectors. By abusing notation, we also use $\langle \cdot, \cdot \rangle$ to denote the Euclidean inner product in $\mathbb{R}^9$. With these convections, each summand on the left hand side of (3.50) is a quadratic form in p. For example, we have

$$\langle X, g_1 \rangle \langle Y, g_7 \rangle = \langle p, v_1 \rangle \langle p, v_7 \rangle = (p^T v_1)(v_7^T p) = p^T (v_1 v_7^T) p.$$

Hence, (3.50) is equivalent to

$$p^T M p \leq C_{opt}\, p^T D p, \tag{B.13}$$

where M and D are given by

$$\begin{aligned} M &= v_1 v_3^T + v_1 v_7^T - (\lambda_2 - \lambda_3 \bar{d}_\theta) v_1 v_5^T + \lambda_2 v_1 v_2^T \\ &\quad - \lambda_3 v_5 v_6^T + \lambda_3 v_5 v_4^T + \lambda_2 v_1 v_8^T - \lambda_3 v_5 v_9^T, \\ D &= Id + s_1 v_1 v_1^T + s_2 v_5 v_5^T. \end{aligned} \tag{B.14}$$

By definition of $\mathbf{e}_1, \mathbf{e}_5$, i.e. $\mathbf{e}_1 = \frac{g_1}{||g_1||_2}$, $\mathbf{e}_5 = \frac{g_5}{||g_5||_2}$, we have $v_1 = ||g_1||_2 E_1$, $v_5 = ||g_5||_2 E_5$, where $E_i \in \mathbb{R}^9$ is the standard basis of $\mathbb{R}^9$, i.e. the i-th coordinate of E_i is 1 and 0 otherwise. Therefore, D is a diagonal matrix

$$D = \mathrm{diag}(1 + s_1 ||g_1||_2^2,\ 1,\ 1,\ 1,\ 1 + s_2 ||g_5||_2^2,\ 1,\ 1,\ 1,\ 1) \in \mathbb{R}^{9\times 9}.$$

Symmetrizing the left hand side of (B.13) and using a change of variable $q = D^{1/2} p$, we obtain

$$C_{opt} = \lambda_{\max}(D^{-1/2} M_s D^{-1/2}), \quad M_s = \frac{1}{2}(M + M^T).$$

Firstly, M can be written as

$$\begin{aligned} &M = V_1 V_2^T, \quad V_2 = (v_3, v_7, v_5, v_2, v_6, v_4, v_8, v_9), \\ &V_1 = (v_1, v_1, -(\lambda_2 - \bar{d}_\theta \lambda_3) v_1, \lambda_2 v_1, -\lambda_3 v_5, \lambda_3 v_5, \lambda_2 v_1, -\lambda_3 v_5). \end{aligned}$$

Then $M_s = \frac{1}{2}(V_1V_2^T + V_2V_1^T) = \frac{1}{2}U_1U_2^T$ with $U_1 = [V_1, V_2], U_2 = [V_2, V_1] \in \mathbb{R}^{9\times 16}$. Using the argument in [11], for any even integer $p \geq 2$, we obtain

$$\begin{aligned} C_{opt} &\leq (\mathrm{Tr}|D^{-1/2}M_sD^{-1/2}|^p)^{1/p} = 2^{-1}(\mathrm{Tr}(D^{-1/2}U_1U_2^TD^{-1/2})^p)^{1/p} \\ &= 2^{-1}(\mathrm{Tr}(U_2^TD^{-1}U_1)^p)^{1/p}. \end{aligned} \tag{B.15}$$

We will explain how to rigorously estimate the bound above in the Supplementary Material [10].

B.6 Estimate of $\mathcal{T}$ in Section 3.12

For $\lambda_2, \lambda_3, t_{61}, \kappa, r_{c_\omega} > 0$ chosen in (C.3), Appendix C and t_{62} determined by these parameters, we define T_i and s_i

$$\begin{aligned} &T_1 = (-\lambda_1 D_\omega - A_\omega\varphi^{-1} - \lambda_1\kappa)\varphi - t_{61}x^{-4}, \quad T_2 = (-D_\theta - A_\theta\psi^{-1} - \kappa)\psi, \\ &T_3 = 25t_{61}x^{-4} + t_{62}x^{-4/3}, \quad s_1 = -\frac{\pi}{2}\lambda_2(\bar{c}_\omega + \bar{u}_x(0)) - r_{c_\omega} - \frac{\pi\lambda_1 e_3\alpha_6}{12} - G_c, \\ &s_2 = -2\bar{c}_\omega\lambda_3 - \kappa\lambda_3, \end{aligned} \tag{B.16}$$

We will verify that $T_i > 0, s_i > 0$ later. The parameter r_{c_ω} is essentially determined by κ. See Appendix C.2 for the procedure to determine these parameters. Plugging the above T_i and s_i in (3.48), we can compute the upper bound of C_{opt} in (3.48) using (B.15) with $p = 36$

$$C_{opt} \leq 2^{-1}(\mathrm{Tr}(U_2^TD^{-1}U_1)^p)^{1/p} < 0.9930 < 1, \tag{B.17}$$

which is verified in (D.7), Appendix D. Thus from (3.48), we obtain

$$\mathcal{T} \leq ||\omega T_1^{1/2}||_2^2 + ||\theta_x T_2^{1/2}||_2^2 + ||\frac{u_\Delta}{x}T_3^{1/2}||_2^2 + s_1c_\omega^2 + s_2d_\theta^2,$$

which is exactly (3.53). By definition of T_1, T_2, we have

$$\begin{aligned} \langle(D_\theta + A_\theta\psi^{-1})\psi, \theta_x^2\rangle + \langle T_2, \theta_x^2\rangle &= -\kappa\langle\theta_x^2, \psi\rangle, \\ \langle(\lambda_1 D_\omega + A_\omega\varphi^{-1})\varphi, \omega^2\rangle + \langle T_1, \omega^2\rangle &= -\kappa\lambda_1\langle\omega^2, \varphi\rangle - t_{61}\langle\omega^2, x^{-4}\rangle. \end{aligned}$$

Hence, plugging the above estimate on $\mathcal{T}$ in (3.52), we yield

$$\begin{aligned} J = &-\kappa||\theta_x\psi^{1/2}||_2^2 - \kappa\lambda_1||\omega\varphi^{1/2}||_2^2 - t_{61}||\omega x^{-2}||_2^2 + s_1c_\omega^2 + s_2d_\theta^2 \\ &+ ||\frac{u_\Delta}{x}T_3^{1/2}||_2^2 - \Big(D_u - \frac{9}{49}t_{12} - \frac{72\lambda_1}{49}\cdot 10^{-5}\Big)||\tilde{u}_x x^{-2/3}||_2^2 + A(u) + G_c c_\omega^2. \end{aligned} \tag{B.18}$$

It remains to estimate the u_Δ term. Recall u_Δ in (3.41) and T_3 in (B.16). A direct calculation yields

$$||\frac{u_\Delta}{x}T_3^{1/2}||_2^2 = \int_0^\infty (\tilde{u} - \frac{1}{5}\tilde{u}_x x)^2 \cdot 25 t_{61} x^{-6} dx$$
$$+ \int_0^\infty (\tilde{u} - \frac{1}{5}\tilde{u}_x x)^2 \cdot t_{62} x^{-10/3} dx \triangleq I_1 + I_2$$

Using (2.9) with $p = 3$ and Lemma A.2, we get

$$I_1 = t_{61}||\tilde{u}_x x^{-2}||_2^2 = t_{61}||\omega x^{-2}||_2^2.$$

For I_2, using integration by parts and Lemma A.8 about $\tilde{u}$ with $\alpha = \beta = 0$, we get

$$I_2 = t_{62}\int_0^\infty \frac{1}{25}\frac{\tilde{u}_x^2}{x^{4/3}} - \frac{2}{5}\frac{\tilde{u}\tilde{u}_x}{x^{7/3}} + \frac{\tilde{u}^2}{x^{10/3}} dx = t_{62}\int_0^\infty \frac{1}{25}\frac{\tilde{u}_x^2}{x^{4/3}} + \frac{1}{5}\tilde{u}^2\partial_x x^{-7/3} + \frac{\tilde{u}^2}{x^{10/3}} dx$$
$$= t_{62}\int_0^\infty \frac{1}{25}\frac{\tilde{u}_x^2}{x^{4/3}} + (1 - \frac{7}{15})\frac{\tilde{u}^2}{x^{10/3}} dx \le t_{62}\int_0^\infty \frac{\tilde{u}_x^2}{x^{4/3}}\left(\frac{1}{25} + \frac{8}{15}\cdot\frac{36}{49}\right) dx.$$

Combining the estimates of I_1, I_2 yields

$$||\frac{u_\Delta}{x}T_3^{1/2}||_2^2 \le t_{61}||\omega x^{-2}||_2^2 + \left(\frac{1}{25} + \frac{8}{15}\cdot\frac{36}{49}\right)t_{62}||\tilde{u}_x x^{-2/3}||_2^2, \tag{B.19}$$

We define t_{62} in Appendix C so that the terms $||\tilde{u}_x x^{-2/3}||_2^2$ in (B.19) and (B.18) are almost canceled. We establish (3.54), i.e.

$$J \le -\kappa||\theta_x \psi^{1/2}||_2^2 - \kappa\lambda_1||\omega\varphi^{1/2}||_2^2 + (s_1 + G_c)c_\omega^2$$
$$+ s_2 d_\theta^2 - 10^{-6}||\tilde{u}_x x^{-2/3}||_2^2 + A(u).$$

Appendix C. Parameters in the estimates

C.1. Parameters

Parameters e_1, e_2, e_3 introduced in (3.7) are determined by the approximate self-similar profiles

$$e_1 = 1.5349, \quad e_2 = 1.2650, \quad e_3 = 1.3729. \tag{C.1}$$

We choose the following parameters for the weights ψ, φ (3.8),(3.9)

$$\alpha_1 = 5.3, \quad \alpha_2 = 3.3, \quad \alpha_3 = 0.68, \quad \alpha_4 = 12.1, \quad \alpha_5 = 2.1, \quad \alpha_6 = 0.77, \tag{C.2}$$

and the following parameters in the linear stability analysis in Section 3

$$\begin{aligned} &\lambda_1 = 0.32, \quad t_1 = 1.29, \quad t_{12} = \frac{49}{9} \cdot 0.9 D_u, \quad t_2 = 5.5, \quad t_{22} = 13.5, \quad t_{31} = 3.2, \\ &t_{32} = 0.5, \quad t_{34} = 2.9, \quad \tau_1 = 4.7, \quad t_4 = 3.8, \quad \lambda_2 = 2.15, \quad \lambda_3 = 0.135, \\ &t_{61} = 0.16, \quad \kappa = 0.03, \quad r_{c_\omega} = 0.15. \end{aligned} \tag{C.3}$$

Parameter λ_1 is introduced in (3.12), (3.14); t_2, t_{22} are introduced in the estimates of I_n (3.18), (3.20); t_1, t_{12} are introduced in the estimate of I_f (3.23), (3.25); t_4 is introduced in the estimate of I_s in (3.28); (t_{31}, t_{32}), t_{34}, τ_1 are introduced in the estimate of $I_{u\omega}$ in (3.33), (3.32) and (3.30), respectively; $\lambda_2, \lambda_3, t_{61}, \kappa, r_{c_\omega}$ are introduced in (B.16) to estimate $\mathcal{T}$ in (3.53).

The parameter D_u introduced in (3.25), t_{62} in (B.16) are determined by the above parameters

$$D_u = \frac{t_1 \alpha_3 \lambda_1 \alpha_6}{\sqrt{3}}, \quad t_{62} = (D_u - \frac{9}{49} t_{12} - \frac{72\lambda_1}{49} \cdot 10^{-5} - 10^{-6})(\frac{1}{25} + \frac{8}{15} \cdot \frac{36}{49})^{-1}.$$

After we complete the weighted L^2 estimate, we choose the following parameters in the weighted H^1 estimates and nonlinear stability estimates

$$\begin{aligned} &\kappa_2 = 0.024, \quad t_{71} = 2.8, \quad t_{72} = 2, \quad t_{81} = 5, \quad t_{82} = 0.7, \quad t_{91} = 1, \quad t_{92} = 1.2, \\ &\gamma_1 = 0.98, \quad \gamma_2 = 0.07, \quad \lambda_4 = 0.005, \quad E_* = 2.5 \cdot 10^{-5}, \quad a_{H^1} = 0.31. \end{aligned} \tag{C.4}$$

Parameters t_{7i}, t_{8i}, t_{9i} are introduced in the estimates of Q_2 (5.11), (5.17); κ_2 in (5.23); γ_1, γ_2 in (5.22); λ_4 in (5.29). Parameter a_{H1} is determined by the above parameters via $A_{\omega 2}$ (5.20) and (5.24)

$$a_{H^1} = 0.31.$$

C.2. Choosing parameters in $\mathcal{T}$ and determining κ

We first choose $r_{c_\omega} = \kappa \frac{\pi}{2} \lambda_2$ with small $\kappa = 0.001$. The remaining unknown parameters in the linear stability analysis are $\lambda_2, \lambda_3, t_{61} > 0$. Once $\lambda_2, \lambda_3, t_{61}$ are chosen, the functions T_i and scalars s_i in (B.16) are determined and then we can compute C_{opt} in (3.48) using the argument in Section (3.47) and Appendix B.5. We optimize $\lambda_2, \lambda_3, t_{61} > 0$ subject to the constraints $T_i > 0, s_i > 0$, such that $C_{opt} < 0.98$ and C_{opt} is as small as possible. Then we obtain the approximate values for $\lambda_2, \lambda_3, t_{61}$.

Our goal is to obtain κ as large as possible. The estimate of C_{opt} depends on all the parameters in (C.2)-(C.3). We gradually increase κ until $C_{opt} < 0.98$ is violated. We further refine all the parameters in (C.2)-(C.3) one by one and by modifying them around their approximate values to obtain smaller C_{opt}. Then we increase κ again. Repeating this process several times, we obtain larger κ and $\kappa = 0.03$. Finally, we increase r_{c_ω} until $C_{opt} < 0.98$ is violated. This allows us to obtain a damping term for

c_ω^2 with a larger coefficient in the weighted L^2 estimate (3.57), Using this procedure, we determine the parameters in (C.2), (C.3) and further establish (3.57).

In our process of determining the parameters, we actually first use the grid point values of the functions and only need to track the constraints, e.g. $T_i > 0$, on the grid points instead of every $x \in \mathbb{R}$. After we determine all parameters, we verify the constraints rigorously by using computer-assisted analysis and establish the desired bound $C_{opt} < 0.993 < 1$ (B.17).

Appendix D. Rigorous Verification

This section is a collection of inequalities that will be rigorously verified with the help of computer programs. The methods of computer-assisted verification are introduced and discussed in detail in the Supplementary Material [10]. All the numerical computations and quantitative verifications are performed in MATLAB (version 2020a) in double-precision floating-point operations. The MATLAB codes can be found via the link [9].

D.1. Ranges of the parameters

Denote by

$$G_1(\lambda_1, t_2, t_{22}) \triangleq t_2 x^{-4} + \frac{t_{22}}{25} x^{-4} + t_2(\lambda_1\alpha_5)^2 x^{-2},\ G_2(t_2, t_{22}) \triangleq \frac{1}{4t_2}(\alpha_2 x^{-1} + \alpha_1 x^{-2})^2 + \frac{1}{4t_{22}}(x^3\bar{\theta}_{xx}\psi_n)^2$$

the coefficients in (3.21). Applying estimate (3.21) on I_n, we establish (3.22) with $c = 0.01$ if

$$\frac{1}{\lambda_1} G_1(\lambda_1, t_2, t_{22})\varphi^{-1} + D_\omega \le -c, \quad G_2(t_2, t_{22})\psi^{-1} + D_\theta \le -c,$$

where D_ω, D_θ defined in (3.13) are the coefficients in D_1, D_2. To verify the above estimate for $\lambda_1 \in [\lambda_{1l}, \lambda_{1u}] = [0.31, 0.33], t_2 \in [t_{2l}, t_{2u}] = [5.0, 5.8]$, $t_{22} \in [t_{22l}, t_{22u}] = [13, 14]$, since G_1, G_2 are monotone in λ_1, t_2, t_{22}, it suffices to verify

$$\frac{1}{\lambda_{1l}} G_1(\lambda_{1u}, t_{2u}, t_{22u})\varphi^{-1} + D_\omega \le -c, \quad G_2(t_{2l}, t_{22l})\psi^{-1} + D_\theta \le -c. \quad \text{(D.1)}$$

Similar, in order for $I_f + D_1 + D_2 \le -0.01(||\theta_x\psi^{1/2}||_2 + \lambda_1||\omega\varphi^{1/2}||_2^2)$ with estimate 3.27 on I_f and $\lambda_1 \in [\lambda_{1l}, \lambda_{1u}] = [0.31, 0.33]$, $t_1 \in [t_{1l}, t_{1u}] = [1.2, 1.4]$, $t_{12} \in [t_{12l}, t_{12u}] = [0.55, 0.65]$, it suffices to verify

$$\frac{1}{\lambda_{1l}} G_3(\lambda_{1u}, t_{1u}, t_{12u})\varphi^{-1} + D_\omega \le -c, \quad G_4(t_{1l}, t_{12l})\psi^{-1} + D_\theta \le -c, \quad \text{(D.2)}$$

where

$$G_3(\lambda_1, t_1, t_{12}) = t_1\Big(\alpha_3^2 x^{-2} + \frac{\alpha_3\lambda_1\alpha_6}{\sqrt{3}}x^{-4/3} + (\lambda_1\alpha_6)^2 x^{-2/3}\Big),$$
$$G_4(t_1, t_{12}) = \frac{1}{4t_1}x^{-2/3} + \frac{1}{4t_{12}}(\psi_f\bar{\theta}_{xx}x^{5/3})^2.$$

In order for $I_s + D_1 + D_2 \le -0.01(||\theta_x\psi^{1/2}||_2 + \lambda_1||\omega\varphi^{1/2}||_2^2)$ with estimate (3.28) on I_s and $\lambda_1 \in [\lambda_{1l}, \lambda_{1u}] = [0.31, 0.33]$, $t_4 \in [t_{4l}, t_{4u}] = [3.5, 4.0]$, it suffices to verify

$$\frac{1}{\lambda_{1l}}G_5(t_{4u}) + D_\omega \le -c, \quad G_6(\lambda_{1u}, t_{4l}) + D_\theta \le -c, \tag{D.3}$$

where

$$G_5(t_4) = t_4 x^{-3}\varphi^{-1}, \quad G_6(\lambda_1, t_4) = \frac{(\lambda_1\alpha_4)^2}{4t_4}x^{-5}\psi^{-1}.$$

Remark D.1 We do not actually use the above estimates. Yet, they provide a useful guideline to determine the parameters t_{ij} in the estimates.

D.2. Inequalities on the approximate steady state

To establish the nonlinear estimates in Sections 3 and 5, we have used several inequalities on the approximate steady state and the parameters defined in Appendix 1. These inequalities are summarized below.

In (3.13), we derive the damping terms in the weighted L^2 estimate with coefficients D_θ, D_ω. These coefficients are negative uniformly. That is, for some $c > 0$, we have

$$D_\theta, D_\omega \le -c < 0. \tag{D.4}$$

Recall that we choose the weights T_i and s_i defined in (B.16) and apply the argument in Section 3.11.3 to obtain the sharp estimate of the $\mathcal{T}$ term defined in (3.47). This estimate requires that the weights are nonnegative, i.e.

$$\begin{aligned} T_1 &= (-\lambda_1 D_\omega - A_\omega\varphi^{-1} - \lambda_1\kappa)\varphi - t_{61}x^{-4} > 0,\\ T_2 &= (-D_\theta - A_\theta\psi^{-1} - \kappa)\psi > 0,\\ T_3 &= 25t_{61}x^{-4} + t_{62}x^{-4/3} > 0. \end{aligned} \tag{D.5}$$

and

$$\begin{aligned} s_1 &= -\frac{\pi}{2}\lambda_2(\bar{c}_\omega + \bar{u}_x(0)) - r_{c_\omega} - \frac{\pi\lambda_1 e_3\alpha_6}{12} - G_c > 0,\\ s_2 &= -2\bar{c}_\omega\lambda_3 - \kappa\lambda_3 > 0. \end{aligned} \tag{D.6}$$

Using the above T_i, s_i and the argument in Section B.5, we establish the following estimate for the constant C_{opt} in (3.48)

$$C_{opt} \leq 2^{-1}(\mathrm{Tr}(U_2^T D^{-1} U_1)^p)^{1/p} < 0.9930 < 1. \tag{D.7}$$

The fact that $C_{opt} < 1$ implies (3.53).

In the weighted H^1 estimates, we have used

$$(x^2 \bar{u}_{xx} \psi)_x \leq 0.02\psi \tag{D.8}$$

in (5.9) to establish (5.10). We have also used

$$\begin{aligned} D_\theta + A_\theta \psi^{-1} - \left(\bar{u}_x - \frac{\bar{u}}{x}\right) + B_\theta \psi^{-1} &\leq -\kappa_2, \\ \lambda_1 D_\omega + A_\omega \varphi^{-1} - \lambda_1 \left(\bar{u}_x - \frac{\bar{u}}{x}\right) + B_\omega \varphi^{-1} &\leq -\kappa_2 \lambda_1. \end{aligned} \tag{D.9}$$

and

$$||A_{\omega 2} \varphi^{-1}||_\infty \leq a_{H^1}, \tag{D.10}$$

originated from (5.9) and (5.24) to establish (5.25).

References

1. Castelli, R., Gameiro, M., Lessard, J.-P.: Rigorous numerics for ill-posed PDEs: periodic orbits in the Boussinesq equation. Archive for Rational Mechanics and Analysis **228**(1), 129–157 (2018)
2. Castro, A., Córdoba, D.: Infinite energy solutions of the surface quasi-geostrophic equation. Advances in Mathematics **225**(4), 1820–1829 (2010)
3. Castro, A., Córdoba, D., Gómez-Serrano, J.: Global smooth solutions for the inviscid sqg equation. (2020)
4. Castro, A., Córdoba, D., Gómez-Serrano, J., Zamora, A.M.: Remarks on geometric properties of SQG sharp fronts and α-patches. arXiv preprint arXiv:1401.5376, (2014)
5. Chen, J.: On the slightly perturbed De Gregorio model on S^1. To appear in ARMA, arXiv preprint arXiv:2010.12700, (2020)
6. Chen, J.: Singularity formation and global well-posedness for the generalized Constantin-Lax-Majda equation with dissipation. Nonlinearity **33**(5), 2502 (2020)
7. Chen, J., Hou, T.Y.: Finite time blowup of 2D Boussinesq and 3D Euler equations with $C^{1,\alpha}$ velocity and boundary. Communications in Mathematical Physics **383**(3), 1559–1667 (2021)
8. Chen, J., Hou, T.Y., Huang, D.: Asymptotically self-similar blowup of the Hou–Luo model for the 3D Euler equations. arXiv preprint arXiv:2106.05422
9. Chen, J., Hou, T.Y., Huang, D.: Matlab codes for computer-aided proofs in the paper "asymptotically self-similar blowup of the Hou–Luo model for the 3D Euler equations". https://www.dropbox.com/sh/qjs6p6d9n3uiq8r/AABCDI-rZeVuTmBxGQuLJbUva?dl=0
10. Chen, J., Hou, T.Y., Huang, D.: Supplementary materials for the paper for the paper "asymptotically self-similar blowup of the Hou–Luo model for the 3D Euler equations". arXiv preprint arXiv:2106.05422
11. Chen, J., Hou, T.Y., Huang, D.: On the finite time blowup of the De Gregorio model for the 3D Euler equations. Communications on Pure and Applied Mathematics **74**(6), 1282–1350 (2021)

12. Choi, K., Hou, T., Kiselev, A., Luo, G., Sverak, V., Yao, Y.: On the finite-time blowup of a 1D model for the 3D axisymmetric Euler equations. CPAM **70**(11), 2218–2243 (2017)
13. Choi, K., Kiselev, A., Yao, Y.: Finite time blow up for a 1D model of 2D Boussinesq system. Comm. Math. Phys. **334**(3), 1667–1679 (2015)
14. Constantin, P.: On the Euler equations of incompressible fluids. Bulletin of the American Mathematical Society **44**(4), 603–621 (2007)
15. Constantin, P., Fefferman, C., Majda, A.: Geometric constraints on potentially singular solutions for the 3D Euler equations. Communications in Partial Differential Equations, 21(3-4), (1996)
16. Constantin, P., Lax, P.D., Majda, A.: A simple one-dimensional model for the three-dimensional vorticity equation. CPAM **38**(6), 715–724 (1985)
17. Córdoba, A., Córdoba, D., Fontelos, M.: Formation of singularities for a transport equation with nonlocal velocity. Annals of Mathematics, pages 1377–1389, (2005)
18. Córdoba, A., Córdoba, D., Fontelos, M.A.: Integral inequalities for the hilbert transform applied to a nonlocal transport equation. Journal de Mathématiques Pures et Appliquées **88**(6), 529–540 (2006)
19. Córdoba, D., Gómez-Serrano, J., Zlatoš, A.: A note on stability shifting for the Muskat problem, II: From stable to unstable and back to stable. Analysis & PDE **10**(2), 367–378 (2017)
20. De Gregorio, S.: On a one-dimensional model for the three-dimensional vorticity equation. Journal of Statistical Physics **59**(5–6), 1251–1263 (1990)
21. De Gregorio, S.: A partial differential equation arising in a 1D model for the 3D vorticity equation. Mathematical Methods in the Applied Sciences **19**(15), 1233–1255 (1996)
22. Deng, J., Hou, T., Yu, X.: Geometric properties and nonblowup of 3D incompressible Euler flow. Communications in Partial Difference Equations **30**(1–2), 225–243 (2005)
23. Duoandikoetxea, J., Zuazo, J.D.: Fourier analysis, vol. 29. American Mathematical Soc (2001)
24. Elgindi, T.M.: Finite-time singularity formation for $C^{1,\alpha}$ solutions to the incompressible Euler equations on $\mathbb{R}^3$. arXiv:1904.04795, (2019)
25. Elgindi, T.M., Ghoul, T.-E., Masmoudi, N.: On the stability of self-similar blow-up for $C^{1,\alpha}$ solutions to the incompressible Euler equations on $\mathbb{R}^3$. arXiv preprint arXiv:1910.14071, (2019)
26. Elgindi, T.M., Ghoul, T.-E., Masmoudi, N.: Stable self-similar blow-up for a family of nonlocal transport equations. Analysis & PDE **14**(3), 891–908 (2021)
27. Elgindi, T.M., Jeong, I.-J.: Finite-time singularity formation for strong solutions to the axi-symmetric 3 d euler equations. Annals of PDE **5**(2), 1–51 (2019)
28. Elgindi, T.M., Jeong, I.-J.: On the effects of advection and vortex stretching. Archive for Rational Mechanics and Analysis, (Oct 2019)
29. Elgindi, T.M., Jeong, I.-J.: Finite-time singularity formation for strong solutions to the boussinesq system. Annals of PDE **6**, 1–50 (2020)
30. Enciso, A., Gómez-Serrano, J., Vergara, B.: Convexity of Whitham's highest cusped wave. arXiv preprint arXiv:1810.10935, (2018)
31. Gabai, D., Meyerhoff, G.R., Thurston, N.: Homotopy hyperbolic 3-manifolds are hyperbolic. Annals of Mathematics **157**(2), 335–431 (2003)
32. Gibbon, J.: The three-dimensional Euler equations: Where do we stand? Physica D: Nonlinear Phenomena **237**(14), 1894–1904 (2008)
33. Gómez-Serrano, J.: Computer-assisted proofs in pde: a survey. SeMA Journal **76**(3), 459–484 (2019)
34. Gómez-Serrano, J., Granero-Belinchón, R.: On turning waves for the inhomogeneous Muskat problem: a computer-assisted proof. Nonlinearity **27**(6), 1471 (2014)
35. Hales, T.: A proof of the Kepler conjecture. Annals of Mathematics, pages 1065–1185, (2005)
36. Hardy, G., Littlewood, J., Pólya, G.: Inequalities. Cambridge University Press (1952)
37. Hoang, V., Orcan-Ekmekci, B., Radosz, M., Yang, H.: Blowup with vorticity control for a 2d model of the boussinesq equations. Journal of Differential Equations **264**(12), 7328–7356 (2018)
38. Hoang, V., Radosz, M.: Cusp formation for a nonlocal evolution equation. Archive for Rational Mechanics and Analysis **224**(3), 1021–1036 (2017)
39. Hoang, V., Radosz, M.: Singular solutions for nonlocal systems of evolution equations with vorticity stretching. SIAM Journal on Mathematical Analysis **52**(2), 2158–2178 (2020)
40. Hou, T.: Blow-up or no blow-up? a unified computational and analytic approach to 3D incompressible Euler and Navier-Stokes equations. Acta Numerica **18**(1), 277–346 (2009)
41. Hou, T., Li, R.: Dynamic depletion of vortex stretching and non-blowup of the 3D incompressible Euler equations. Journal of Nonlinear Science **16**(6), 639–664 (2006)

42. Hou, T., Liu, P.: Self-similar singularity of a 1D model for the 3D axisymmetric Euler equations. Research in the Mathematical Sciences **2**(1), 1–26 (2015)
43. Jia, H., Stewart, S., Sverak, V.: On the de gregorio modification of the constantin-lax-majda model. Archive for Rational Mechanics and Analysis **231**(2), 1269–1304 (2019)
44. Kenig, C.E., Merle, F.: Global well-posedness, scattering and blow-up for the energy-critical, focusing, non-linear Schrödinger equation in the radial case. Inventiones mathematicae **166**(3), 645–675 (2006)
45. Kiselev, A.: Regularity and blow up for active scalars. Mathematical Modelling of Natural Phenomena **5**(04), 225–255 (2010)
46. Kiselev, A.: Small scales and singularity formation in fluid dynamics. In: Proceedings of the International Congress of Mathematicians, volume **3**, (2018)
47. Kiselev, A., Ryzhik, L., Yao, Y., Zlatos, A.: Finite time singularity for the modified SQG patch equation. Ann. Math. **184**, 909–948 (2016)
48. Kiselev, A., Sverak, V.: Small scale creation for solutions of the incompressible two dimensional Euler equation. Annals of Mathematics **180**, 1205–1220 (2014)
49. Kiselev, A., Tan, C.: Finite time blow up in the hyperbolic boussinesq system. Adv. Math. **325**, 34–55 (2018)
50. Landman, M., Papanicolaou, G., Sulem, C., Sulem, P.: Rate of blowup for solutions of the nonlinear Schrödinger equation at critical dimension. Physical Review A **38**(8), 3837 (1988)
51. Lanford, O.E.: A computer-assisted proof of the Feigenbaum conjectures. In: Universality in Chaos, pages 245–252. Routledge, (2017)
52. Li, D., Rodrigo, J.: Blow-up of solutions for a 1d transport equation with nonlocal velocity and supercritical dissipation. Advances in Mathematics **217**(6), 2563–2568 (2008)
53. Liu, P.: Spatial Profiles in the Singular Solutions of the 3D Euler Equations and Simplified Models. PhD thesis, California Institute of Technology, (2017). https://resolver.caltech.edu/CaltechTHESIS:09092016-000915850
54. Luo, G., Hou, T.: Toward the finite-time blowup of the 3D incompressible Euler equations: a numerical investigation. SIAM Multiscale Modeling and Simulation **12**(4), 1722–1776 (2014)
55. Luo, G., Hou, T.Y.: Potentially singular solutions of the 3d axisymmetric euler equations. Proceedings of the National Academy of Sciences **111**(36), 12968–12973 (2014)
56. Lushnikov, P.M., Silantyev, D.A., Siegel, M.: Collapse vs. blow up and global existence in the generalized constantin-lax-majda equation. arXiv preprint arXiv:2010.01201, (2020)
57. Majda, A., Bertozzi, A.: Vorticity and incompressible flow, vol. 27. Cambridge University Press (2002)
58. Martel, Y., Merle, F., Raphaël, P.: Blow up for the critical generalized Korteweg-de Vries equation. I: Dynamics near the soliton. Acta Mathematica **212**(1), 59–140 (2014)
59. McLaughlin, D., Papanicolaou, G., Sulem, C., Sulem, P.: Focusing singularity of the cubic Schrödinger equation. Physical Review A **34**(2), 1200 (1986)
60. Merle, F., Raphael, P.: The blow-up dynamic and upper bound on the blow-up rate for critical nonlinear Schrödinger equation. Annals of mathematics, pages 157–222, (2005)
61. Merle, F., Zaag, H.: Stability of the blow-up profile for equations of the type $u_t = \delta u + |u|^{p-1}u$. Duke Math. J **86**(1), 143–195 (1997)
62. Merle, F., Zaag, H.: On the stability of the notion of non-characteristic point and blow-up profile for semilinear wave equations. Communications in Mathematical Physics **333**(3), 1529–1562 (2015)
63. Moore, R.E., Kearfott, R.B., Cloud, M.J.: Introduction to interval analysis, volume 110. Siam, (2009)
64. Okamoto, H., Sakajo, T., Wunsch, M.: On a generalization of the constantin-lax-majda equation. Nonlinearity **21**(10), 2447–2461 (2008)
65. Rump, S.M.: Verification methods: Rigorous results using floating-point arithmetic. Acta Numerica **19**, 287–449 (2010)
66. Schochet, S.: Explicit solutions of the viscous model vorticity equation. Communications on pure and applied mathematics **39**(4), 531–537 (1986)
67. Schwartz, R.E.: Obtuse triangular billiards II: One hundred degrees worth of periodic trajectories. Experimental Mathematics **18**(2), 137–171 (2009)
68. Silvestre, L., Vicol, V.: On a transport equation with nonlocal drift. transactions of the American Mathematical Society **368**(9), 6159–6188 (2016)